

THE MECHANISM OF SOIL-
BIOENGINEERING FOR SLOPE STABILITY DURING HEAVY RAINFALL ON UNSATURATED
SOIL.

Mr. Kreng Hav Eab



บทคัดย่อและแฟ้มข้อมูลฉบับเต็มของวิทยานิพนธ์ตั้งแต่ปีการศึกษา 2554 ที่ให้บริการในคลังปัญญาจุฬาฯ (CUIR)
เป็นแฟ้มข้อมูลของนิสิตเจ้าของวิทยานิพนธ์ ที่ส่งผ่านทางบัณฑิตวิทยาลัย

The abstract and full text of theses from the academic year 2011 in Chulalongkorn University Intellectual Repository (CUIR)
are the thesis authors' files submitted through the University Graduate School.

A Dissertation Submitted in Partial Fulfillment of the Requirements
for the Degree of Doctor of Philosophy Program in Civil Engineering
Department of Civil Engineering
Faculty of Engineering
Chulalongkorn University
Academic Year 2014

Copyright of Chulalongkorn University

กลไกวิศวกรรมชีวภาพดินสำหรับการเพิ่มเสถียรภาพลาดดินในสถานะไม่อิ่มตัวด้วยน้ำ



วิทยานิพนธ์นี้เป็นส่วนหนึ่งของการศึกษาตามหลักสูตรปริญญาวิศวกรรมศาสตรดุษฎีบัณฑิต

สาขาวิชาวิศวกรรมโยธา ภาควิชาวิศวกรรมโยธา

คณะวิศวกรรมศาสตร์ จุฬาลงกรณ์มหาวิทยาลัย

ปีการศึกษา 2557

ลิขสิทธิ์ของจุฬาลงกรณ์มหาวิทยาลัย

Thesis Title	THE MECHANISM OF SOIL-BIOENGINEERING FOR SLOPE STABILITY DURING HEAVY RAINFALL ON UNSATURATED SOIL.
By	Mr. Kreng Hav Eab
Field of Study	Civil Engineering
Thesis Advisor	Professor Suched Likitlersuang, DPhil.

Accepted by the Faculty of Engineering, Chulalongkorn University in Partial Fulfillment of the Requirements for the Doctoral Degree

.....Dean of the Faculty of Engineering
(Professor Bundhit Eua-arporn, Ph.D.)

THESIS COMMITTEE

.....Chairman
(Associate Professor Supot Teachavorasinskun, D.Eng.)

.....Thesis Advisor
(Professor Suched Likitlersuang, DPhil.)

.....Examiner
(Associate Professor Tirawat Boonyatee, D.Eng.)

.....Examiner
(Associate Professor Boonchai Ukritchon, Sc.D.)

.....External Examiner
(Professor Akihiro Takahashi)

เกรียง ฮัฟ เอบ : กลไกวิศวกรรมชีวภาพดินสำหรับการเพิ่มเสถียรภาพลาดดินในสภาวะไม่อิ่มตัวด้วยน้ำ (THE MECHANISM OF SOIL-BIOENGINEERING FOR SLOPE STABILITY DURING HEAVY RAINFALL ON UNSATURATED SOIL.) อ.ที่ปรึกษาวิทยานิพนธ์หลัก: สุเชษฐ์ ลิขิตเลอสรวง, 127 หน้า.

การสูญเสียเสถียรภาพของลาดดินจากปริมาณน้ำฝนที่ตกอย่างต่อเนื่องนั้นถือเป็นภัยพิบัติทางธรณีเทคนิคที่สำคัญและพบเจอทั่วไป ปัจจัยที่สำคัญต่อกลไกการวิบัติของลาดดินเช่น พฤติกรรม การไหลของน้ำ การเปลี่ยนแปลงแรงดันน้ำโพรง และกำลังรับแรงเฉือนของดิน งานวิจัยนี้เริ่มจากการศึกษาผลของพีชต่อกำลังรับแรงเฉือนของดิน โดยใช้หญ้าแฝกเป็นกรณีศึกษา ดำเนินการสังเกตการเจริญเติบโตของรากและวัดอัตราส่วนพื้นที่รากในห้องปฏิบัติการ รวมทั้งดำเนินการทดสอบวัดกำลังรับแรงเฉือนของหญ้าแฝกอายุ 4 และ 6 เดือนด้วยเครื่องทดสอบกำลังรับแรงเฉือนทางตรง การศึกษานี้ยังรวมถึงการอธิบายกลไกวิศวกรรมชีวภาพดินผ่านการจำลองลาดดินภายใต้ปริมาณน้ำฝนด้วยแบบจำลองหมุนเหวี่ยง การศึกษานี้ได้ใช้เทคนิคการสร้างแบบจำลองขนาดเล็กของเสถียรภาพลาดดินโดยใช้โพลีเอสเตอร์ไฟเบอร์ผสมเข้ากับดินตัวอย่าง ขั้นตอนการทดสอบจะบันทึกค่าการเพิ่มขึ้นของระดับน้ำใต้ดินอันเนื่องมาจากปริมาณน้ำฝนที่ค่อยๆแทรกซึมสู่ดิน ผลการทดสอบแสดงให้เห็นว่าการเพิ่มขึ้นของระดับน้ำใต้ดินทำให้เกิดการวิบัติของลาดดินโดยเริ่มจากด้านล่างของลาดดินและจะค่อยๆแผ่ขยายไปด้านบนในกรณีของดินที่ไม่ได้มีพีชปกคลุม และผลการทดสอบยังแสดงให้เห็นอีกด้วยว่า รากที่เสริมเข้าไปจะช่วยลดการซึมของน้ำฝนสู่ดิน ชะลอการเพิ่มขึ้นระดับน้ำใต้ดิน และทำให้ดินมีกำลังรับแรงเฉือนเพิ่มมากขึ้นอีกด้วย และเพื่อเป็นการสนับสนุนผลการทดสอบจึงนำเอาการวิเคราะห์สมมูลลิมิตด้วยเทคนิคการแปรเปลี่ยนแรงดันน้ำใต้ดินมาช่วยในการพิจารณา ค่าพารามิเตอร์ที่สำคัญของการวิเคราะห์ คือปริมาณน้ำในดินเชิงปริมาตรและค่าการนำทางชลศาสตร์ของดิน ตลอดจนค่าการยึดเกาะและมุมเสียดทานปรากฏของดินที่เสริมแรงด้วยรากพีช ผลจากการวิเคราะห์แสดงให้เห็นในแนวโน้มของค่าความปลอดภัยที่เพิ่มขึ้นจากการปลูกพีช ซึ่งสอดคล้องกับผลจากแบบจำลองหมุนเหวี่ยง

ภาควิชา วิศวกรรมโยธา

ลายมือชื่อนิสิต

สาขาวิชา วิศวกรรมโยธา

ลายมือชื่อ อ.ที่ปรึกษาหลัก

ปีการศึกษา 2557

5471459921 : MAJOR CIVIL ENGINEERING

KEYWORDS: SLOPE STABILITY; VEGETATION; LARGE DIRECT SHEAR TEST; CENTRIFUGE MODELLING; TRANSIENT ANALYSIS; LIMIT EQUILIBRIUM ANALYSIS.

KRENG HAV EAB: THE MECHANISM OF SOIL-BIOENGINEERING FOR SLOPE STABILITY DURING HEAVY RAINFALL ON UNSATURATED SOIL.. ADVISOR: PROF. SUCHED LIKITLERSUANG, DPhil., 127 pp.

Slope instability induced by rainfall is a serious geotechnical hazard all over the world. The characteristics of water flow, pore water pressure changes and shear strength of the soil are the main factors involved in slope failure mechanisms. This research begins with a study of the vegetation contribution on shear strength using vetiver as a vegetation specimen. Root observation and determination of root area ratios were carried out in the laboratory. To observe the shear strength, vetiver specimens at 4 and 6 months were tested using direct shear tests. This research also aims to illustrate the mechanism of soil bio-engineering for slope stability induced by rainfall using a rainfall simulator in a geotechnical centrifuge. A sloping rooted surface layer was simulated by polyester fibre in the centrifuge tests. The results indicate that a rise in the groundwater table due to rainwater infiltration was responsible for slope failure and failure near the toe propagated up-slope in a bare soil slope. The test results also reveal that roots can help to reduce the infiltration of rainwater into the ground, delay a rise in groundwater table and increase the shear strength of the soil. To confirm this, the transient and limit equilibrium analysis were conducted. The important parameters incorporated in transient analysis are volumetric of water content and hydraulic conductivity as well as apparent cohesion and friction angle of root-reinforced soils. The analysis result has shown agreement with the trends observed in the centrifuge tests.

Department: Civil Engineering

Student's Signature

Field of Study: Civil Engineering

Advisor's Signature

Academic Year: 2014

ACKNOWLEDGEMENTS

First of all, I would like to express my highest gratitude to my scholarship sponsor, AUN/Seed-Net project (JICA), who has financially and technically supported me during this doctoral program. Also, many thanks go to Chulalongkorn University (CU) and the Civil Engineering Department for being host institute, under the AUN/SEED-Net program.

Secondly, I would like to express my gratefulness to my principal advisor, Prof. Dr. Suched Likitlersuang, for his excellent guidance, advises, and encouragement. During my doctoral studies, he gave me the best supervision, which could lead me to finish my study successfully with a great credit of knowledge.

Thirdly, I would like to express my gratitude to my co-advisor, Prof. Dr. Akihiro Takahashi for spending his value time to instruct me about physical modelling using centrifuge apparatus at Tokyo Institute of Technology, Japan. And he also guides me how to do a good experiment and explain the concept of analysis the data from centrifuge.

Unforgettably, I am heartily thankful to all lectures in Civil Engineering Department for providing the valuable knowledge and advices during the three-year doctoral student in Thailand. Moreover, it is a pleasure to thank to all program officers of Civil Engineering Department and AUN Seed-Net for their facility in processing all administrative matters. Plus, I would like to thank Mr. Adithep Wangbooncong for sharing his data.

Finally, I would like to express my greatest gratitude to my parents for their unlimited supports, advices, encouragements, endorsements and believes. They always give me hope and believe in what I do. Most of all, they are my source of strength to struggle against every obstacle in my life.

Thank you.

CONTENTS

	Page
THAI ABSTRACT	iv
ENGLISH ABSTRACT	v
ACKNOWLEDGEMENTS	vi
CONTENTS	vii
CONTENTS OF TABLES	xii
CONTENTS OF FIGURES	xiii
1 CHAPTER INTRODUCTION	1
1.1 Background	1
1.2 Statement of the Problem	3
1.3 Research Objectives and scopes	5
1.4 Research Methodology	6
1.5 Thesis Structure	8
2 CHAPTER LITERATURE REVIEW	11
2.1 Introduction	11
2.2 Role of vegetation in the stability of slope	12
2.3 Root reinforcement theory	13
2.3.1. Root system architectures	15
2.3.1.1. Structure classification and terminology	15
2.3.1.2. Depth and distribution of root system	17
2.3.2. Root reinforcement measurement	18
2.4 Principle of soil bioengineering	19
2.5 Limitations of Soil bioengineering	20

2.6 The Soil-bioengineering Design	21
2.6.1. Vetiver system.....	21
2.6.2. Tensile and Shear Strength of Vetiver root.....	22
2.7 Unsaturated soil mechanics	24
2.7.1. Stress state variables	24
2.7.2. Suction in unsaturated soil.....	25
2.7.3. Transient flow in unsaturated soil	27
2.7.4. Hydraulic conductivity function in unsaturated soil	28
2.7.5. Soil-Water Characteristic curve	29
2.7.5.1. Brooks and Corey estimation.....	30
2.7.5.2. Van Genuchten estimation	31
2.7.5.3. Fredlund's estimation	31
2.8 Vegetation and slope Stability Analysis	32
2.8.1. The influence of vegetation on slope stability	33
2.8.2. Slope stability analysis	33
2.8.2.1. Limit equilibrium method	34
2.8.2.2. Finite element method	35
2.8.2.3. Infinite slope analysis	36
2.9 Physical modelling in geotechnical centrifuge	39
2.9.1. Scaling laws	41
2.9.2. Apparatus test.....	43
2.10 Numerical modelling for slope stability in Geo-studio	44
2.10.1. Slope/W.....	46

	Page
2.10.1.1. General limit equilibrium method	47
2.10.1.2. Moment equilibrium factor of safety	48
2.10.1.3. Force equilibrium factor of safety.....	48
2.10.2. Seep/W	48
2.10.2.1. Darcy's law.....	49
3 CHAPTER VETIVER GRASS EXPERIMENTAL IN LABORATORY.....	50
3.1. Introduction	50
3.2 Sample preparation.....	52
3.2.1. Soil sample testing.....	52
3.2.2. Vetiver sample preparation.....	53
3.3 Vetiver Roots Observation	56
3.4 Shear strength of vetiver roots	59
3.4.1. Direct shear box.....	60
3.4.2. Large direct shear box.....	62
3.5 Image processing.....	63
3.6 Results and discussion.....	66
4 CHAPTER PHYSICAL MODELLING.....	68
4.1 Introduction	68
4.2 Soil bioengineering	69
4.3 Instrumentation.....	71
4.3.1. Centrifuge apparatus.....	71
4.3.2. Pore water pressure transducer and accelerometers.....	72
4.3.3. Steel box and bedrock.....	74

	Page
4.4 Properties of soil and fibre used in the model.....	75
4.5 Shear strength of soils	77
4.6 Description of centrifuge model tests.....	79
4.6.1. Rainfall model test.....	82
4.6.2. Centrifuge slope stability model tests and testing procedure	84
4.7 Test Results and Discussion.....	86
4.7.1. Test results	86
4.7.1.1. Phreatic surface and slope displacement.....	86
4.7.1.2. Safety factor of slope model	91
4.8 Results discussion.....	92
5 CHAPTER NUMERICAL MODELLING.....	95
5.1 Introduction	95
5.2 Slope/W using limit equilibrium analysis.....	96
5.2.1. Ordinary of Fellenius method.....	97
5.2.2. Bishop's simplified method	97
5.2.3. Morgenstern-Price method.....	98
5.3 Seep/W using transient analysis	98
5.4 Unsaturated soil mechanics principle	99
5.4.1. Soil water characteristic curve	100
5.4.2. Permeability function	101
5.5 Numerical analysis.....	102
5.5.1. Model of root reinforcement.....	102
5.5.2. Seepage and slope stability modelling.....	103

	Page
5.6 Results and discussion.....	105
5.6.1. Pore water pressure distribution	105
5.6.2. Slip surface for factor of safety	105
5.6.3. Pore water pressure comparison between centrifuge and geo-slope	108
6 CHAPTER CONCLUSION AND RECOMMENDATION	111
6.1 Conclusion.....	111
6.2 Recommendation	112
REFERENCES	113
Appendix: Rainfall simulator	124
VITA.....	127



CONTENTS OF TABLES

Table 2-1: Strength of some plants root (Truong et al., 2008).....	23
Table 2-2: Influence of vegetation on soil slope (Coppin & Richards, 1990).....	33
Table 2-3: Some common for centrifugal scaling test	42
Table 2-4: Specification of centrifugal apparatus (Akihiro Takahashi, 2002)	44
Table 3-1: Chemical test result of planted soil	52
Table 3-2: Results of root area ratio.....	65
Table 3-3: Results of direct shear tests.....	67
Table 4-1: Properties of compacted soils	76
Table 4-2: Classification of Rainfall intensity (Llasat, 2001).....	84
Table 4-3: Summaries of the rainfall model test	84
Table 4-4: Summaries of centrifuge tests.....	94
Table 5-1: Principle and equations for unsaturated soil mechanics modified from (Harianto Rahardjo & Satyanaga, 2014).....	100
Table 5-2: Input soil material for slope stability.....	104
Table 5-3: Summarized of safety factors.....	110

CONTENTS OF FIGURES

Figure 1-1: Mechanism of rainfall-induced slope failure (H. Rahardjo, Satyanaga, & Leong, 2012).....	4
Figure 1-2: Flow chart of research work.....	7
Figure 1-3: schematic of interaction between different parts of the dissertation	8
Figure 2-1: Schematic diagram of perpendicular root fiber reinforcement model modified from (Gray & Sotir, 1996).....	15
Figure 2-2: Main components of woody root system (Gray & Sotir, 1996).....	16
Figure 2-3: Five basic types of root systems modified from (Ghestem, Sidle, & Stokes, 2011). (a) Bunch of grass root systems. (b) Tap-root system. (c) Heart shaped root system. (d) Root system with a large tap-root and large horizontal lateral roots from which emerge vertical sinkers. (e) Plate-shaped root system.	17
Figure 2-4: Influence of slope stratigraphy on the stabilizing effect of roots against slope failure (Gray & Sotir, 1996)	18
Figure 2-5: Vetiver root in soil (left and middle), in water (right) (Truong et al., 2008)	22
Figure 2-6: Root diameter distribution (Truong et al., 2008).....	23
Figure 2-7: a) Development of surface tension at the interface of the water and air, b) Changes in the radius of the meniscus with water content (Askarinejad, 2013)	27
Figure 2-8: Relative hydraulic conductivity function after (Lu & Likos, 2004).....	28
Figure 2-9: Typical chart of soil water characteristic curve (Delwyn G Fredlund, Rahardjo, & Fredlund, 2012)	30
Figure 2-10: Infinite slope: a) without the effect of vegetation roots and b) with the effect of vegetation root modified from (Gray & Sotir, 1996).....	37

Figure 2-11: Centrifuge apparatus at TIT (Oblozinsky & Kuwano, 2004).....	40
Figure 2-12: Principle of Centrifuge Modeling (Schofield, 1981)	42
Figure 2-13: Section view of centrifuge apparatus at TIT (Akihiro Takahashi, 2002)	43
Figure 3-1: Flow chart of experimental in laboratory	52
Figure 3-2: Vetiver specimens grew in hydroponic condition.....	53
Figure 3-3: Root observation for highland within 3 months	54
Figure 3-4: Root observation for lowland within 3 months.....	54
Figure 3-5: Vetiver grass specimens prepared for the shear tests: a) 4 months old single vetiver grass for the direct shear test and b) 6 months old group vetiver grass for the large direct shear test	55
Figure 3-6: Tested samples for shear tests: a) a 60 mm diameter direct shear apparatus and b) a 300mm x 300mm large direct shear apparatus	56
Figure 3-7: Relationship between length and radius of roots bundle for highland.....	57
Figure 3-8: Relationship between length and radius of roots bundle for lowland.	58
Figure 3-9: Comparison growing rate of vetiver roots with (Kaewsang, 2000).	58
Figure 3-10: Direct shear apparatus	60
Figure 3-11: Single vetiver grass planting sample: a) before testing and b) after testing	61
Figure 3-12: 4 months old single vetiver grass from direct shear test	61
Figure 3-13: Large direct shear apparatus.....	62
Figure 3-14: Group vetiver grass planting sample: a) planting in wood box and b) before testing.....	63
Figure 3-15: 6 months old group vetiver grass from large direct shear test	63
Figure 3-16: Definition of root-area ratio: a) in the shear plane and b) parallel plane.....	64

Figure 3-17: Root photograph taken from the 6 months group vetiver.....	65
Figure 3-18: Binary image processing by using Photoshop.....	65
Figure 4-1: Stability of vetiver grass on Slope.....	70
Figure 4-2: Centrifuge apparatus at Tokyo Institute of Technology (Tokyo tech).....	72
Figure 4-3: a) pore water pressure transducer and b) accelerometer.....	73
Figure 4-4: Pore water pressure transducers and accelerometers arrangement.....	73
Figure 4-5: a) steel box and b) bedrock.....	74
Figure 4-6: Grain size distribution curve of Edosaki Sand.....	75
Figure 4-7: Polyester fibers before and after mixed with Edosaki sand at 2% by mass: a) Before mixing and b) After mixing.....	76
Figure 4-8: Edosaki sand specimens with and without 2% of polyester fibres.....	78
Figure 4-9: 4 months old single vetiver from direct shear test.....	78
Figure 4-10: Flow chart of centrifuge model test.....	79
Figure 4-11: The detail schematic of centrifuge model tests: a) rainfall model test, b) case 1, c) case 2, and d) case 3.....	81
Figure 4-12: Rainfall simulator apparatus.....	83
Figure 4-13: Schematic rainfall system in centrifuge test.....	83
Figure 4-14: Schematic slope testing systems for centrifuge tests.....	86
Figure 4-15: Variation of phreatic surface and location of pore water pressure gauges used: a) Pore water pressure location, b) Case 1, c) Case 2, and d) Case 3.....	88
Figure 4-16: Slope displacement for case 1: (a) displacement calculated from ACCs; (b) slip surface of soil slope at 26 s.....	90
Figure 4-17: Slope displacement for case 2: (a) displacement calculated from ACCs; (b) exaggerated displacement vector at 50 s.....	90

Figure 4-18: Slope displacement for case 3: (a) displacement calculated from ACCs; (b) exaggerated displacement vector at 58 s.....	91
Figure 4-19: Relationships between safety factor with time history.....	92
Figure 4-20: Evolutions of (a) average water pressure head; (b) displacement at toe slope.....	93
Figure 5-1: Fitting of soil water characteristic data using grain size assumption	101
Figure 5-2: Hydraulic conductivity with soil suction using grain size assumption	102
Figure 5-3: Geometry of boundary condition for slope models: a) for seepage analysis and b) for slope stability analysis.....	104
Figure 5-4: Results pore water pressure change at the end of rainfall: a) unreinforced case, b) 1 m depth of vegetation root case and c) 2 m depth of vegetation root case.....	106
Figure 5-5: Results slip surface at the end of rainfall: a) un-reinforced case, b) 1 m depth of vegetation root case, and c) 2 m depth of vegetation root case.....	107
Figure 5-6: Variation of safety factor during rainfall.....	108
Figure 5-7: Comparison of pore water pressure change for unreinforced case: a) centrifuge result and b) seep/W result.....	109
Figure 5-8: Comparison of pore water pressure change for 1m depth of vegetation root: a) centrifuge result and b) seep/W result	109
Figure 5-9: Comparison of pore water pressure change for 2m depth of vegetation root: a) centrifuge result and b) seep/W result	110

1 CHAPTER INTRODUCTION

1.1 Background

Landslides are one of the most widespread earth processes, which involve the failure of sloping earth material. Landslides are concerned as one of the important problems with Geotechnical engineering. This is because landslides are usually among the most costly natural hazards in terms of human life and economic loss. In recent years, the natural slope instability has increasingly occurred, especially in the tropical monsoon zone such as Southeast Asia countries. There are several factors that could cause the natural slope failure, such as geological activity, hydrological influence and human interference, but seepage and rainfall are the main factors. The infiltration of rain water could develop the ground water level rise up by increasing in pore water pressure or decreasing in soil matric suction of unsaturated soil. On other hand, the matric suction has been defined as an important factor to the stability of unsaturated soil (D.G. Fredlund & Rahardjo, 1993). In addition, the physical process of rainfall infiltration into the ground and its seepage through the soil layers have been studied by the hydrogeologists, soil scientists and geotechnical engineers (Ng & Shi, 1998)

To increase the slope stability, several methods have been used such as; soil nail, retaining structure, geosynthetic reinforcement and shotcrete. However, these methods are costly and may not suitable for natural slope. In ancient time, the use of vegetation in soil slopes and earthen covers for the landfill has been recognised and it is also well-known that the effect of vegetation plays an important role to increase soil slope stability. Soil Bioengineering is an environmentally friendly alternative the uses vegetation for improving slope failure. There are two main contributions that vegetation could affect to the slope stability (i.e., hydrological and mechanical processes). Firstly, changing through the soil moisture regime and drain

the water from the soil via evapotranspiration (Ali & Osman, 2008) could induce the soil suction. Secondly, the roots of vegetation could enhance the slope stability by increasing the shear strength of soil ((Gray & Sotir, 1996) and (T.H. Wu, McKinnell, & Swanston, 1979)). The role of vegetation on slope stability has been defined by (Greenway, 1978) , (Coppin & Richards, 1990), and (T. H. Wu, 1995)). In addition, this method is applied against the shallow failure and as well as to the soil surface erosion in the natural slopes.

Vetiver grass (*Chrysopogon zizanioides*), a plant had been promoted to help conserve the soil erosion and water runoff or infiltration by the World Bank in the 1980's, has been developed to become an important soil Bioengineering (Greenfield, 1996). Recently, the Chaipattana Foundation and the office of the Royal Development Project Board, Thailand, had promoted the use of Vetiver grass for soil and water conservation for many royal projects in Thailand. Vetiver grass is kind of vegetation that is very fast growing and requires low maintenance. The length of Vetiver root was observed that it could grow up to 2-3.5 m (Chinapan, Sukhasem, & Moncharoen, 1997). The Vetiver root can penetrate deeply into the ground to form a net-like barrier capable of filtering silt and containing top soil. Normally, the region with prolonged and heavy rainfall, the shallow failure is a typical failure mode of the soil slope and it has always occurred 1-3 m depth from the surface (Au, 1998; Gray & Leiser, 1982; Meisina & Scarabelli, 2007). Hence, the shallow failure of the natural slope could be protected by the rooting depth of the Vetiver grass which interlocks with the soil particle against the slope collapsed. Planting this vetiver grass is required a simple technology and it is low cost to do the maintenance. Some previous researches have performed the tensile root strength properties of vetiver grass for the resistance to shallow failure and surficial erosion (D. Hengchaovanich & N. S. Nilaweera, 1996).

Recently, stability of model soil slopes that were reinforced by plant roots has been investigated by (Sonnenberg et al., 2010) at 15-g using a centrifuge. By continuously raising groundwater table in model slopes, contributions of mechanical root reinforcement were back-analysed based on the observed slip surface on failure.

(Sonnenberg, Bransby, Bengough, Hallett, & Davies, 2011) developed and vegetated root models on their model soil slopes to explore the effects of model materials (i.e., tensile strength and elastic modulus) and root architecture on slope stability in a centrifuge. (A. Takahashi, Nakamura, & Likitlersuang, 2014) studied the effect of vegetation structures on the seepage-induced slope failure using a 50-g centrifuge model.

Although monitoring of such vegetated slopes is undertaken in Geotechnical centrifuge modelling, it is important to verify with numerical analysis. The natural slope stability has become an important issue in Geotechnical practices due to the influence of suction on unsaturated soil (D.G. Fredlund & Rahardjo, 1993). Due to the rainfall infiltration of unsaturated soil plays an important role in the process of making slope failure, the steady state analysis, which is conventionally used to analyze the slope is not suitable for the case rainfall induced the slope instability. As the theory, steady state analysis is based on the strength properties of the soil sampled along the failure plane that normally used to investigate the cause of slope failure. Moreover, the steady state analysis has been performed for the worst case which slope is either dry or fully saturated (Gofar, Lee, & Asof, 2006). To analyze the rainfall induced slope stability; hence, transient seepage analysis and limit equilibrium analysis are needed to perform in this research. (Ng & Shi, 1998) studied on a numerical investigation of slope instability on unsaturated soil by using the transient seepage analysis. The combination of transient seepage and limit equilibrium analysis have been modelled by using seep/W and slope/W from Geo-Slope International, Ltd. (Blatz, Ferreira, & Graham, 2004).

1.2 Statement of the Problem

A study of the stability of slope on unsaturated soil mechanics has become a common analytical tool in Geotechnical engineering. Landslide or slope failures in residual soils are liable to occur due to several factors, such as hydrological influence, weathering process, geological activities, human interference, and climatic

condition. Climate has been an important issue in whether a soil is saturated or unsaturated. In warm and wet climate regions with more rainy days in a hilly or mountainous area, landslides are usually occurring and it is a big concern not only in the Southeast Asia, but also around the world. For the slopes on unsaturated zone above the ground water table is commonly occurring during or shortly after heavy rainfall, as water infiltrates into the soil slope to reduce near surface suction. On unsaturated soil with higher permeability, the pore-water pressure will increase because of the increasing of rain water infiltration into the soil. In addition, the ground water table will rise up to the result of increasing the pore-water pressure. As a result, the slopes become more instability because of the decrease of the shear strength of the soil. Figure 1-1 shows the mechanism of rainfall induced the slope failure.

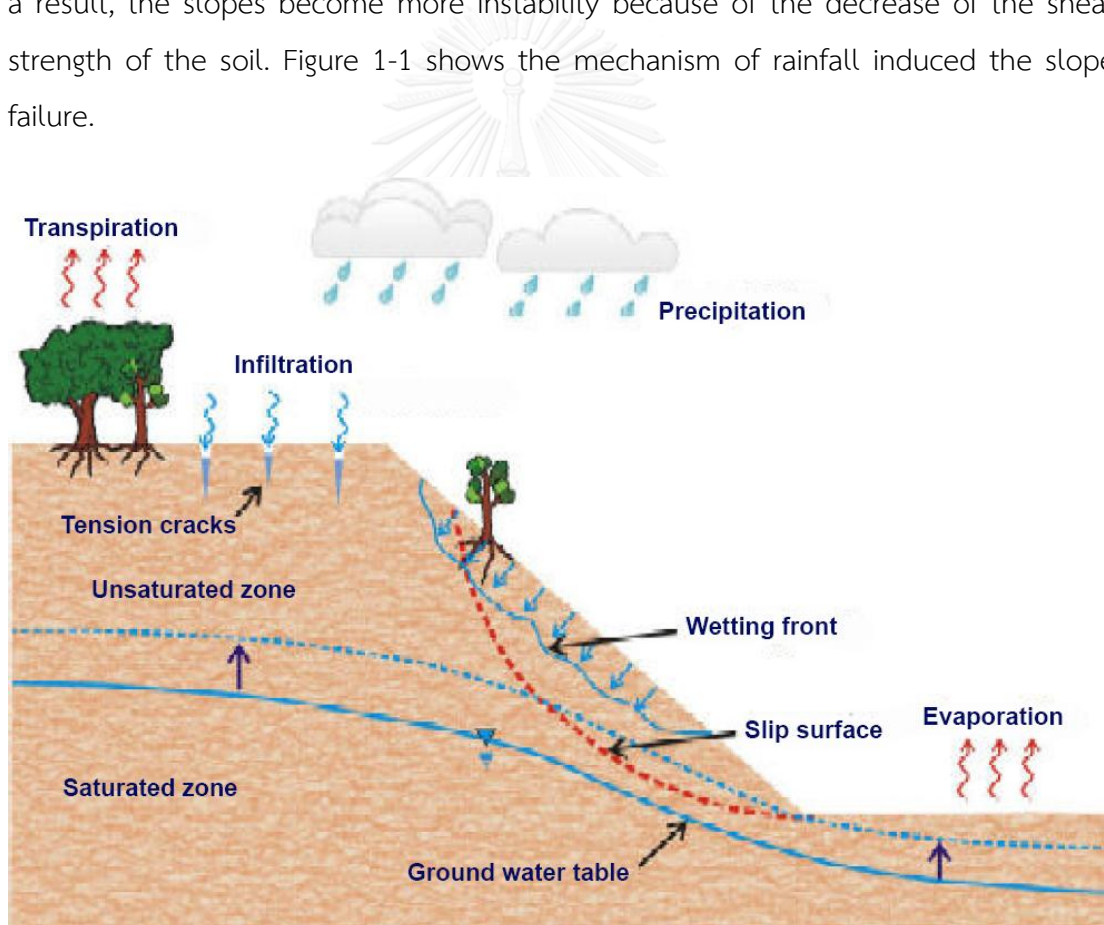


Figure 1-1: Mechanism of rainfall-induced slope failure (H. Rahardjo, Satyanaga, & Leong, 2012)

1.3 Research Objectives and scopes

Based on the problem description in section 1.2, there are three main categories have been pointed out such as: (1) the infiltration of water through porous media, (2) the changing behavior of unsaturated soil, and (3) the shear strength of soil. Therefore, the aim of this doctoral research is to obtain a main objective that to investigate the mechanism of soil Bioengineering technology for slope stabilization subjected to heavy rainfall on unsaturated soil. The investigation can be divided into small four objectives as described in the following:

- 1 To observe feasible alternative of soil bio-engineering approaches for slope stabilization by doing the experimental investigation on the roots of Vetiver grass in the process of planting.
- 2 To characterize the shear strength of soil interaction with the root fibres by conducting the large direct shear test and direct shear test based on the ASTM D3080 standard.
- 3 To correlate the effect of root fibres in soil slope between the pore water pressure and slope deformation by conducting physical modelling: Geotechnical centrifuge tests.
- 4 To study the hydro-mechanical interaction between root fibres and soil slope by using numerical analysis based on the seep/W and slope/W analysis in geo-slope studio.

1.4 Research Methodology

To get more understanding in implementing of the research, the research methodology has built to be prepared in advance to acquire the successful and smooth running research work. Based on this research, there are three steps of the research framework as follows (See Fig. 1.2):

- Research Preparation: it is the preliminary step. After the statement of problem have been set up, the literature review and data collection need to be prepared to get more understanding and finding the solution responding to those problems.
- Laboratory Work: in this step, the detail investigations on the root of Vetiver grass have been observed by determining the behavior of root fibres and physical modelling have been performed to define the mechanism of slope failure under heavy rainfall.
- Studio Work: numerical analysis has been performed by using the finite element program seep/W and limit equilibrium slope/W in geo slope studio to study the hydro-mechanical and root fibres in soil slope.

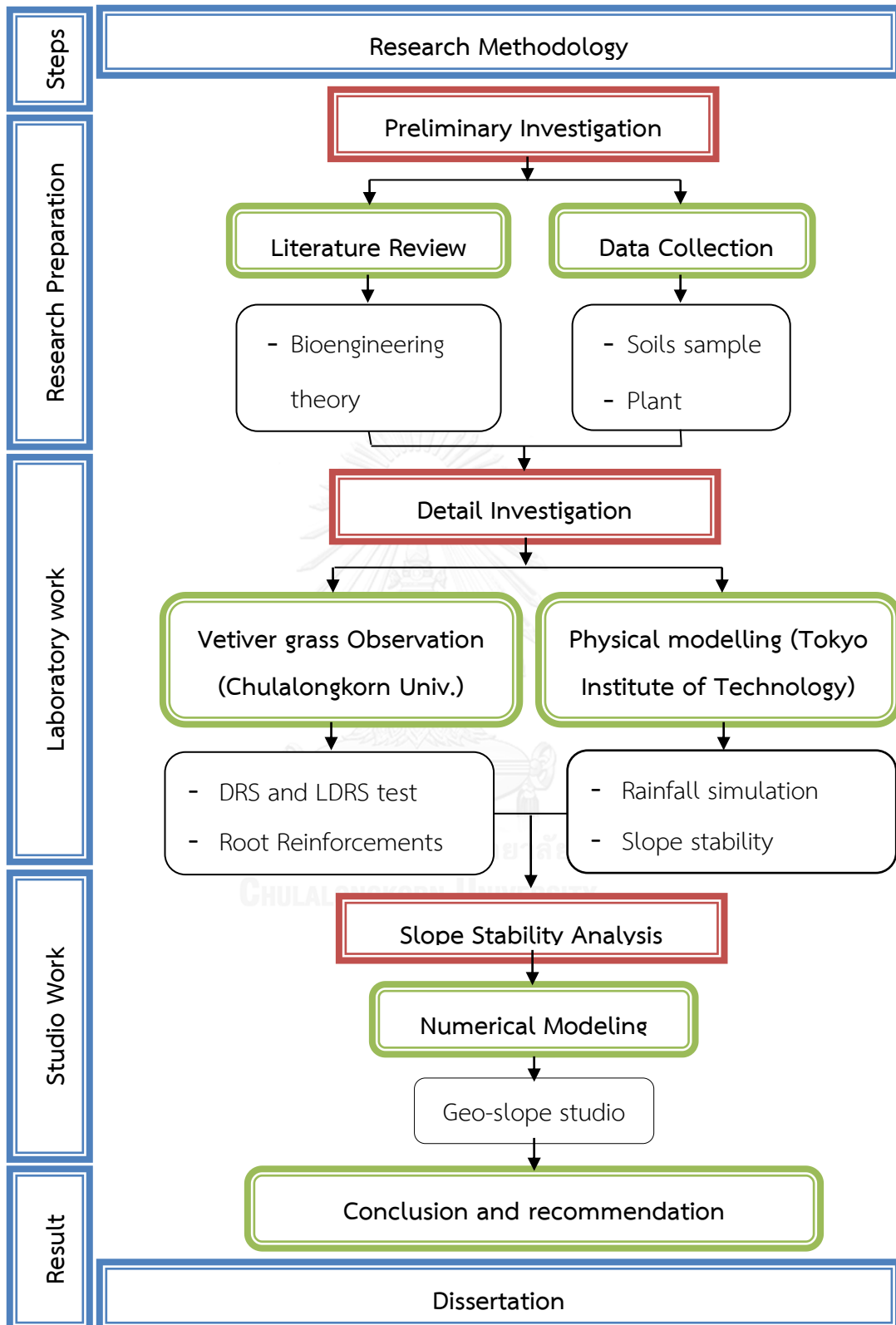


Figure 1-2: Flow chart of research work

1.5 Thesis Structure

This dissertation is chronologically crafted based on the following structures with brief description into 6 chapters. Figure 1-3 shows the schematic of interaction between different parts of the dissertation.

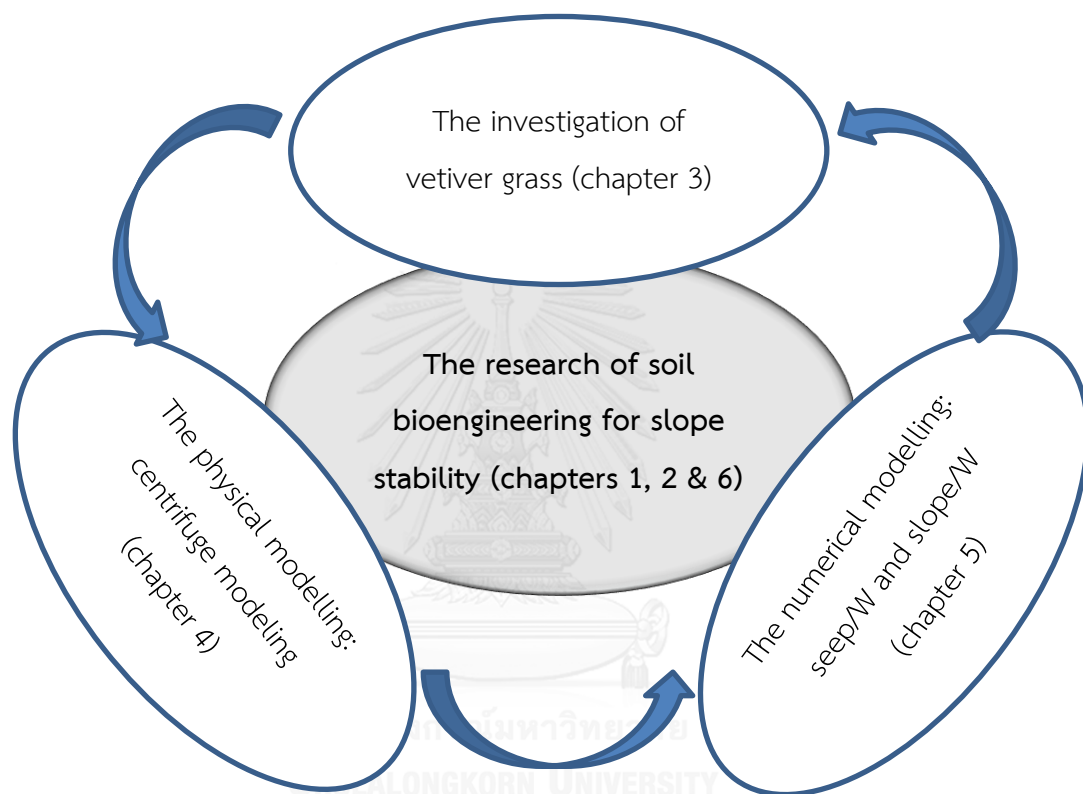


Figure 1-3: schematic of interaction between different parts of the dissertation

- Chapter 2: Review of literature on the topics of the study, which are related to the work in this research, such as; soil Bioengineering is presented including: unsaturated soil mechanic, methods of slope stability, theory of Vetiver grass, effect of vegetation on slope stability, Geotechnical centrifuge test, and the concept of transient seepage analysis.
- Chapter 3: The experimental observations of Vetiver grass have been presented in this chapter by using three steps: (1) observe the length of the roots and radius of root bundle by planting the Vetiver grass in hydroponic (liquid nutrient).

The measurement of the length of the root and the radius of root bundle was carried out continuously until 6 months. (2) Direct shear tests have performed to define the increase of cohesion of shear strength of the single Vetiver root reinforcement and the bare soils with the same density and water content associated with the four months. (3) Large direct shear tests have performed to define the increase of cohesion of shear strength from the group Vetiver grass which associated with six months. And the root area ratio also defined by transferring a digital camera to binary image via the histogram function of Photoshop software.

- Chapter 4: Physical modelling has been performed in this chapter. The concepts of Geotechnical centrifuge tests have been described, including the scaling laws and the detail of centrifuge equipment in Tokyo Institute of Technology. The soil slope models were prepared in a steel box and a 50g of centrifugal acceleration was used to model the slope stability problem. The tests have been conducted by using the rainfall simulator. The details of the design and construction of a soil slope in centrifuge chamber and rain simulator will be explained in this chapter. Three cases have been performed to examine the reinforcing effect of the 'roots' against slope failure, rooting depth was selected as a parameter. The results of test are reported and interpreted to study the mechanism of slope failure during the heavy rainfall correlated between the effects of the hydraulic interactions overlying soil mass with the contribution of the root fibres to strengthening the slope.

- Chapter 5: is devoted the numerical analysis. The effect of root reinforcement is incorporated in the existing finite element slope stability model. Parametric studies are conducted to investigate and quantify the effect of root reinforcement on slope stability. The volumetric of water content and hydraulic conductivity chart have been defined by using Van Genuchten method (Krahn, 2009; van Genuchten, 1980). Transient seepage analysis has been used to define the pore water pressure change with time in the slope model. In addition, Limit equilibrium analysis is used for these simulations. The pore pressure distributions inside the soil slope after the first and second experiments are simulated using the finite element program seep/W (Krahn,

2009) and the results are used to quantify the factor of safety of the slope using the limit equilibrium program, slop/W (Krahn, 2008).

- Chapter 6: Conclusion and Recommendation. It is the closing part of the research where, final judgments, ideas and comments are quantitatively given this section based on the research results.



2 CHAPTER LITERATURE REVIEW

2.1 Introduction

Soil Bioengineering is a discipline of civil engineering. Soil Bioengineering is the use of live material such as vegetation, alone or in combination with the mechanical, biological, and ecological concepts to achieve the civil engineering design goal that seek to arrest soil erosion and prevent the shallow slope failures (Gray & Sotir, 1996). It might sometimes work as a substitute for classical engineering. This soil Bioengineering's application has suggested itself in all fields of soil and hydraulic engineering, especially for slope and embankment stabilization and erosion control. Plus, soil Bioengineering has been mostly used in controlling erosion, but it has also been shown to be successful in the stabilization of slopes against shallow failures. In soil Bioengineering, the installations of vegetation/plants play an important role for the major structural immediately or the major structure component over time. The mechanism of interlocking the soil mass with plant roots can increase the shear strength and, also, through dewatering of the soil. Therefore, the engineer who desires successful employment of a bioengineered design requires a fundamental understanding of the growth requirements of commonly used plant species and, in the natural context, environmental benefits in secondary interest to the plant. Some of researches noted that the fiber roots of vegetation reinforced the soil slope is involved as a natural consequence of environments. However, the limitation of Bioengineering techniques, in general, to shallow mass movements and is inappropriate for controlling deep-seated slope failures due the limited depth of plant roots.

2.2 Role of vegetation in the stability of slope

The role of vegetation plays an important role in stabilizing slopes by intercepting and absorbing water, retaining soil below ground with roots and above ground with stems, retarding runoff velocity by providing a break in the path of the water and increasing surface roughness, and increasing water infiltration rates, soil porosity, and permeability (Schor & Gray, 2007). Vegetation is developed by natural selection in order to survive. Each type of vegetation serves a critical function. Grasses, or herbaceous cover, protects sloped surfaces from rain and wind erosion. Shrubs, trees, and other vegetation with deeper roots are more effective at preventing shallow soil failures, as they provide mechanical reinforcement and restraint with the roots and stems and modify the slope hydrology by root uptake and foliage interception (Schor & Gray, 2007). Therefore, although engineers prefer indicating it in terms of say strength and structural stability, in the natural context, environmental benefits in secondary interest to the plant (Mafian, Huat, & Ghiasi, 2009). Moreover, (Gray & Sotir, 1996) said vegetation affected with both surficial and mass stability of slope in the significant and important ways. The type of vegetation and the type of slope degradation process were mentioned as an important benefit of stabilization or protection. In the case of mass stability, the root and the stems of vegetation, which used the protective benefits of woody from mechanical reinforcement, have been modified to slope hydrology as a result of soil moisture extraction via evapotranspiration. The increasing of soil erosion or higher frequencies of slope failure is caused by the loss or removal of slope vegetation. “This Cause-and-effect relationship can be demonstrated convincingly as a result of many field and laboratory studies reported in the technical literature” (Gray & Sotir, 1996).

2.3 Root reinforcement theory

The basis of root reinforcement theory of slope stability is focused on the plant roots which penetrate into the weakness zone of the soil as an anchor to provide the soil slope become more stable. The reinforcing effect of plant roots intermixed with soil resembles soil cohesion has been reported by (Endo & Tsuruta, 1969). (Mafian et al., 2009) said there are two ways which have developed in the root reinforcement theory. The first approach is based on an effort to quantify impact of deforestation and rainfall on the stability of the slope and entailed a description of the root interaction in the soil by the shear band through the force equilibrium. The formulations were proposed by (Waldron, 1977) and (Tien H Wu, McKinnell III, & Swanston, 1979). The second approach to the root reinforcement theory has been established by the description of the behaviors of composite material based on its owned original. This method is focusing on the apparent of the root properties. For example, (Michalowski & Zhao, 1996) studied on the macroscopic properties of composites and it has been homogenized or averaged the root fibres and root matrix based on the distinct their characteristics. "Within this context of fibre reinforcement, root reinforcement is clearly identified as a specific case" (Mafian et al., 2009). In addition, there are many researches have investigated on the root reinforcement into the soil and clarified that the roots generally failed in tension which is meant the root system has a negligible effect on the components of the friction force (Endo & Tsuruta, 1969; O'Loughlin, 1974; Waldron, 1977; Waldron & Dakessian, 1981). These observations have been used to demonstrate that root reinforcement of soil is best approximated by an increase in apparent soil cohesion that varies in proportion to the concentration of roots within the soil. (Coppin & Richards, 1990) reported that the root which have 2 cm in diameter, is limited, has shown the increase in apparent soil cohesion.

A root reinforcement model must also be incorporated into the overall stability analysis. In terms of shear strength of soil, the contribution of the root reinforcement into the soil can be considered as an additional.

$$S = C + (\sigma - u_a) \tan \phi' \quad (2-1)$$

$$C = c' + (u_a - u_w) \tan \phi^b + S_r \quad (2-1.1)$$

$$S_r = T_r \left(\frac{A_r}{A} \right) (\sin \theta + \cos \theta \tan \phi') \quad (2-1.2)$$

C: total cohesion (kPa); c': effective cohesion of soil (kPa); u_a : pore air pressure (kPa); u_w : pore water pressure (kPa); ϕ^b : angle indicating the change in shear strength related to the changes in matric suction ($u_a - u_w$), ϕ' : effective friction angle of soil (degree); S_r : roots cohesion (kPa); T_r : tensile strength of roots (kPa); A_r/A : area of the shear surface occupied by the roots, per unit area; θ : shear deformation from vertical (degree). Figure 2-1 illustrates the root fibers increase the shear strength of the soil primarily by transferring shear stresses that develop in the soil matrix into tensile resistance in the fiber oriented perpendicularly to the shear surface. The value bracketed term ($\sin \theta + \cos \theta \tan \phi'$) in equation (2-1.2) is relatively insensitive to normal variation in θ and ϕ , so (Tien H Wu et al., 1979) proposed an average value of 1.2 for this term. Equation (2-1.2) can be then simplified to:

$$S_r = 1.2 T_r \left(\frac{A_r}{A} \right) \quad (2-2)$$

(Waldron, 1977) and (Tien H Wu et al., 1979) have developed a simple model which used to define the contribution of tree roots to soil shear strength (i.e. to determine S_r). The model was designed to simulate the idealised situation of a tree's vertical root extending across a potential sliding surface in a slope. It consists of a flexible, elastic root extending vertically across a horizontal shear zone of thickness z (Fig. 2.1).

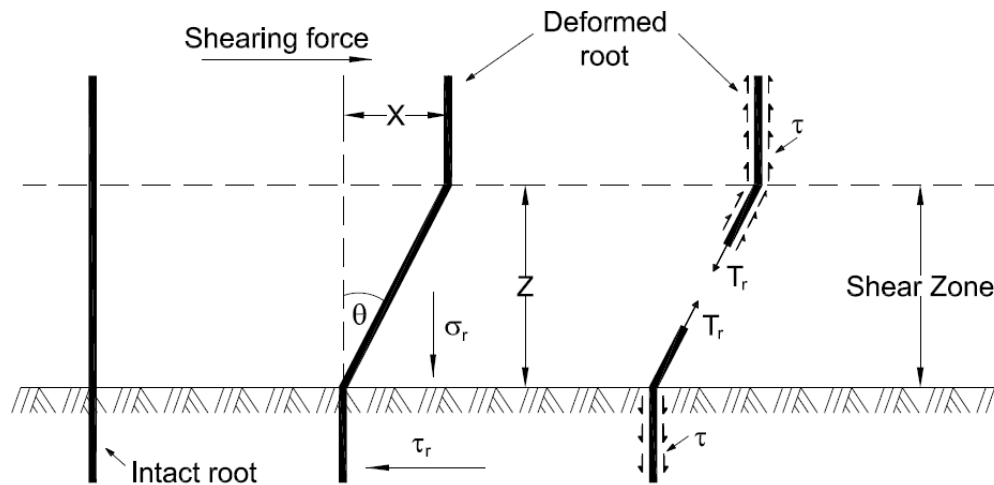


Figure 2-1: Schematic diagram of perpendicular root fiber reinforcement model modified from (Gray & Sotir, 1996)

2.3.1. Root system architectures

2.3.1.1. Structure classification and terminology

The morphology of the root system architectures is important information which helps to understand the contribution of a plant's roots to particular slope stability. Although the importance of this fact have been well recognized (T. H. Wu, 1995), a system of root morphology is still less understood aspect of arboriculture (Helliwell, 1986). This is due mainly to the difficulties of observation and variation, not only from environmental area, but also from a lesser extent of the root system. (Kozłowski, 1971) observed that root structure as well as depth and rate of root growth are chiefly controlled by the rooting environment. Local soil and site conditions such as moisture availability, soil aeration, temperature, nutrient availability, and mechanical impedance, all affect the development of a plant's root system. The major components of a tree's root system are illustrated in Figure 2-2. The root crown or root stock includes the bases of the lateral roots and the concentration of small roots beneath the root crown. Plate-shaped root systems are composed mainly of lateral roots. The diameter of lateral roots decreases rapidly

with the distance from the root crown. The mass which contains most of lateral roots is sometimes called the root mat. (Sutton, 1969) and (Kozlowski, 1971) have reported the comprehensive descriptions of root system morphology. The lateral roots are mostly found close to the soil surface while tap-roots and sinker roots are to a large extent located close to the zone directly below the tree stem. Trees tend to have most of their roots in the upper layers of soil where the mass of laterals is located in what is often referred to as the 'root mat'. Although the lateral root system may play a role in binding the soil into a single mass, the main resistance to shear failure in slopes is provided by vertical roots which are more likely to intercept potential failure planes (Gray & Leiser, 1982). The depth to which vertical roots extend is therefore important and varies considerably between species and rooting environment. Many tree species have the inherent capability to develop deep and far-reaching roots in the absence of restrictive soil or substrate characteristics (Stone & Kalisz, 1991).

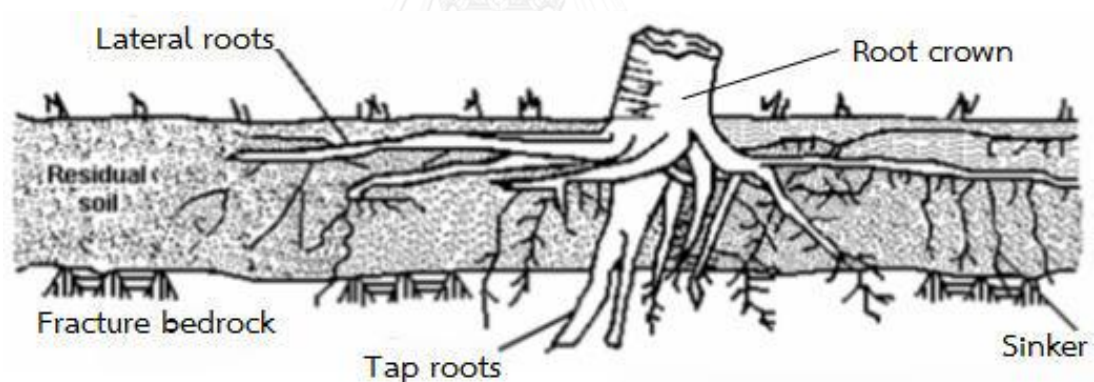


Figure 2-2: Main components of woody root system (Gray & Sotir, 1996)

The architecture of a root system is a critical factor controlling the extent to which vegetation can reinforce the earth and stabilise a slope. The quantity and size of roots crossing a potential shear surface are of particular importance (equation (2-2)).

This appears to be the case for trees of all ages and it follows that the magnitude of potential earth reinforcement will exhibit a similar spatial pattern. In the comprehensive sense, root geometry denotes all the properties which are necessary

to define the positions and dimensions of the roots in the system. Figure 2-3 shows the five different basic types of root system.

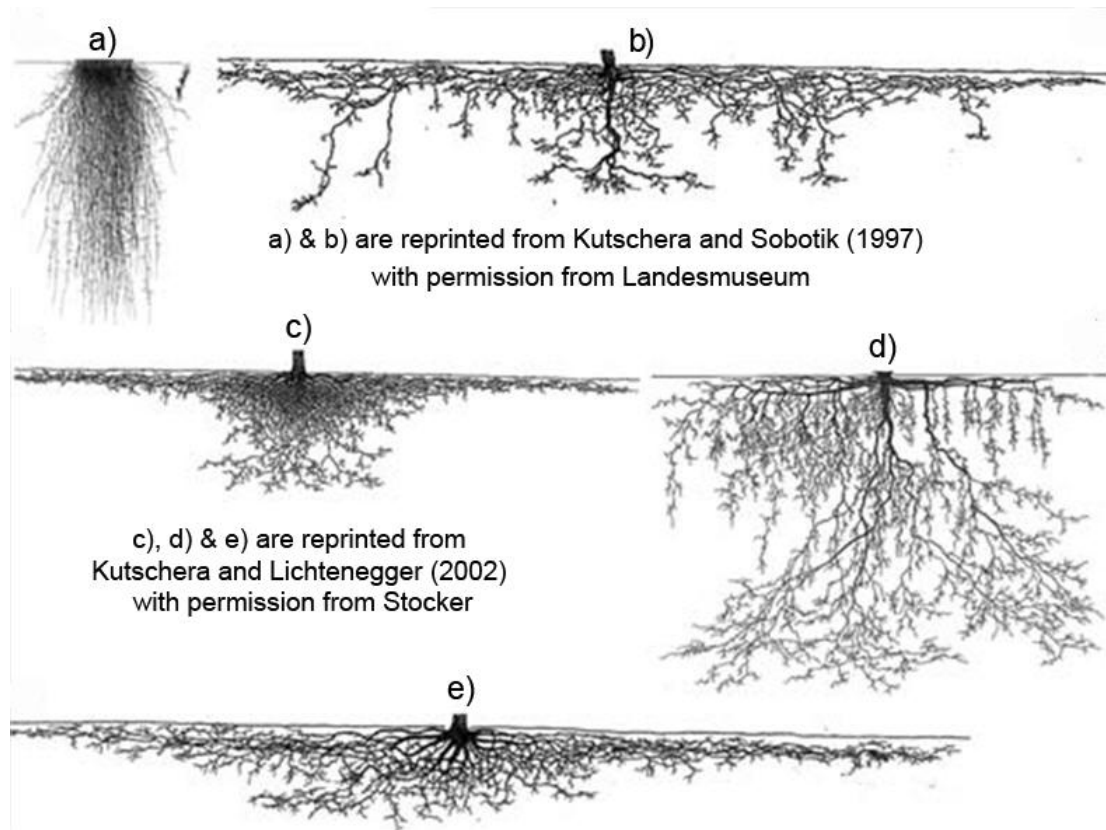


Figure 2-3: Five basic types of root systems modified from (Ghestem, Sidle, & Stokes, 2011). (a) Bunch of grass root systems. (b) Tap-root system. (c) Heart shaped root system. (d) Root system with a large tap-root and large horizontal lateral roots from which emerge vertical sinkers. (e) Plate-shaped root system.

2.3.1.2. *Depth and distribution of root system*

Deeply penetrating vertical taproots and sinker roots provide the main contribution to the stability of slope vis-à-vis resistance to shallow sliding. The mechanical resistant against sliding only extends as far as the depth of root penetration. In addition, the roots must penetrate across the failure surface to have a significant effect. The influence of root reinforcement and restraint for different slope stratigraphy and condition is summarized in Figure 2-4.

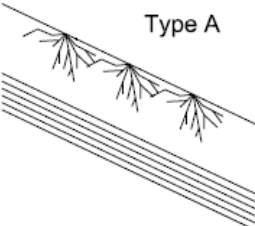
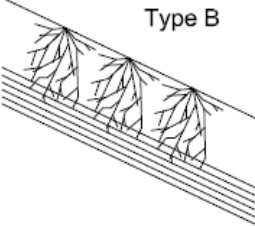
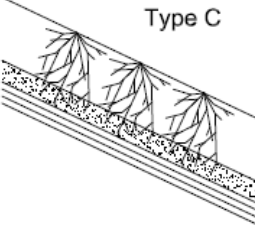
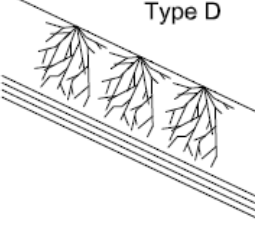
<u>Slope Type</u>	<u>Description</u>	<u>Stability effect of roots</u>
 <p>Type A</p> <p>Soil</p> <p>Bedrock</p>	<p>A. Relatively thin soil mantle, fully reinforced with tree roots, underlain by massive bedrock that is impenetrable to roots</p>	<p>Slight. plane of weakness occurs at bedrock</p>
 <p>Type B</p>	<p>B. Similar to type A, except bedrock contains discontinuities (fractures) which are penetrated by roots; trunks can act as restraint piles.</p>	<p>Major</p>
 <p>Type C</p> <p>Transition layer</p>	<p>C. Thicker soil mantle containing a transition layer with soil density & shear strength increasing w/ depth. Roots that penetrate the transition layer stabilize the slope.</p>	<p>Substantial</p>
 <p>Type D</p>	<p>D. Thick soil mantle extends below the root zone; roots may effect hydrologic regime but do not penetrate across deep seated failure surfaces.</p>	<p>Minor. little effect on deep seated stability</p>

Figure 2-4: Influence of slope stratigraphy on the stabilizing effect of roots against slope failure (Gray & Sotir, 1996)

2.3.2. Root reinforcement measurement

The study method which used to measure the direct contribution of root reinforcement to soil shear strength were reported by (Endo & Tsuruta, 1969; O'Loughlin, 1974; Tien. H. Wu, Bettadapura, & Beal, 1988; Robert R Ziemer, 1981) with using the in situ tests; and (Waldron, 1977; Waldron & Dakessian, 1981) by using laboratory tests. It is generally accepted from these studies that the increase in soil

strength is a measure of increased apparent cohesion and that this increases as the root quantity across the shear zone increases.

The tensile strength of roots varies enormously not only between species but also within species growing at different locations (Greenway, 1987). It generally reduces with increasing root diameter, leading to claims that the finest roots have the potential to contribute most to soil reinforcement (Burroughs & Thomas, 1977; O'Loughlin & Watson, 1979). This is also probably due to the fact that smaller roots are more likely to be located at the margins of a root system where instability is more likely to occur; and because they are the first to decay upon death of the tree, resulting in a bigger influence on slope stability after clear-cutting. The strength of small roots is much easier to measure than for larger roots, which is the most probable reason that no studies can be identified that measure the influence of large roots (> 4 cm) on soil shear resistance.

While most root reinforcement investigations have focused on an increase in soil shear strength, Zhou *et al.* (1997) studied the traction effect of lateral roots of *Pinus yunnanensis* by direct *in-situ* test in the Hutiaoxia Gorge, Southwest China. In contrast to the effect of vertically-extending roots, the traction effect reinforces the soil not by increasing shear strength, but by enhancing the tensile strength of the rooted soil zone. It was found that the traction effect of the roots increased the tensile strength of the shallow rooted soil by 4.2~5.6 kPa. The results of this study indicate that together with the pine's vertical roots, which may potentially anchor the shallow rooted soil zone to a more stable substrate, the lateral roots through a traction effect, are able to mitigate against shallow instability in forested slopes.

2.4 Principle of soil bioengineering

The nature of Bioengineering and its empathy and response to local conditions requires that each area or project be assessed individually. A Bioengineering solution cannot simply be transferred from one Geo-ecosystem to the next. This means that rather than transferring techniques, what should be transferred from area to area are

the principles which an engineer should follow in order to develop a Bioengineering strategy applicable to the conditions where he/she is working. When using soil Bioengineering and biotechnical stabilization practices on the slopes, consider a partnership among many disciplines, including soil scientists, hydrologists, botanists, engineering geologists, maintenance personnel, civil engineers, and landscape architects. The following basic concepts will aid in selection of soil Bioengineering and biotechnical treatments:

- Fit the system to the site. Consider topography, geology, soils, vegetation, and hydrology. Avoid extensive grading and earthwork in critical areas.
- Test soils to determine if amendments are necessary.
- Use on-site vegetation whenever possible.
- Limit the amount of disturbed areas at each site. Any materials removed from the site are to be kept on site and reused if possible.
- Clear sites during times of low precipitation.
- Stockpile or protect the topsoil and reuse during planting.
- Utilize temporary erosion and sediment control measures.

2.5 Limitations of Soil bioengineering

(Menashe, 2001) said an effective cover of vegetation on a slope are may not be established if the undisturbed mature native vegetation are weak and cannot provide erosion control and slope stabilization benefits on slope surface. Soil bio-engineering, likewise, is not appropriate for all sites and situation. In certain case, a conventional vegetation treatment, for example, grass seeds and hydro mulching, works satisfactorily at less cost. In another case, the more appropriate and most effective solution is a structural retaining system alone or possibly in combination with soil Bioengineering. Biotechnical stabilization differs in significant respects from conventional approaches to slope protection and repair, provides important advantages. These advantages notwithstanding, biotechnical stabilization should not be viewed as a panacea for all slope failure and surface erosion problems.

Vegetation is inappropriate, for example, where highly toxic conditions exist or in sites subjected to high water velocity or extreme wave action (Gray & Sotir, 1996).

2.6 The Soil-bioengineering Design

Soil Bioengineering design methods range from installations that merely resist erosion to systems which provide slope stabilizing reinforcement and drainage through the strategic establishment of vegetation. Some examples of the numerous established techniques are live staking, live poles, fascines, brush layers, vegetative Geo-grids, branch packing, vegetated crib walls, live slope grating, wattle fences, furrow planting, and vegetated gabions. To select the vegetation for the slope stability, it depends on hydrological condition of the slope area such as: soil properties, evaporation rate, temperature, and rainfall intensity. Common vegetation used as slope cover is vetiver grass by (H. Rahardjo et al., 2012).

2.6.1. Vetiver system

The Vetiver system is an application system, which is used based on the Vetiver grass. Due to Vetiver grass extraordinary characteristic, Vetiver system now is known as Bioengineering technique for steep slope stabilization, wastewater disposal, and also the environmental protection purpose. Vetiver system is a very simple, inexpensive, practical, low and easy maintenance and very effective means of soil and water conservation, land stabilization and rehabilitation, and sediment control (Truong, Van, & Pinnars, 2008). When the Vetiver grass is planted into the soil, it will form as a hedge which is a very effective in decreasing the speed of running off water, reducing soil erosion, and conserving soil moisture. In addition, it has the extremely deep and massively thick root system (Fig. 2.5) which is very fast growing and can be dislodged under high velocity water flows and it is highly suitable for steep slope stabilization.



Figure 2-5: Vetiver root in soil (left and middle), in water (right) (Truong et al., 2008)

2.6.2. Tensile and Shear Strength of Vetiver root

The tensile strength of Vetiver roots increases with the reduction in root diameters. The fine roots are provided the greater resistance than thicker roots. Work by (Truong et al., 2008) illustrates that the tensile strength of Vetiver root is between 40-120 MPa in the range of root diameter 0.2-2.2 mm (Fig 2.6 and Table 2-1). And between 0.7-0.8 mm root diameter, the means of design tensile strength is about 75 MPa, which is equal to one sixth of mild steel approximately. Therefore, Vetiver roots are as strong, even stronger than the hardwood species that have been proven positive for slope reinforcement.

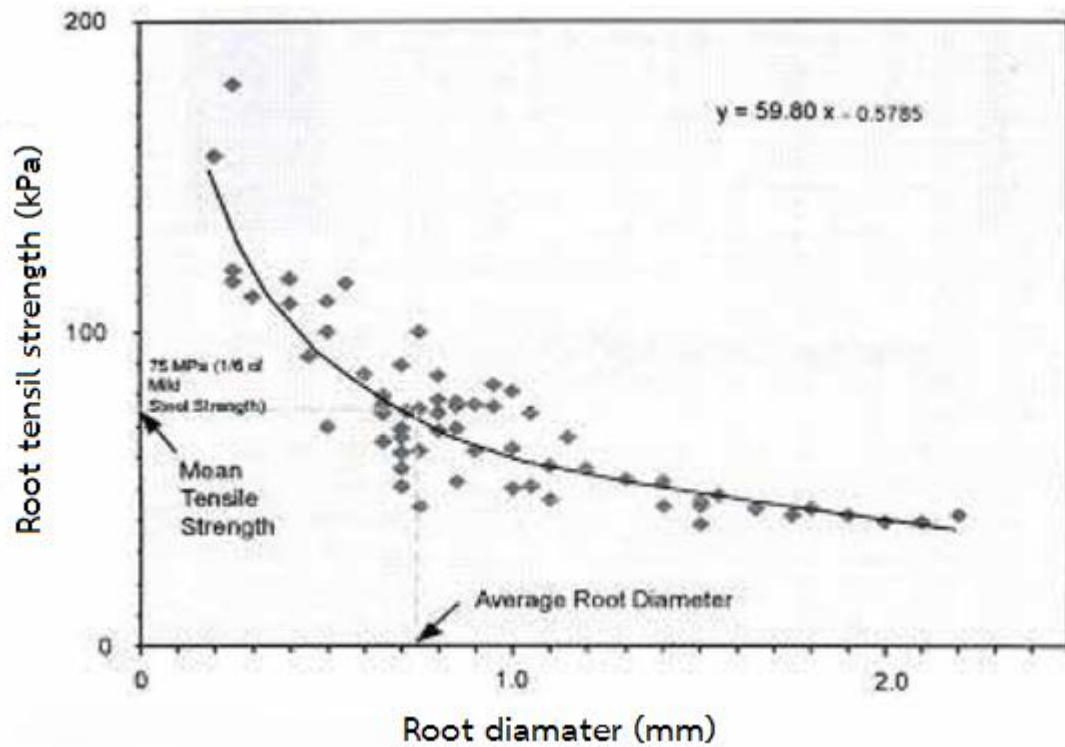


Figure 2-6: Root diameter distribution (Truong et al., 2008)

Table 2-1: Strength of some plants root (Truong et al., 2008)

Name of Vegetation	Tensile Strength (MPa)
Willow	9-36
Poplars	5-38
Alders	4-74
Douglas fir	19-61
Silver maple	15-30
Western hemlock	27
Huckleberry	16
Barley grass	15-31
Forbs moss	2-20
Vetiver grass	40-120 (average 75)

2.7 Unsaturated soil mechanics

Pioneers of unsaturated soil mechanics called upon that certain Geotechnical engineering problems may be analyzed with more knowledge and understanding of the unsaturated soil behavior. Identification of the primary needs and difficulties in the discipline which needs to be addressed were stated as follows (D.G. Fredlund & Rahardjo, 1993): (1) Negative pore-water pressure measurement which may either be direct or indirect. (2) Integration of SWCC information. It is important to collect data for diverse kinds of soils. (3) Simplification of formulas for distinct and various unsaturated soil problems. (4) Documentation of case histories involving unsaturated soil behavior. (W Mairiang, Jotisankasa, & Soralump, 2011) called upon pertinent application of suitable technology for unsaturated soil mechanics such as rainfall-induced landslide, dam engineering and other volume change problems in Thailand. The research called upon further adaptive study and application of Unsaturated Soil Mechanics not only in Thailand but also for South-East Asian countries; to provide cost-effective and appropriate technology to achieve a better understanding of the subject matter in their own respective circumstances. The majority of the landslides were induced by rainfall events occur in the unsaturated zones of the slope area. In unsaturated soils, four phases in equilibrium are defining the system: the soil particle, the contractile skin, and the phases of air and water. In each phase, the measurable stresses (σ , u_a and u_w) at equilibrium are formulated in equilibrium under the context of continuum mechanics. (D. G. Fredlund & Morgenstern, 1977), defined the stress state in an unsaturated soil by using two independent stress tensors. The formulations are presented. Four main concepts are reviewed in detail: the stress state variables and the transient flow in unsaturated soils; the matric suction and the soil–water characteristic curve.

2.7.1. Stress state variables

(Terzaghi et al., 1943), introduced terms to understand the unsaturated soil behavior. His works were focused on saturated soil for which he defined the concept of

“effective stress variable” as the most important variable or “effective” variable to define the state of stress in such soil. The effective stress is defined as:

$$\sigma' = \sigma - u_w \quad (2-3)$$

Where: σ' = Effective stress; σ = total stress; and u_w = pore water pressure.

After Terzaghi, several researchers attempted to express the stress state of unsaturated soils. In the 1950's, Bishop, introduced the pore air pressure as an independent and measurable variable in order to define the effective stress in unsaturated soils (Alan Wilfred Bishop, 1960). Bishop proposed the following expression to estimate the effective stress.

$$\sigma' = (\sigma - u_a) + \chi(u_a - u_w) \quad (2-4)$$

Where: σ' = Effective stress; σ = total stress; u_a = pore air pressure; u_w = pore water pressure; and χ = parameter related to the degree of saturation.

Two stress state variables are required to describe the behaviour of unsaturated soil (D. G. Fredlund & Morgenstern, 1977): net normal stress ($\sigma - u_a$), and matric suction ($u_a - u_w$). Relationships between shear strength or volume change with stress state variables are expressed as constitutive equations. All constitutive equations used to describe the mechanical behaviour of unsaturated soils can be presented as an extension of the equations used for saturated soils. The constitutive equations for unsaturated soils show a smooth transition to the constitutive equations for saturated soils when the degree of saturation approaches 100% or matric suction goes to zero.

2.7.2. Suction in unsaturated soil

Unsaturated soil or soils with negative pore-water pressure can be occurred in essentially any geological deposit. On soil cover with vegetation, as the soil, water moves into the roots and through the plants, the negative pressure or suction is

applied by the roots to the soil through a decrease of soil water potential. Moreover, the negative pore-water pressure (or matric suction) in unsaturated soil has been influenced by the flux boundary condition changes (infiltration, evaporation and transpiration) these changes came up from the climatic conditions. On the other hand, a better understanding of shear strength of the soil has increased due to the development of negative pore-water pressure. The soil Water Characteristic Curve (SWCC) is the relationship between water content and suction for the soil. Proper and accurate characterization is required since it has been a basis for prediction of other unsaturated soil properties such as hydraulic conductivity and shear-strength. SWCC has become essential in application of unsaturated soil mechanic in Geotechnical engineering (Delwyn G Fredlund, Sheng, & Zhao, 2011; Delwyn G Fredlund & Xing, 1994). SWCC and permeability function are the main parameters for seepage analysis.

Suction between the soil grains affects different aspects of the soil behaviour and plays a major role in the volumetric and mechanical responses of a soil element. Unbalanced intermolecular forces are experienced by a water molecule at the interface of the air and water which leads to a “tensile pull” along the interface (Fig. 2.7a)). This tensile pull is known as surface tension and is temperature dependent. The water molecules, which are connected by the surface tension, form a membrane along the interface. The pressure on the water side is lower than the air pressure, therefore a concave shape form at the interface. The radius of the membrane curvature is related to the radius of the container (pores in the soil) and the contact angle. The contact angle is a function of the soil grain material. The geometry of the membrane governs the pressure difference between both sides. This pressure difference is determined based on the force equilibrium in vertical direction:

$$u_a - u_w = \left(\frac{2T_s \times \cos \alpha}{R} \right) \quad (2-5)$$

where, T_s is the surface tension, u_a is the air pressure, u_w is the water pressure and α is the contact angle of the membrane to the container wall (soil grains).

The value of $(u_a - u_w)$ in the soil pores is called matric suction, and the equation implies that smaller meniscus radii correspond to higher values of matric suction and vice versa. Accordingly, higher values of suction develop in soils with smaller pores and/or less water content (Fig. 2.7b)).

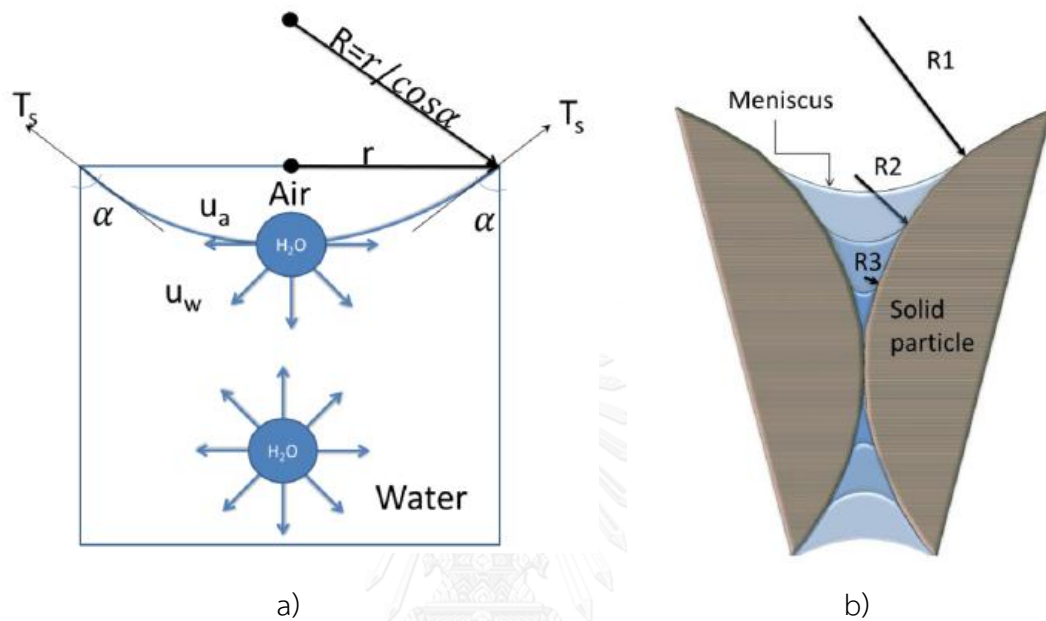


Figure 2-7: a) Development of surface tension at the interface of the water and air, b) Changes in the radius of the meniscus with water content (Askarinejad, 2013)

2.7.3. Transient flow in unsaturated soil

The moisture flow can be analyzed in terms of energy or “head” when water–air flows from a point of high energy to a point of low energy. This energy gradient is known as “hydraulic head gradient”. The behavior of the moisture flow is described under the principles of Bernoulli and Darcy. These principles apply equally for both saturated and unsaturated soils. Bernoulli’s law considers the total energy or head as the sum of three heads: velocity head, pressure head and the position head. In Geotechnical practice, the velocity head is very low when compared with pressure head and position head (D.G. Fredlund & Rahardjo, 1993). The pressure head (p/γ_w) suction is made of two components: matric suction and osmotic suction. Therefore, the pressure head and position head, combined, define the hydraulic head gradient

in an unsaturated or saturated soil. Equation 2-5, expresses the hydraulic head gradient, h , at any point in the soil mass.

$$h = \frac{p}{\gamma_w} + H \quad (2-6)$$

Where: p = total suction (matric suction + osmotic suction); γ_w = unit weight of water; and H = position head. .

2.7.4. Hydraulic conductivity function in unsaturated soil

The hydraulic conductivity of a soil reduces with decrease of the water content and the relationship between the degree of saturation (or water content or suction) and hydraulic conductivity is defined as the hydraulic conductivity function. An example of relative hydraulic conductivity functions for clay and sand is shown in Figure 2-8. K_r is this figure is the ratio between the unsaturated hydraulic conductivity to the saturated one ($K_r = K_{\text{unsat}}(s)/K_{\text{sat}}$).

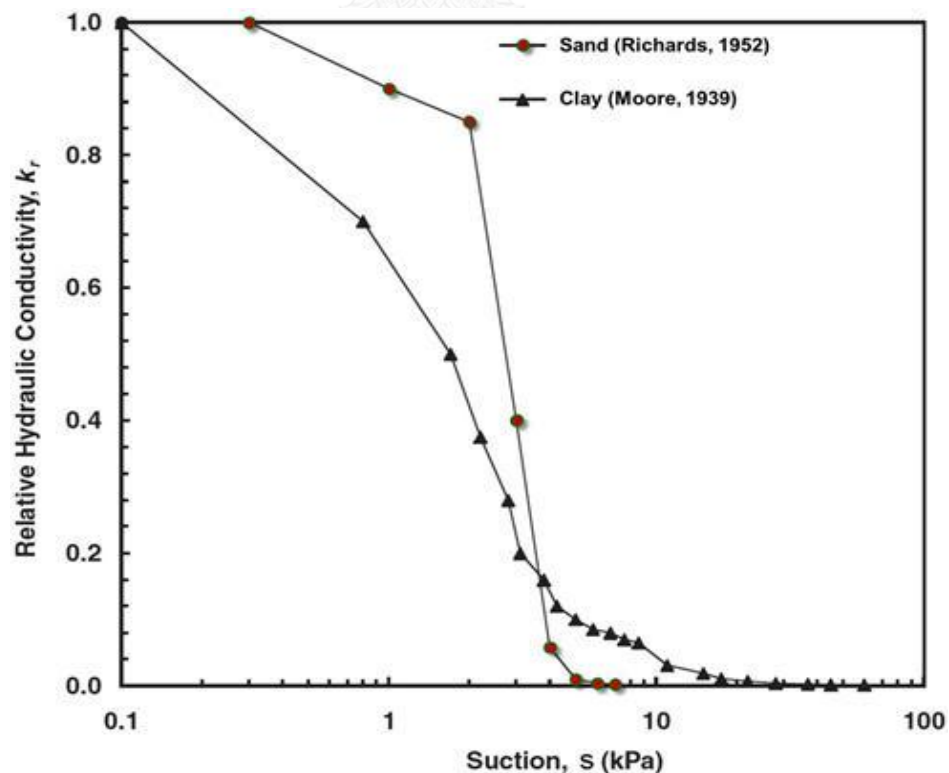


Figure 2-8: Relative hydraulic conductivity function after (Lu & Likos, 2004)

2.7.5. Soil-Water Characteristic curve

The soil-water characteristic curve is the relationship between water content and suction for the soil and it is usually described by both a drying curve and a wetting curve as shown in Figure 2-9. The value of volumetric water content in this figure is determined from the following equation:

$$\theta = \frac{V_w}{V_t} = S_r \times n \Rightarrow \theta = n \quad (2-7)$$

Where: V_w and V_t are the volume of water and total volume of the soil, respectively. S_r is the degree of saturation ($S_r = V_w/V_v$, where, V_v is the pore volume) and n is the porosity of the soil ($n = V_v/V_t$). The definition of volumetric water content implies that its value at full saturation (θ_s) is equal to the porosity of the material. The residual value of water content (θ_r) represents the situation where water is isolated at the particle contacts and suction attains an infinite asymptote.

The SWCC could be used to represent the relationship between volumetric water content (θ_w) and matric suction which is suggested by (D. Fredlund, Rahardjo, Leong, & Ng, 2001). The requirement of the proper and accurate characterization has been a basis for the prediction of other unsaturated soil properties such as hydraulic conductivity and shear-strength parameters. It has become essential in the application of unsaturated soil mechanics in Geotechnical engineering. (Delwyn G Fredlund et al., 2011; Delwyn G Fredlund & Xing, 1994). Three models were particularly selected from the Equations of the soil-water characteristic curve published by (Delwyn G Fredlund & Xing, 1994) to fit the experimental data the three equations chosen are: the (Brooks & Corey, 1964; van Genuchten, 1980), and (Delwyn G Fredlund & Xing, 1994) models. These equations have already established good correlation for a wide range of suction and various soil types.

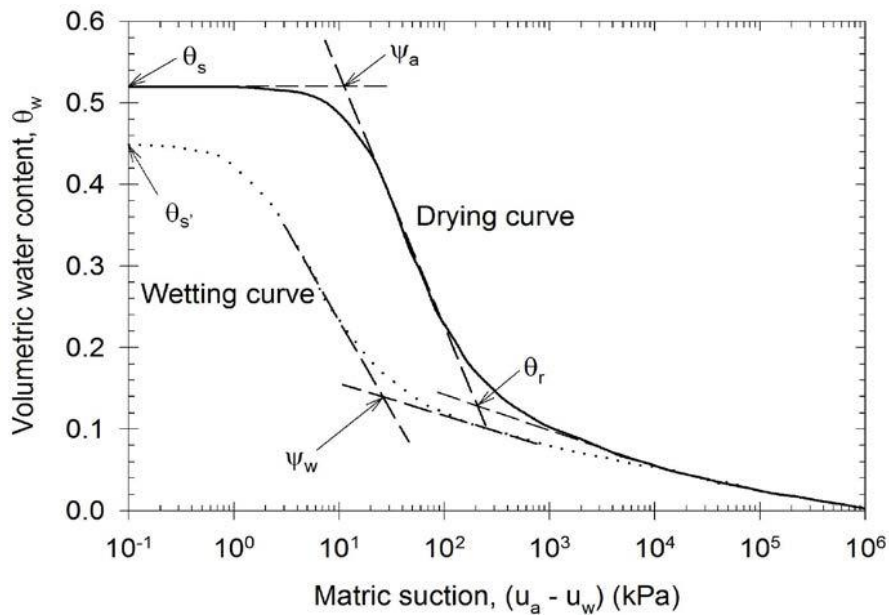


Figure 2-9: Typical chart of soil water characteristic curve (Delwyn G Fredlund, Rahardjo, & Fredlund, 2012)

2.7.5.1. Brooks and Corey estimation

A method to predict the unsaturated coefficient of hydraulic conductivity is proposed by (Brooks & Corey, 1964). The method is based on the fit of the soil–water characteristic curve with the (Brooks & Corey, 1964) equation and the saturated permeability hydraulic conductivity of a soil. The (Brooks & Corey, 1964) equation that is used to best-fit the soil–water characteristic curve data is as follows:

$$\theta = \theta_r + (\theta_s - \theta_r) \left(\frac{\psi_b}{\psi} \right)^\lambda \quad \text{for } \psi \geq \psi_b \quad (2-8)$$

$$\theta = \theta_s \quad \text{for } \psi < \psi_b \quad (2-9)$$

where θ is the volumetric water content, θ_s the saturated volumetric water content, θ_r the residual volumetric water content, ψ the soil suction (kPa), ψ_b the curve fitting parameter (air-entry value) (kPa), and λ the fitting parameter (pore-size distribution index).

2.7.5.2. Van Genuchten estimation

Since the Brooks and Corey (1964) equation does not converge rapidly when used in numerical simulations of seepage in saturated–unsaturated soils, (van Genuchten, 1980) proposed a closed-form equation to estimate the hydraulic conductivity that may be used for the flow modelling of saturated–unsaturated soils. (van Genuchten, 1980) proposed a method based on the saturated hydraulic conductivity and fitting of soil–water characteristic data by the (van Genuchten, 1980) equation. Equation (2-10) presents the equations proposed by (van Genuchten, 1980) for the soil–water characteristics and the hydraulic conductivity, respectively, of unsaturated soils.

$$\theta = \theta_r + \frac{(\theta_s - \theta_r)}{\left[1 + (\alpha\psi^n)\right]^m} \quad (2-10)$$

where θ is the volumetric water content, θ_s the saturated volumetric water content, θ_r the residual volumetric water content, ψ the soil suction (kPa), α and n are the curve fitting parameters, and $m = 1-1/n$.

2.7.5.3. Fredlund's estimation

A method to estimate the hydraulic conductivity of a soil as a function of soil suction is presented by (Delwyn G Fredlund & Xing, 1994). The method describe the soil–water characteristic curve by using the approach of (Delwyn G Fredlund & Xing, 1994) and basing on saturated hydraulic conductivity. (Delwyn G Fredlund & Xing, 1994) proposed the equation (2-11) to fit soil–water characteristic data. The integration in equation (2-11) is complex and a closed-form solution is not available. Therefore, in numerical software, such as Soil Vision (2006), seep/W (2004), and vadose/W (2004), Simpson's rule is generally used to integrate equation (2-11).

$$\theta = \left\{ 1 - \frac{\ln\left(1 + \frac{\psi}{\psi_r}\right)}{\ln\left(1 + \frac{10^6}{\psi_r}\right)} \right\} \left\{ \frac{\theta_s}{\ln\left[e + \left(\frac{\psi}{a}\right)^n\right]^m} \right\} \quad (2-11)$$

where θ is the volumetric water content, θ_s the saturated volumetric water content, θ_r the residual volumetric water content, ψ the soil suction (kPa), $e = a$ a natural number (2.71828...), and $a, m, n =$ fitting parameters (Parameter a has the unit of pressure (kPa)).

2.8 Vegetation and slope Stability Analysis

The link between vegetation and slope stability has been examined by a number of investigators, who have established a strong cause and effect relationship ascribing a decrease in slope stability with loss of root reinforcement due to clear-cutting and timber harvesting. (D. M. Bishop & Stevens, 1964) is reported within ten years for the increasing in the number of shallow landslides by following clear-cutting. This accelerated slope failure occurrence was principally attributed to the destruction and gradual decay of the interconnected root system. A finding reiterated by (Swanston, 1970, 1974), (O'Loughlin, 1974), (Tien H Wu, 1976), (R. R. Ziemer & Swanston, 1977), (Tien H Wu et al., 1979), (TIEN H Wu & Swanston, 1980), and (Robert R Ziemer, 1981) in similar studies undertaken in North America. The level of reinforcement attributed to tree roots depends, however on the specific hydrologic, slope, soil-mantle, and plant conditions present at any given site. To examine the effect of vegetation on slope stability various analytical methods have been modified to include vegetative factors. These factors include: a) the increased effective soil cohesion due to root reinforcement, b) soil suction resulting from evapotranspiration or a decrease in pore water pressure, c) an increased surcharge due to the weight of vegetation, d) an increased disturbing force due to wind-throw, and e) an increased restoring force due to large diameter inclined roots acting as discrete tensile elements (Coppin & Richards, 1990). Not all factors contribute significantly in every analysis. This will depend on the prevailing conditions within a particular environment. The particular model chosen will also depend on actual on-site conditions. A brief review of general slope stability models that incorporate vegetative effects is presented in the following section.

2.8.1. The influence of vegetation on slope stability

The protective roles of vegetation on the slope stability have gained increasing recognition and provide a good summary of the hydro mechanical influences of vegetation as related to slope stability. It depicts the benefits and limitations that must be considered when choosing a soil Bioengineering method and when analyzing the stability. Vegetation may have an overall stabilizing or destabilizing effect on the slope and this can change over time due to seasonal variances and other perceivable factors. The main beneficial effects of woody vegetation on the mass stability of slope are listed in Table 2-2:

Table 2-2: Influence of vegetation on soil slope (Coppin & Richards, 1990)

Surface	Depth
Protection against wind erosion	Increase water infiltration
Protection against foot traffic	Water up take by roots
Protection against raindrop impact	Reinforcement of soil by roots
Protection of surface water runoff	Anchoring and buttressing by taproots
Protection against erosion by surface water flow	
Interception of rainfall	

2.8.2. Slope stability analysis

Normally, slope stability analysis is performed to define the safety of the natural slope, excavations, embankments, earth dams and landfills, etc. The ability to quantify the stability of earthen slopes is of paramount importance to the Geotechnical engineer. Stability problems involving shallow movement are typically analyzed using limit equilibrium approaches like infinite slope models or the many circular or non-circular analysis methods.

2.8.2.1. *Limit equilibrium method*

In practice, the stability of a slope is usually assessed using limit equilibrium methods. Stability analysis using the limit equilibrium approach involves solving the equilibrium problem by assuming force and/or moment equilibrium. Over the years, many limit equilibrium methods for slope stability analysis have been developed and applied in practice, including the ordinary method of slices (Fellenius, 1936), Bishop's modified method (A. W. Bishop, 1955), force equilibrium methods (e.g. (Lowe & Karafiath, 1960), Janbu's generalised procedure of slices (Janbu, 1968), Morgenstern and Price's method (Morgenstern & Price, 1965) and Spencer's method (Spencer, 1967). Slope stability charts based on these limit equilibrium methods have also been developed (e.g. (A. Bishop & Morgenstern, 1960); (Spencer, 1967); (Janbu, 1968); which are useful for preliminary analysis and quick estimation of the stability of a slope. However, in practice, detailed slope stability analysis is usually performed using a computer program and most of the available computer programs are based on the limit equilibrium approach. In the conventional limit equilibrium approach, the stability of a slope is measured by a factor of safety (FOS), which is defined as the ratio between the shear strength of the soil to the shear stress required for equilibrium (Duncan, 1996). A slip surface, which can be planar, circular or non-circular in shape, is required to be assumed prior to the equilibrium analysis. At the point of failure the shear strength is assumed to be fully mobilised along the slip surface and FOS is assumed to be constant for the entire slip surface. The stability analysis eventually involves an iterative process until the critical slip surface is found, which the slip surface with the lowest FOS is. Over the years, many studies have been conducted to investigate the computational accuracy of different limit equilibrium methods and to develop techniques for searching the critical slip surface (Duncan, 1996). However, (Duncan, 1996) pointed out that the critical slip surface can be assumed to be circular, in most cases, with little inaccuracy unless there are geological layers that constrain the slip surface with a non-circular shape.

It should be noted that most conventional slope stability analyses are performed within a deterministic framework. This means the input parameters (e.g. shear

strength parameters, pore pressure, etc.) are based on the single best estimate value of the available field or laboratory test data. In most cases, due to limited test data, engineering judgments based on previous experience are required to generate the best estimate for each parameter. As a result, the calculated FOS not only depends on the accuracy of the chosen method of analysis and the assumed failure mode, but also the uncertainty associated with the input parameters and the reliability of judgmental assumptions made in relation to the input parameters. In practice, the uncertainty and variability in soil parameters are traditionally accounted for by adopting a higher FOS. However, the FOS has been proved to be an inadequate tool for quantifying the effects of uncertainty and variability in soil properties (Duncan 2000). Hence, it is readily accepted that more reliable tool to incorporate soil variability and uncertainty into slope stability analysis are required. This has led to the development of probabilistic slope stability analysis in the 1970s (e.g. Wu and Kraft 1970; Alonso 1976; Tang et al. 1976; Vanmarcke 1977b), and this will be discussed later.

2.8.2.2. *Finite element method*

As computer performance has improved, the application of finite element in Geotechnical analysis has become increasingly common. These methods have several advantages: to model slopes with a degree of very high realism (complex geometry, sequences of loading, presence of material for reinforcement, the action of water, laws for complex soil behaviour) and to better visualise the deformations of soils in place. However, it is critical to understand the analysis output due to the large number of variables offered to the engineer. Cases where severe failure has occurred, such as that of the Nicoll Highway, Singapore, highlight the importance of understanding the chosen numerical method and the failure criteria. To analyse slopes, the strength reduction method is applied. For example, the reduction of the cohesion (c) and the tangent of the friction angle ($\tan\phi$) of the soil are defined in this method. The parameters are reduced in steps until the soil mass fails. The study used Oasys Safe, a program for soil analysis by finite elements. When developing the strength reduction methodology to be applied in Safe, a comparison was made

between three differing techniques. For all techniques, an initialisation run for a given slope model was carried out and the strains and displacements obtained in that run set to zero for the subsequent FoS assessment. In the first method, an incremental strength reduction was applied to the elastic Mohr-Coulomb material whereby for each follow-on increment the same reduction in global strength was applied. The second method involved specifying separate, independent model runs with revised material parameters corresponding to specific percentage reductions in material strength. The third method used a new feature in Safe, in which the program automatically applies the same strength reduction in successive analysis increments, but once failure is observed, reverts to the last converged increment and refines the strength reduction to obtain an estimate of FoS to an acceptable accuracy. In this study the failure criterion was set to be displacement-related. Other finite element programs may use different criteria to establish when failure is occurring.

2.8.2.3. *Infinite slope analysis*

The classical “infinite slope” analysis procedure is appropriate for analyzing the stability for shallow, transitional slides. This method is suitable for slopes where the slip surface can be assumed to be parallel to the ground surface and the depth to length ratio of the sliding mass is small. In other words, the infinite slope approach is suitable for the sliding of a long shallow mass of soil. The geometry of the infinite slope simplifies the analysis to that of a single element where the forces acting on the element’s sides are equal, opposite and collinear, and the overall end effects in the sliding mass can be ignored. Because this approach is relatively simple, one may incorporate nearly every conceivable force which may act on a slope. For this reason, the infinite slope analysis can assume many forms and may be analyzed using drained or undrained shear strength parameters provided one is consistent in using each approach with regard to the groundwater conditions; the two basic approaches are (1) total soil unit weight and boundary pore water pressure or (2) buoyant soil unit weight and seepage forces. The infinite slope analysis uses force equilibrium where the ratio of the stabilizing and the destabilizing forces acting on the element are identified and compared to yield a factor of safety. Two examples of the infinite

slope procedure are presented in (Gray & Sotir, 1996); (1) a general form of the infinite slope analysis for determining the factor of safety against sliding for a slope with surcharge and water table, and (2) a modified infinite slope model which accounts for seepage and seepage direction, root contributions to increased soil shear strength or root cohesion, and vertical surcharge.

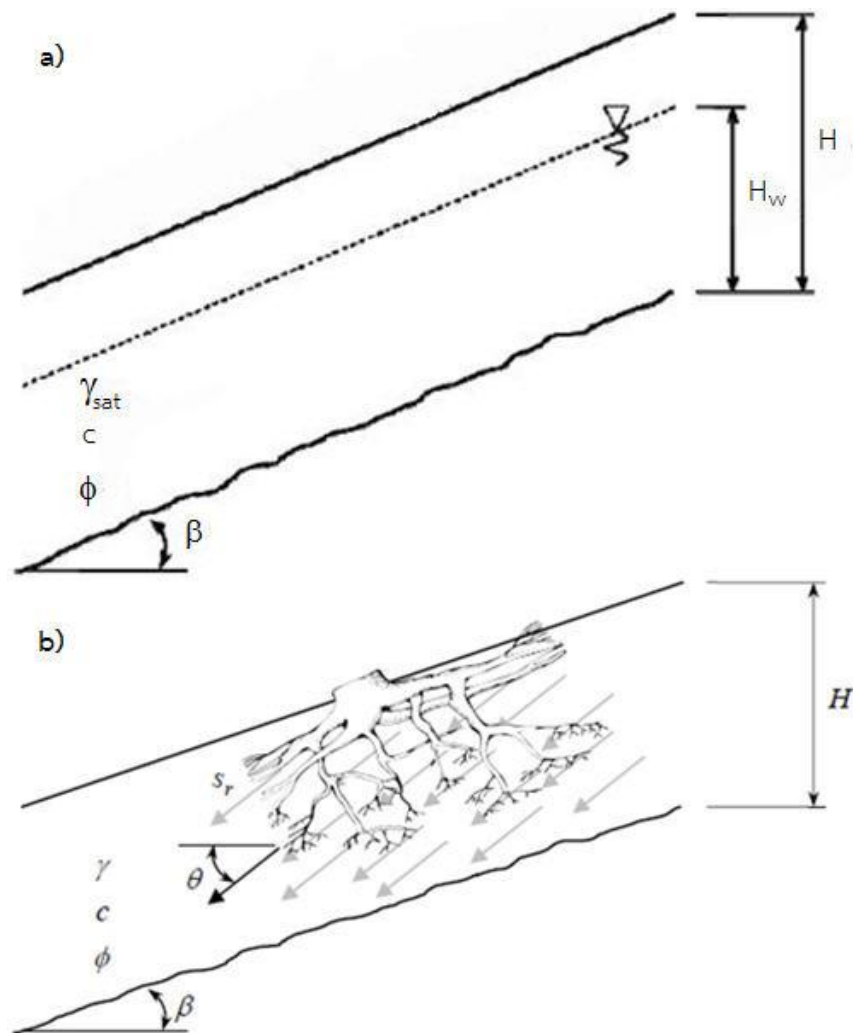


Figure 2-10: Infinite slope: a) without the effect of vegetation roots and b) with the effect of vegetation root modified from (Gray & Sotir, 1996)

The effects of vegetation may be readily incorporated into the infinite slope analysis. The factor of safety for the case where seepage, seepage direction, root cohesion, and no uniform vertical surcharge, are determined by Equation (2-12), and Figure 2-10 shows a schematic representation.

$$FS = A \times \left(\frac{\tan \phi}{\tan \beta} \right) + B \left(\frac{c + S_r}{\gamma H} \right) \quad (2-12)$$

$$A = 1 - \left(\frac{r_u}{\cos^2 \beta} \right); \quad B = \left(\frac{1}{\cos \beta \sin \beta} \right);$$

$$r_u = \frac{H_w}{H} \left(\frac{\gamma_w}{\gamma_t} \right) \cos^2 \beta \quad (\text{Water table parallel the slope surface}) \quad (\text{Fig. 2-10a})$$

$$r_u = \left(\frac{\gamma_w}{\gamma_t + \gamma_t \tan \beta \tan \theta} \right) \quad (\text{Water table not parallel the slope surface}) \quad (\text{Fig. 2-10b})$$

Where:

- β = slope angle of natural ground
- θ = seepage angle (with respect to horizontal)
- ϕ = angle of internal friction
- c = soil cohesion
- S_r = root cohesion
- γ_t = soil density
- γ_w = density of water
- H = vertical thickness (or depth) of sliding surface
- H_w = water table

The root cohesion term, S_r , takes into account the influence of root reinforcement and may be determined based on experience, from published values, or from either laboratory or in situ shear strength tests. This version of the infinite slope analysis also allows the engineer to incorporate the vegetation effect on the soil moisture regime. The moisture content and pore pressure/matric suction at depth within a slope can be accurately measured with instruments such as tensiometers, piezometers, time domain reflectometry (TDR), and porous blocks. The seepage

direction, θ , is determined by identifying pore pressure/matric suction gradients within the slope. Because vegetation removes water from the soil, vegetation will have an effect on the seepage forces as well as soil density, γ_t . For the root cohesion S_r is determined by the equation (2-2).

2.9 Physical modelling in geotechnical centrifuge

The intention of physical modelling is to study the behavior of a given prototype. Physical modelling can be performed as full-scale testing but is often used in a reduced scale. The physical modelling presented in this thesis will be based on a set of centrifuge model tests. Dimensional analysis is used here to deduce dimensional products, which are used to transform model observation to prototype. These non-dimensional products should be identical and scale independent; this implies that a possible diameter effect is neglected. Centrifuge modelling of rainfall induced landslides with controlled material properties, and boundary conditions has the potential to provide an understanding of the triggering mechanisms of landslides due to rainfall. In the centrifuge tests a model is conducted under centrifugal acceleration field with a magnitude of N times the Earth's gravity. The geometry of N times is smaller than the prototype (Schofield, 1980). This process provides a gradient of body stresses within the model similar to the prototype, which ensures similar effective stresses and groundwater pressures at equivalent depths. Seepage dominates the movement of water through the soil during raining over model slopes in centrifuge tests (Kimura, Takemura, Suemasa, & Hiro-Oka, 1991). It has been shown that the seepage velocity in the centrifugal field of Ng is N times that under the Earth's gravitational field, as long as the identical material is used for the model and prototype soil (Goodings, 1985); (Garnier et al., 2007). Since the intensity of rain has the same dimension as the seepage velocity, the intensity of rain in the Ng field is N times that in the Earth's gravitational field. Several failure mechanisms of rainfall induced landslides have been investigated by different researchers using centrifuge modelling. Nowadays, the geotechnical centrifuge is well established among the

geotechnical researcher. It is used for verification of geotechnical design as well as for teaching purpose; to explain the ground deformation and the different failure mechanisms associated with the slope stability, retaining wall or foundation. The basic of centrifuge modeling is to create the stress conditions which would exist in a full-scale construction (prototype), using a model on a greatly reduced scale. It is done by subjecting the model components to an enhanced body force, which is provided by a centripetal acceleration due to the Earth gravity. Stress replication in an N^{th} scale model is achieved when the imposed “gravitational” acceleration is suitable for modeling stress dependent problems. Moreover, reduction of time for model tests such as consolidation time can be achieved by using a reduced size model. By (Oblozinsky & Kuwano, 2004) and (Takemura, Kondoh, Esaki, Kouda, & Kusakabe, 1999); this centrifuge is a beam type centrifuge having a pair of parallel arms that hold platforms on which the model container and a weight for counterbalance are mounted as shown in Figure. 2-11. Radius of rotation is 2.45m, which is the distance from the rotating shaft to the platform base. The surface of the swinging platform is always normal to the resultant acceleration of the centrifugal acceleration, ng , and Earth's gravity.

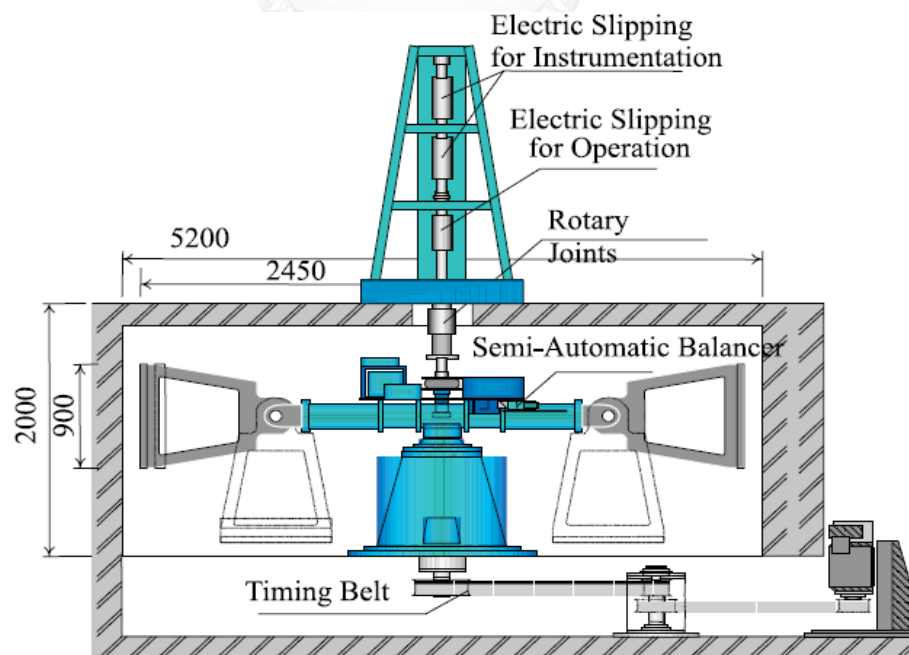


Figure 2-11: Centrifuge apparatus at TIT (Oblozinsky & Kuwano, 2004)

For the centrifuge model tests, the model laws are generally derived through dimensional analysis, from the governing equations for a phenomenon, or from the principle of mechanical similarity between a model and a prototype. Some commonly used scaling laws are summarized in Table 2-3. Modeling of geotechnical earthquake problems in centrifuge has significantly grown since last few decades as it enables the study and analysis of design problems (Taylor, 2003). Physical modeling replicates the properties, dimension and in situ stresses change with depth, i.e. stress history of the prototype scale. The technique involves testing scale models in the increased g environment of a geotechnical centrifuge. A centrifugal in geotechnical is a tool which uses to conduct model tests to study geotechnical issue such as the strength, stiffness and capacity of foundations for bridges and buildings, settlement of embankments, slope stability, retaining structures, tunnel stability and seawalls. The centrifuge is probably useful for scale modeling of any large-scale nonlinear problem for which gravity is a primary driving force.

2.9.1. Scaling laws

The scaling laws described by (Schofield, 1981) for centrifuge modeling is summarized in Table 2-3. The main principle in centrifuge modeling is that a $1/N$ scale model placed at the end of a centrifuge arm subjected to a gravitational acceleration of $N g$ will feel the same stresses as the prototype. For instance, if a ground surface of 50 m depth has to be modeled. The 1 m deep model container is filled with soil, placed on the end of a centrifuge and subject to a centrifugal acceleration of 50 g . The pressures and stresses are increased by a factor of 50. So, the vertical stress at the base of the model container is equivalent to the vertical stress at a depth of 50 m below the ground surface on earth. Thus the 1 m deep model represents 50 m of prototype soil. The reason for the centrifuge is to enable small scale models to feel the same stresses as a full scale prototype. The stress would be 50 times smaller if it is measure under gravity. The scaling laws allow stresses and strains in model and prototype structures to be identical and hence true prototype behavior is observed in the model as shown in Figure 2-12.

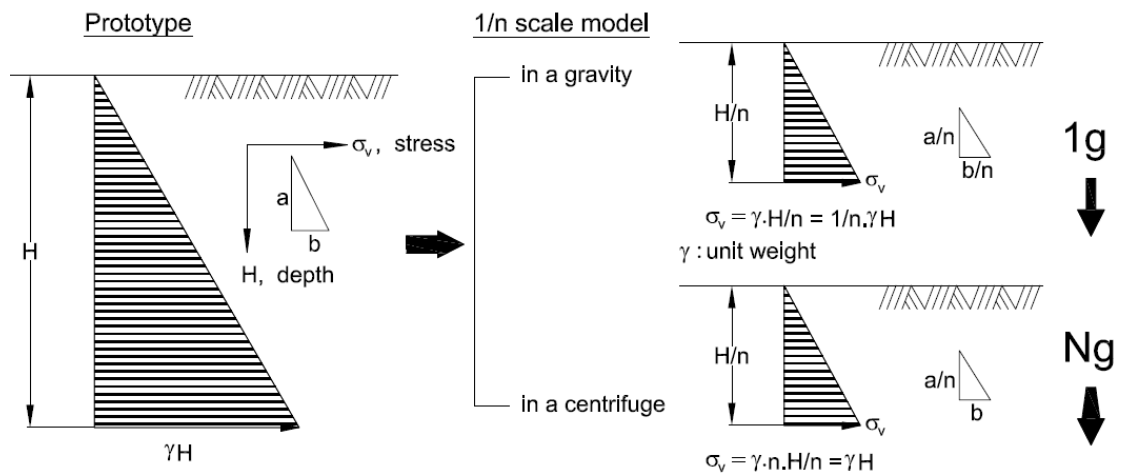


Figure 2-12: Principle of Centrifuge Modeling (Schofield, 1981)

Table 2-3: Some common for centrifugal scaling test

Parameters	Scale (model/prototype)
Acceleration	N
Linear dimension	$1/N$
Area dimension	$1/N^2$
Volume dimension	$1/N^3$
Stress	1
Strain	1
Mass	$1/N^3$
Density	1
Unit weight	N
Force	$1/N^2$
Bending moment	$1/N^3$
Bending moment / unit width	$1/N^2$
Time (consolidation / diffusion)	$1/N^2$
Pore fluid velocity	N
Concentration	1
Velocity (dynamic)	1

The testing of centrifuge apparatus is going to generate for controlling the model slope failure with the root system properties to determine the reinforcing effect of the roots. In a single geometry of a 30° slope with a 2.5 to 3 m height will select for modeling in each test. During the centrifuge test, the slope will provide the water as the rainfall to raise the inner water level within the soil to let the slope failure.

2.9.2. Apparatus test

The centrifuge apparatus of Tokyo Institute of Technology is used for this study. The soil slope model will spin in the soil chamber within dimension of 900 mm x 900 mm x 970 mm. A beam centrifuge apparatus as shown in Figure 2-13 consists of a beam with two swing platform attached on the each end of beam. As the beam rotate around the supporting column in horizontal level the swing platform are lifted under the action of the centrifugal force. Model placed on the swing platform is subjected to the centrifugal force acting like an artificial gravity field. The specifications of the centrifuge are summarized in Table 2-4.

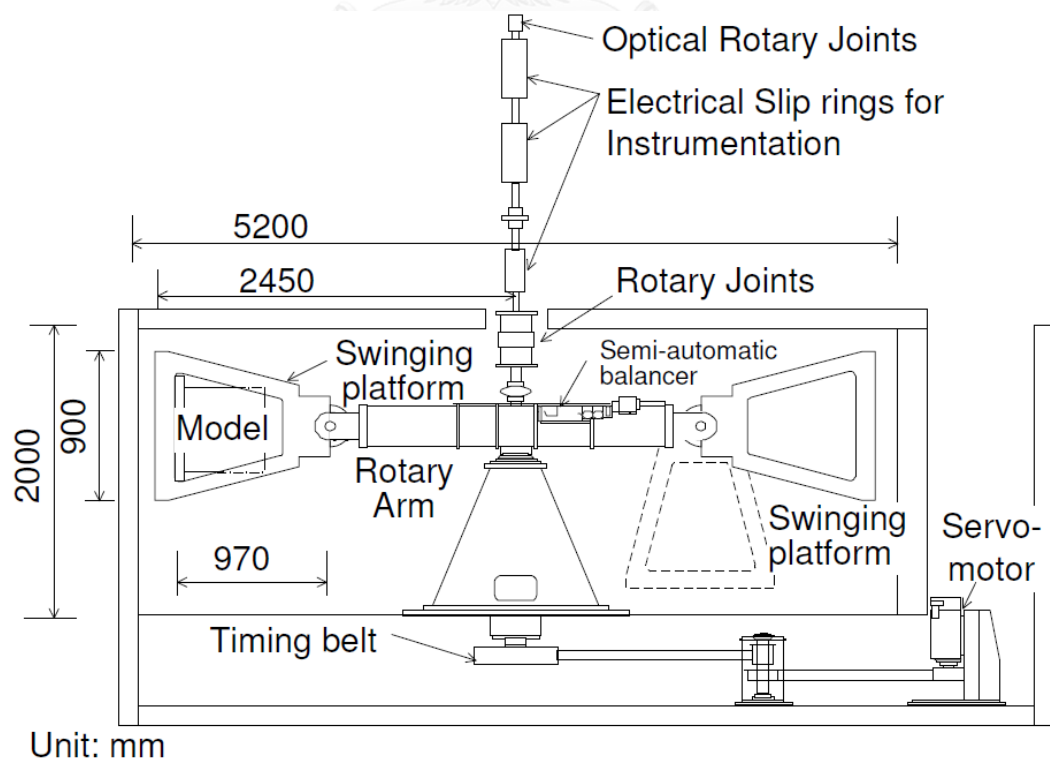


Figure 2-13: Section view of centrifuge apparatus at TIT (Akihiro Takahashi, 2002)

Table 2-4: Specification of centrifugal apparatus (Akihiro Takahashi, 2002)

Radius	Platform radius	2.45	m
	Effective radius	2.0-2.2	m
Platform dimensions	Width	900	mm
	Depth	900	mm
	Maximum height	970	mm
Capacity	Maximum payload	50	g.ton
	Maximum number of rotation	300	rpm
	Maximum payload at 80g	600	kg
Electrical slip rings	For instrumentation	72	Channels
	For operation	20	Channels
Optical rotary joint	Number of sports	4	-
Rotary joint	Number of sports for air and water	2	-
	Working pressure for air and water	1	MPa
	Number of sports for oil	2	-
	Working pressure for oil	21	MPa

2.10 Numerical modelling for slope stability in Geo-studio

Geostudio software is one of geotechnical program that is based on the finite element and can do analysis such as, stress-strain, seepage, slope stability, dynamic analysis. Modeling has been a useful tool for engineering design and analysis. The definition of modeling may vary depending on the application, but the basic concept remains the same: the process of solving physical problems by appropriate

simplification of reality. In engineering, modeling is divided into two major parts: physical/empirical modeling and theoretical/analytical modeling. Laboratory and in situ model tests are examples of physical modeling, from which engineers and scientists obtain useful information to develop empirical or semi-empirical algorithms for tangible application. Theoretical modeling usually consists of four steps. The first step is construction of a mathematical model for corresponding physical problems with appropriate assumptions. This model may take the form of differential or algebraic equations. In most engineering cases, these mathematical models cannot be solved analytically, requiring a numerical solution. The second step is development of an appropriate numerical model or approximation to the mathematical model. The numerical model usually needs to be carefully calibrated and validated against pre-existing data and analytical results. Error analysis of the numerical model is also required in this step. The third step of theoretical modeling is actual implementation of the numerical model to obtain solutions. The fourth step is interpretation of the numerical results in graphics, charts, tables, or other convenient forms, to support engineering design and operation.

With the increase in computational technology, many numerical models and software programs have been developed for various engineering practices. Numerical modeling has been used extensively in industries for both forward problems and inverse problems. Forward problems include simulation of space shuttle flight, ground water flow, material strength, earthquakes, and molecular and medication formulae studies. Inverse problems consist of non-destructive evaluation (NDE), tomography, source location, image processing, and structure deformation during loading tests. Although numerical models enable engineers to solve problems, the potential for abuse and misinformation persists. Colorful impressive graphic presentation of a sophisticated software package does not necessarily provide accurate numerical results.

Fundamental scientific studies and thorough understanding of the physical phenomena provide a reliable and solid guideline for engineering modeling. In this project, the focus is on the thermo effects of drilled shafts after the placement of

concrete, and performance under various loading conditions. The numerical models developed in this project are based on well-developed theories and constitutive laws in chemical and civil engineering, as well as numerical methods widely accepted in engineering. The numerical results are also carefully analyzed against existing laboratory test data.

2.10.1. Slope/W

In this part explains the theory that used to develop the slope/W. A brief description of the General Limit Equilibrium method (GLE) with using some variables is first defined in here. The relevant equations are derived, including the base normal force equation and the factor of safety equations. This is followed by a section describing the iterative procedure adopted to solve the factor safety in nonlinear equations. Attention is then given to aspects of the theory related to soils with negative pore-water pressures. Slope/W solves two factors of safety equations; one equation satisfies force equilibrium and the other satisfies moment equilibrium. All the commonly used methods of slices can be visualized as special cases of the General Limit Equilibrium (GLE) solution. The theory of the Finite Element Stress method is presented as an alternative to the limit equilibrium stability analysis. This method computes the stability factor of a slope based on the stress state in the soil obtained from a finite element stress analysis. Finally, the theory of probabilistic slope stability using the Monte Carlo method is also presented.

Slope/W uses the theory of limit equilibrium of forces and moments to compute the factor of safety against failure. The General Limit Equilibrium (GLE) theory is presented and used as the context for relating the factors of safety for all commonly used methods of slices. A factor of safety is defined as that factor by which the shear strength of the soil must be reduced in order to bring the mass of soil into a state of limiting equilibrium along a selected slip surface.

For an effective stress analysis, the shear strength is defined as:

$$s = c' + (\sigma_n - u) \tan \phi' \quad (2-13)$$

Where: s is shear strength; c' is effective cohesion; ϕ' is internal friction angle; σ_n is total normal stress; u is pore water pressure.

2.10.1.1. General limit equilibrium method

The General Limit Equilibrium method (GLE) uses the following equations of statics in solving for the factor of safety: (1) the summation of forces in a vertical direction for each slice is used to compute the normal force at the base of the slice, N . (2) the summation of forces in a horizontal direction for each slice is used to compute the inter-slice normal force, E . This equation is applied in an integration manner across the sliding mass (i.e., from left to right). (3) the summation of moments about a common point for all slices. The equation can be rearranged and solved for the moment equilibrium factor of safety, F_m . (4) the summation of forces in a horizontal direction for all slices, giving rise to a force equilibrium factor of safety, F_f .

The analysis is still indeterminate, and a further assumption is made regarding the direction of the resultant inter-slice forces. The direction is assumed to be described by a inter-slice force function. The direction together with the inter-slice normal force is used to compute the inter-slice shear force. The factors of safety can now be computed based on moment equilibrium (F_m) and force equilibrium (F_f). These factors of safety may vary depending on the percentage (λ) of the force function used in the computation. The factor of safety satisfying both moment and force equilibrium is considered to be the converged factor of safety of the GLE method.

Using the same GLE approach, it is also possible to specify a variety of inter-slice force conditions and satisfy only the moment or force equilibrium conditions. The assumptions made to the inter-slice forces and the selection of overall force or moment equilibrium in the factor of safety equations, give rise to the various methods of analysis.

2.10.1.2. Moment equilibrium factor of safety

The summation of moments for all slices about an axis point can be written as follows:

$$\sum Wx - \sum S_m R - \sum Nf + \sum kWe \pm \sum Dd \pm \sum Aa = 0 \quad (2-14)$$

After substituting for S_m and rearranging the terms, the safety factor which respected to moment equilibrium is:

$$F_m = \frac{\sum (c' \beta R + (N - u\beta) R \tan \phi')}{\sum Wx - \sum S_m R - \sum Nf + \sum kWe \pm \sum Dd \pm \sum Aa} \quad (2-15)$$

This equation is a nonlinear equation since the normal force, N , is also a function of the factor of safety.

2.10.1.3. Force equilibrium factor of safety

Summation of forces in the horizontal direction for all slices is:

$$\sum (E_L - E_R) - \sum (N \sin \alpha) + \sum (S_m \cos \alpha) - \sum kW + \sum D \cos \omega \pm \sum A = 0 \quad (2-16)$$

The term $\sum (E_L - E_R)$ presents the inter-slice normal forces and must be zero when summed over the entire sliding mass. After substituting for S_m and rearranging the terms, the factor of safety with respect to horizontal force equilibrium is:

$$F_f = \frac{\sum (c' \beta \cos \alpha + (N - u\beta) \tan \phi' \cos \alpha)}{\sum N \sin \alpha + \sum kW - \sum D \cos \omega \pm \sum A} \quad (2-17)$$

2.10.2. Seep/W

The flow of water through soil is one of the fundamental processes in geotechnical and geo-environmental engineering. In fact, there would little need for geotechnical engineering if water were not present in the soil. This is a nonsensical statement: if there were no water in the soil, there would be no way to sustain an ecosystem, no humans on earth and no need for geotechnical and geo-environmental engineering.

However, the statement does highlight the importance of water in working with soil and rock. Flow quantity is a key parameter in quantifying seepage losses from a reservoir or identifying a potential water supply for domestic or industrial use. Pore-pressures associated with groundwater flow are of particular concern in geotechnical engineering. The pore-water pressure, whether positive or negative, is an integral component of the stress state within the soil and consequently has a direct bearing on the shear strength and volume change behavior of soil. Research in the last few decades has highlighted the importance of moisture flow dynamics in unsaturated surficial soils as it relates to the design of soil covers.

2.10.2.1. Darcy's law

Seep/W is defined by following Darcy's law which is based on the basis of the water flow through both saturated and unsaturated soil. It is formulated as:

$$q = ki \quad (2-18)$$

Where: q = the specific discharge, k = the hydraulic conductivity, and i = the gradient of total hydraulic head.

Darcy's Law was originally determined for saturated soil, yet later research has demonstrated that it can likewise be connected to the water flow through unsaturated soil (see (Richards, 1931) and (Childs & Collis-George, 1950)). The only one difference is found out that under condition of water flow through unsaturated soil, the hydraulic conductivity is no more constant, but varies with changes in water content and indirectly varies with change in pore water pressure. Darcy's Law is often written as:

$$v = ki \quad (2-19)$$

Where: v = the Darcian velocity.

Note that the actual average velocity at which water moves through the soil is the linear velocity, which is equal to Darcian velocity divided by the porosity of the soil. In unsaturated soil, it is equal to Darcian velocity divided by the volumetric water content of the soil. Seep/W computes and presents only the Darcian velocity.

3 CHAPTER VETIVER GRASS EXPERIMENTAL IN LABORATORY

3.1. Introduction

In soil bioengineering approach, choosing the suitable vegetation is the first important step needs to do. The root of vegetation is an important part which helps to enhance the shear strength of the soil by the root matrix. An understanding of soil bioengineering has been developed through out a number of researchers including the theoretical of vegetation roots reinforced the soil such as: (Ali & Osman, 2008) studied on large direct shear test in laboratory to define the shear strength of soil based on the differences kind of plant materials and (Endo & Tsuruta, 1969; O'Loughlin, 1974; Terwilliger & Waldron, 1990; Waldron, 1977; Waldron & Dakessian, 1981) have focused on both field and laboratory tests of root reinforced soil. The study of using vetiver root system with applying geo-jute for slope protection and soil erosion control has been reported by (Islam, Nasrin, Islam, & Moury, 2013). Plus, (Jotisankasa, 2013) have studied on bio slope stabilization using seven local plant live stake as a method in slope protection in Thailand. (Mafian et al., 2009) has discussed on root reinforcement theories as bioengineering for slope stability by emphasizing on effect of root strength and soil suction. Moreover, (Waldron, 1977; Tien. H. Wu et al., 1988; Tien H Wu et al., 1979) have reported the theoretical model of fiber roots reinforcement on soil slope. All of these researches noted that the fiber roots of vegetation reinforced the soil slope is involved as a natural consequence of environments. However, the limitation of bioengineering techniques, in general, to shallow mass movements and are inappropriate for controlling deep-seated slope failures due the limited depth of plant roots. It has been illustrated in chapter two that vetiver grass is the best vegetation that has more root matrix in deep into the soil. In addition, vetiver grasses have been selected based on the soil type and the environment which could help them to survive for the last long period. The

Thailand's Land Development Department (Land-Development-Department, 1998) suggested that the root of vetiver grass can penetrate to the ground deeper and it suits for the arid area. Moreover, the vetiver grass had been promoted to control the soil erosion and water runoff or infiltration by World Bank (Greenfield, 1996). The tensile root strength properties of vetiver grass were studied for the resistance to shallow failure and surficial erosion by (Diti Hengchaovanich & Nimal S Nilaweera, 1996). Vetiver grass was proposed to be a soil-bioengineering because of its long root (2 – 3.5 m) and its very fast-growing (only 4 – 6 months). Since the shallow failures, typical failure mode of the slope usually occurs within 1 – 1.5 m depth from the surface in the regions with prolonged and heavy rainfall (Gray & Leiser, 1982), the rooting depth of the vetiver grass may be large enough to protect the slope from the shallow failure. However, the research on engineering aspects of vetiver grass is still limited and undergoing. In this research, the observations of vetiver grasses have been performed in both field and laboratory tests. In the field, vetiver grasses were planted along the slope area to observe the reality of the growing and make a comparison with vetiver specimens that prepared in the laboratory. In the laboratory, the vetiver specimen was prepared in three conditions. Firstly, it has performed on growing rate of vetiver roots by planting the vetiver grass in hydroponic (liquid nutrient). Secondly, the vetiver grasses have been planted in the soil as a single condition. The direct shear test has been performed by using this single vetiver grass to define the ability of cohesion of shear strength with single vegetation. Thirdly, large direct shear test has been set up by using the group of vetiver grass which planted in the cubic box. Figure 3-1 shows the flow chart of experimental in laboratory.

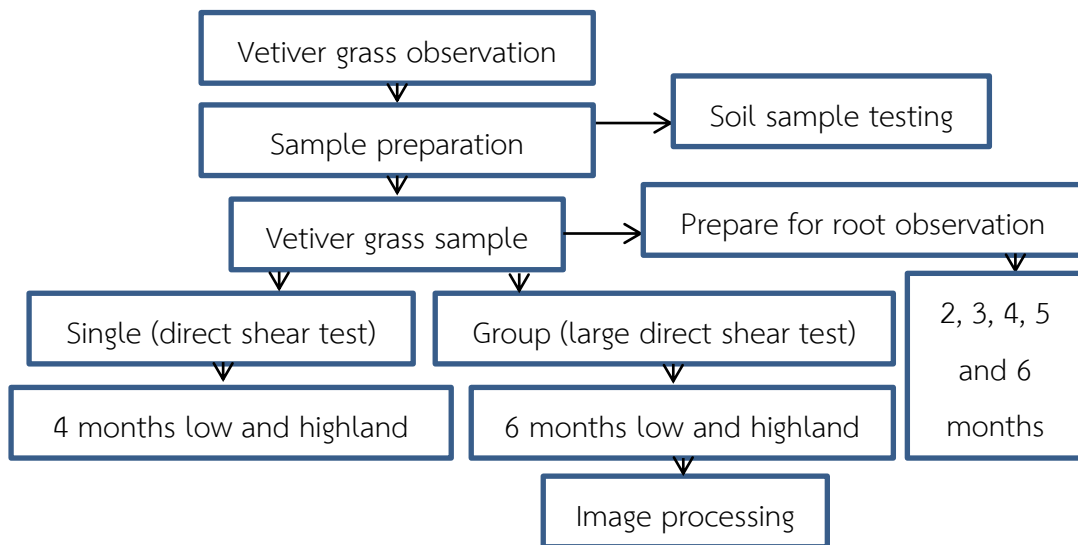


Figure 3-1: Flow chart of experimental in laboratory

3.2 Sample preparation

3.2.1. Soil sample testing

The soil used in this study was collected from the typical slope area. The test was conducted to define the nutrient component in soil which is required for the growth of vetiver plants. The test was performed at Kasetsart University. As the results, the various nutrients have remained relatively high are similar to those used for planting purposes. In other words, this kind of soil can be used for cultivation on the agriculture land. The chemical properties of the soil have presented in Table 3-1

Table 3-1: Chemical test result of planted soil

Test	Value	Level
Alkaline-Acidity (pH)	6.7	Medium
Organic (O)	12.13%	High
Phosphorus (P)	61 mg/kg	High
Calcium (Ca)	7,859 mg/kg	High
Magnesium (Mg)	974 mg/kg	High
Potassium (K)	1,996 mg/kg	Very high

3.2.2. Vetiver sample preparation

As mentioned in the introduction section, vetiver specimens have been prepared with three conditions. The first condition referring to hydroponics, 24 identical single (12 for highland and 12 for lowland) vetiver specimens was grown in a container with a liquid nutrient (without soil). The air pump was also installed in the container to provide the oxygen into the nutrition water as shown in Figure 3-2. This experiment is used to investigate the growing rate of vetiver roots without destroying the roots. The measurement of the length of root and the radius of root bundle were carried out for each specimen continuously until 6 months (Fig. 3.3 highland vetiver specimen and Fig. 3.4 lowland vetiver specimen).

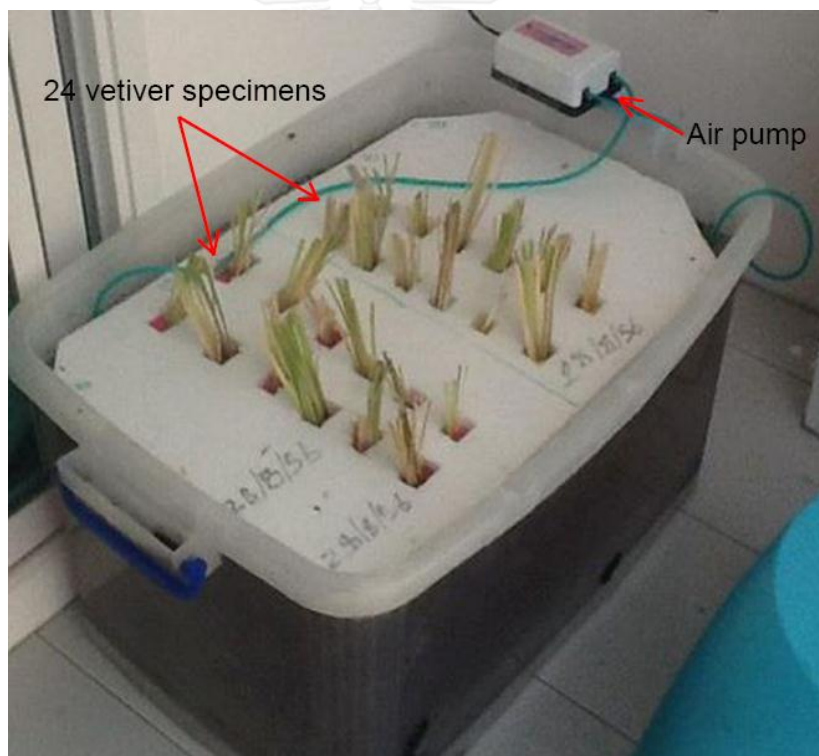


Figure 3-2: Vetiver specimens grew in hydroponic condition



Figure 3-3: Root observation for highland within 3 months



Figure 3-4: Root observation for lowland within 3 months.

For the second and third series of the tests, the vetiver grasses were prepared by planting into the soil. The soil used in this study was collected from the typical slope area. The chemical properties of the soil were tested and reported in Table 3-1. The single vetiver specimens, which planted in the plastic bag and put it the PVC tube

with 150 mm in diameter and 600 mm in length, were prepared for the standard direct shear test. Figure 3-5a) shows the schematic of planting vetiver grass for single specimens. Four tested samples were prepared by cutting at the upper part from top to down direction with 20 mm thickness for each tested sample to fit with the direct shear box as shown in Figure 3-5a) and Figure 3-6a). For the group specimen, the vetiver grasses were prepared by planting in 300 mm cubic wood box. Nine vetiver specimens were planted with a spacing of 75 mm as shown in Figure 3-5b). These group vetiver specimens were prepared for the large direct shear test. Three tested samples were prepared for the test by trimming to fit with large direct shear mould of 300 mm x 300 mm x 200 mm as shown in Figure 3-6b). In addition, this group vetiver grass was prepared for image processing to define the root area ratio as well. It is noted that the group vetiver specimens were planted in the same soil which used to prepare for the single vetiver specimen.

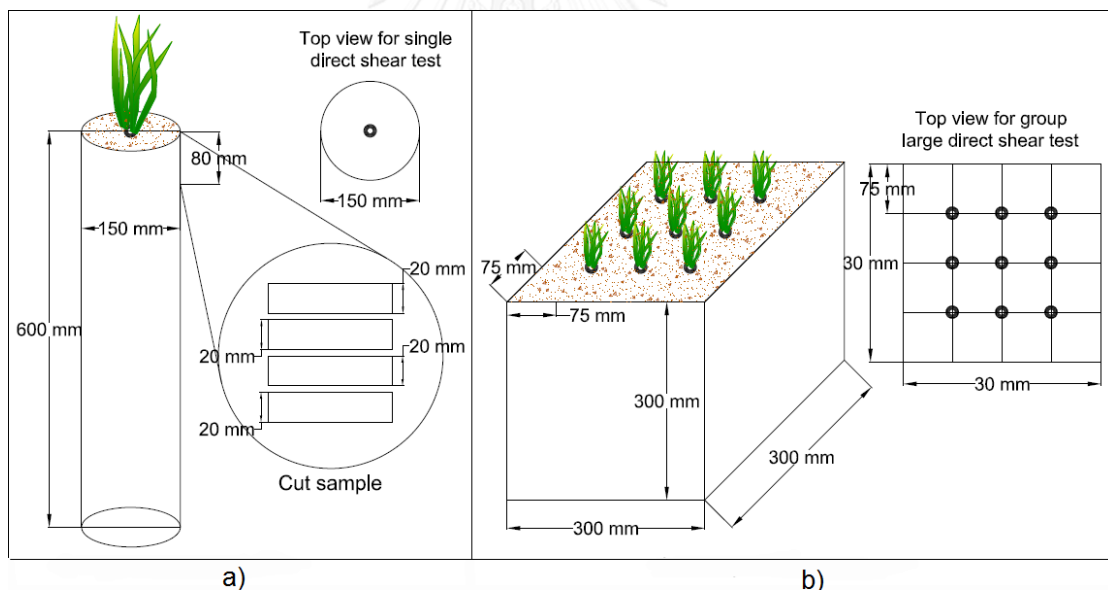


Figure 3-5: Vetiver grass specimens prepared for the shear tests: a) 4 months old single vetiver grass for the direct shear test and b) 6 months old group vetiver grass for the large direct shear test

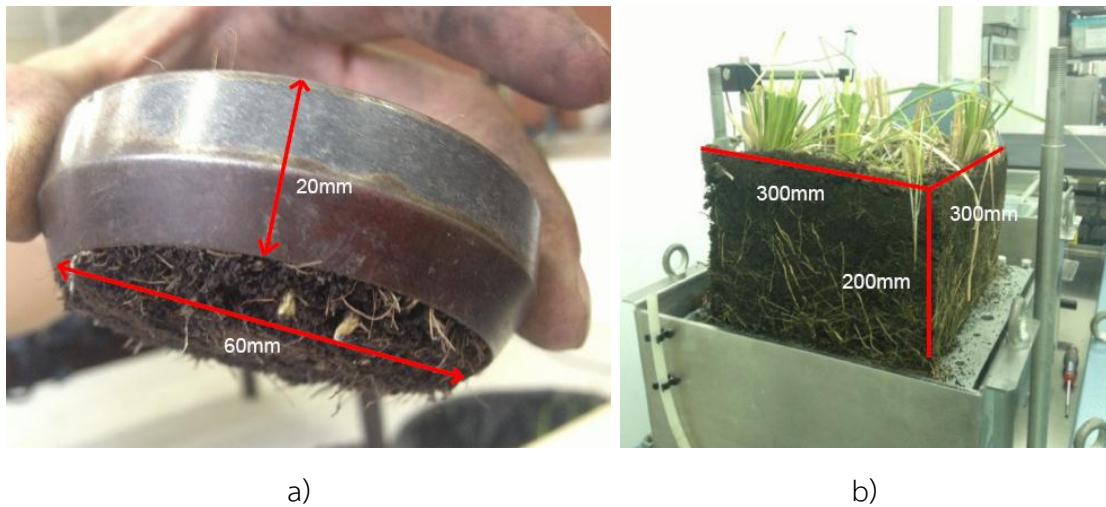


Figure 3-6: Tested samples for shear tests: a) a 60 mm diameter direct shear apparatus and b) a 300mm x 300mm large direct shear apparatus

3.3 Vetiver Roots Observation

Some previous research has studied on measurement of vetiver root in situ test. The method used in the study to measure the root length was directly measured by keeping the root position undisturbed after trenching out of the soil. After measuring the root length, the vetiver clump was replanted into the soil with a special care which could help the plant grow properly (Nasrin, Islam, & Moury, 2013). In this study, the method used to check the root length was the same directly measurement. The difference in this research is on the way of plant the vetiver grass. As mentioned in the vetiver sample preparation above, the vetiver plants were planted in the container with liquid nutrient which is called hydroponic condition. The root length were measured by taking out the vetiver grass from the container (Fig. 3.3 and 3.4) and put it back properly after finished measurement. The plotting graphs below have presented the average values of root length and root bundle diameter from the hydroponic vetiver specimens. The results have been observed and measured continuously from 2 to 6 months. The relationship between the length of roots and the radius of roots bundle is shown in Figure 3-7 for highland vetiver grass and Figure 3-8 for lowland vetiver grass. The growing rate of roots can be determined from a

plot of length of roots with respect to time as shown in Figure 3-9 for both highland vetiver grass and lowland vetiver grass. According to the results, it is indicated that the roots of the grass have spread the radius of roots bundle up to 1.7 cm (Fig. 3.7) and around 1.4 cm (Fig. 3.8). Plus the roots can grow up to 180 cm within 6 months (Fig. 3.9). Based on the results, the radius of roots bundle of highland vetiver specimen are larger than lowland vetiver specimen while the length of the roots are the same. The average growth rate of roots is approximately 30 cm/month.

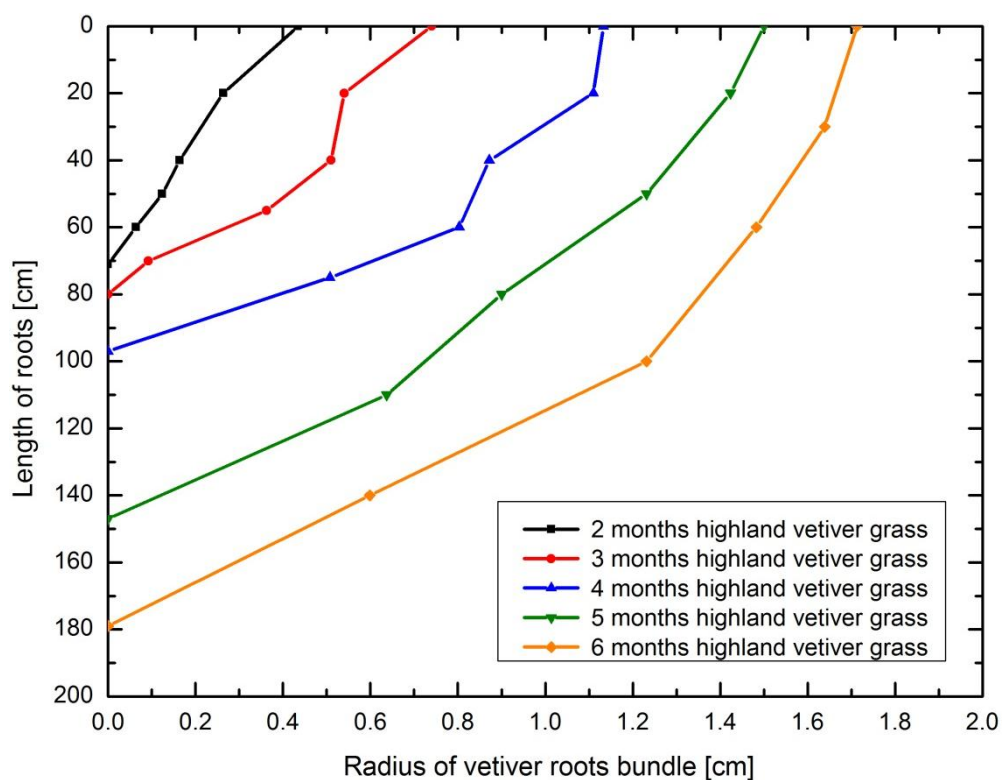


Figure 3-7: Relationship between length and radius of roots bundle for highland.

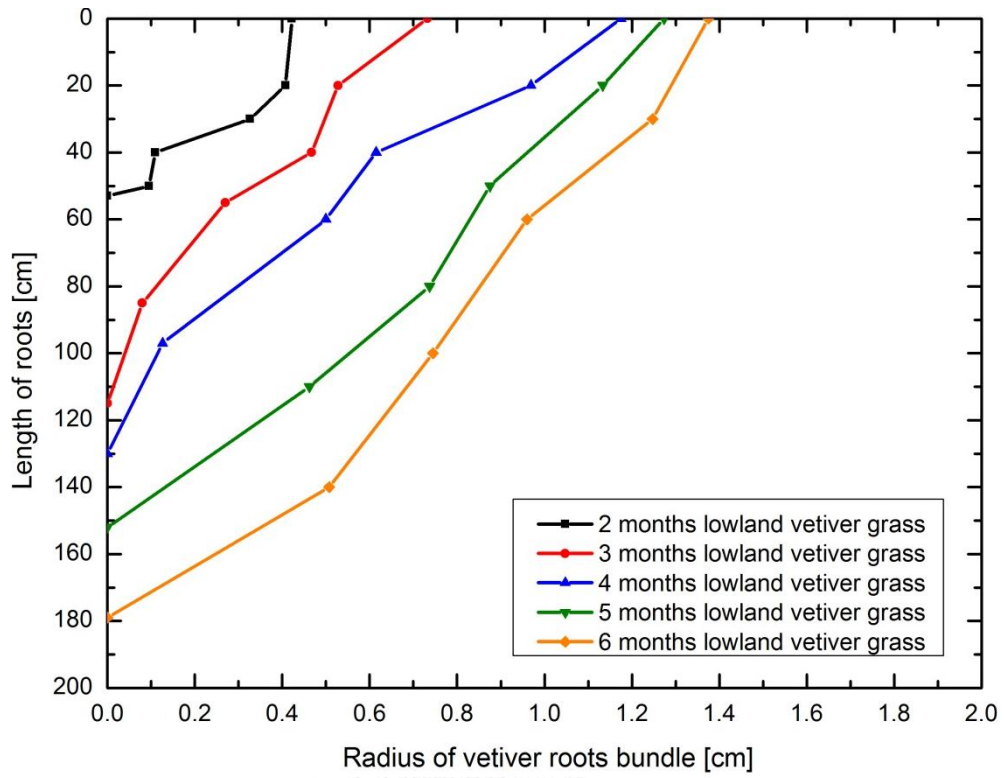


Figure 3-8: Relationship between length and radius of roots bundle for lowland.

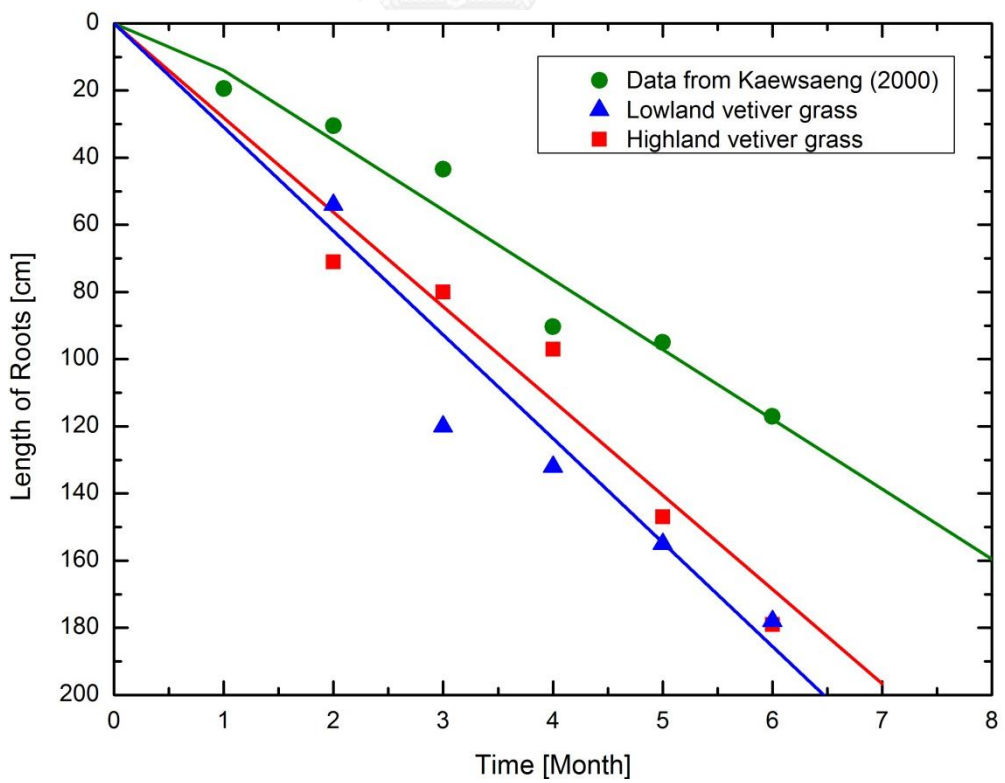


Figure 3-9: Comparison growing rate of vetiver roots with (Kaewsaeng, 2000).

3.4 Shear strength of vetiver roots

The theory of root reinforcement in chapter 2 has mentioned that the soil slope have been improved by the inclusive of fibres root which enhance the shear strength of a soil mass through an increase in the apparent cohesion of the soil. Direct shear test and large direct shear are commonly tests which use the direct shear box and large direct shear box to define the shear strength of root-reinforced soils. In previous study, (Ali & Osman, 2008) studied on large direct shear test in laboratory to define the shear strength of soil based on the differences kind of plant materials and (Endo & Tsuruta, 1969; O'Loughlin, 1974; Terwilliger & Waldron, 1990; Waldron, 1977; Waldron & Dakessian, 1981) have focused on both field and laboratory tests of root reinforced soil. Plus, (Operstein & Frydman, 2000) studied on shear strength of soil which used the direct shear test, pull-out test, and tension test to define the additional shear strength contribute to the soil. In this study, the reinforcements of the vetiver roots system were studied using direct shear box and large direct shear box in laboratory. Hence, the vetiver root system sample can be simply prepared and the density and water content of the soil can be controlled. Two types of specimens were prepared in this study, i.e., single and group vetiver. Four months old single vetiver specimen (Fig. 3.5a)) was prepared for the standard direct shear test. On the other hand, six months old group vetiver specimens (Fig. 3.5b)) were prepared for the large direct shear test. To observe the increase of shear strength from the vetiver root reinforcement, the bare soils with the same density and water content associated with the four months and six months specimens were prepared for direct shear tests as well. Results for the soil-root matrix are compared to soil-only tests to determine the proportion of soil resistance provided by the roots.

3.4.1. Direct shear box

Figure 3-10 shows the direct shear apparatus which is used in this study. Four months old single vetiver grass was individually prepared in the cylindrical plastic bag and put into PVC tube to ensure that the roots of vetiver can growth vertically into the soil as shown in Figure 3-11a). A 60 mm diameter cylindrical mould was used to perform the direct shear test for the fourth month old single specimens as shown in Figure 3-11b). The tests were performed by following the ASTM D3080 (ASTM-Standard-D98, 1998) (similar to JGS 0561) standard with the shear rate of 1.5 mm/min. The normal stresses of 10, 20, 50, and 100 kPa were applied for each test. All specimens were sheared till they reached the peak point or started showing the fairly constant shear stress or the maximum horizontal displacement of 6 mm. The shear strengths of the fourth month vetiver root reinforced soil and the bare soil were obtained as presented in Figure 3-12. The cohesion intercept and the friction angle were determined according the Mohr-Coulomb failure criterion as presented in Table 3-3. The presence of the vetiver roots has improved the strength of the soil. As the results, the vetiver grass could increase the cohesion of shear strength by almost 7 kPa for highland and 1 kPa for lowland. (Ali & Osman, 2008) reported the increasing of cohesion of shear strength of soil by vetiver roots. The results show that the cohesion of shear strength of soil was increased around 11 kPa from the average values of 1 m depth of rooted zone.



Figure 3-10: Direct shear apparatus



Figure 3-11: Single vetiver grass planting sample: a) before testing and b) after testing

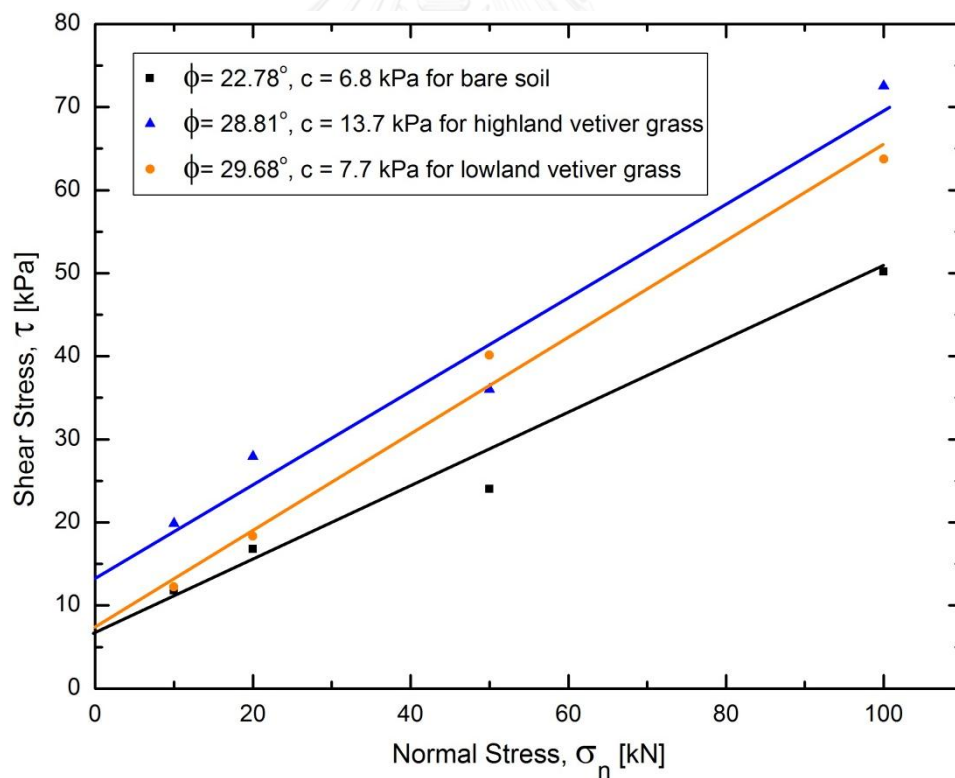


Figure 3-12: 4 months old single vetiver grass from direct shear test

3.4.2. Large direct shear box

Six months of vetiver grass were prepared as a group specimen in the cubic box as shown in Figure 3-14. The large direct shear apparatus was chosen to perform direct shear tests for the group vetiver specimens as shown in Figure 3-13. The tests were performed following the ASTM D3080 (ASTM-Standard-D98, 1998) standard which is used 30, 50, and 75 kPa to apply for the normal stresses by the hydraulic pressure system through the top plate of the machine. The side friction between the sample and the shear box was minimised by applying some oil. All the data from the displacement transducer and load cell are acquired by an automatic data logging system. All samples were sheared to reach the maximum horizontal displacement at 50 mm. The friction angles were determined based on Mohr-Coulomb failure criterion as presented in Table 3-3. The results of cohesion of shear strength have been plotted in the graph in Figure 3-15 by comparing between bare soil with lowland and highland of vetiver grass. As showing in the graph, the cohesion of shear strength of soil was increased around 3 kPa for lowland and 6 kPa for highland.

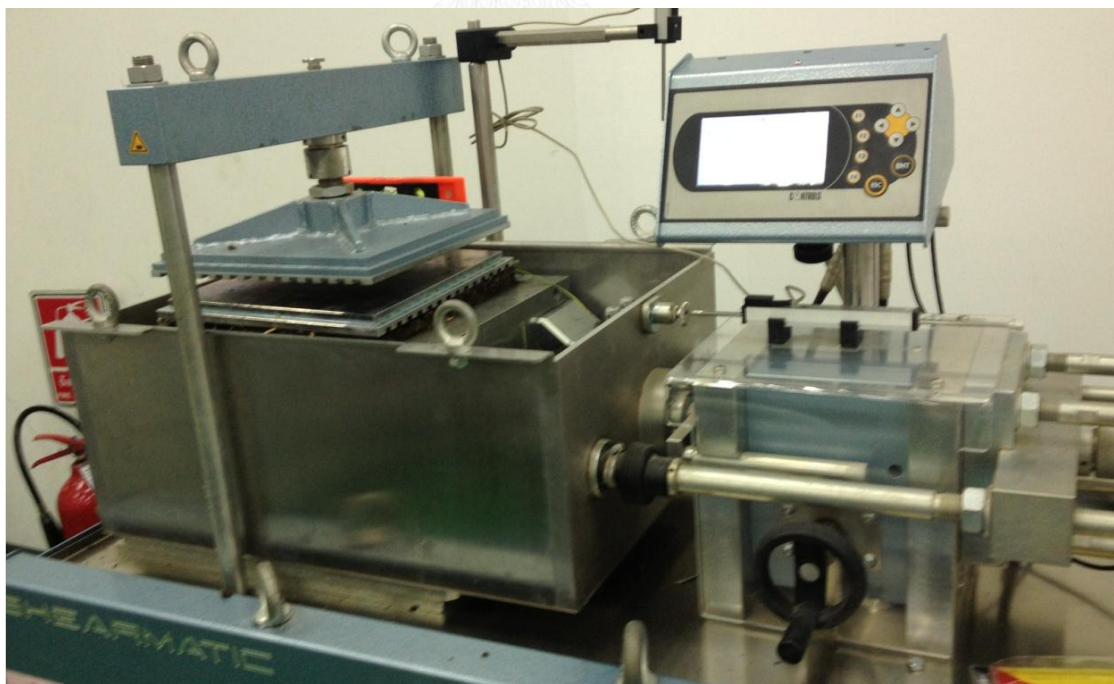


Figure 3-13: Large direct shear apparatus

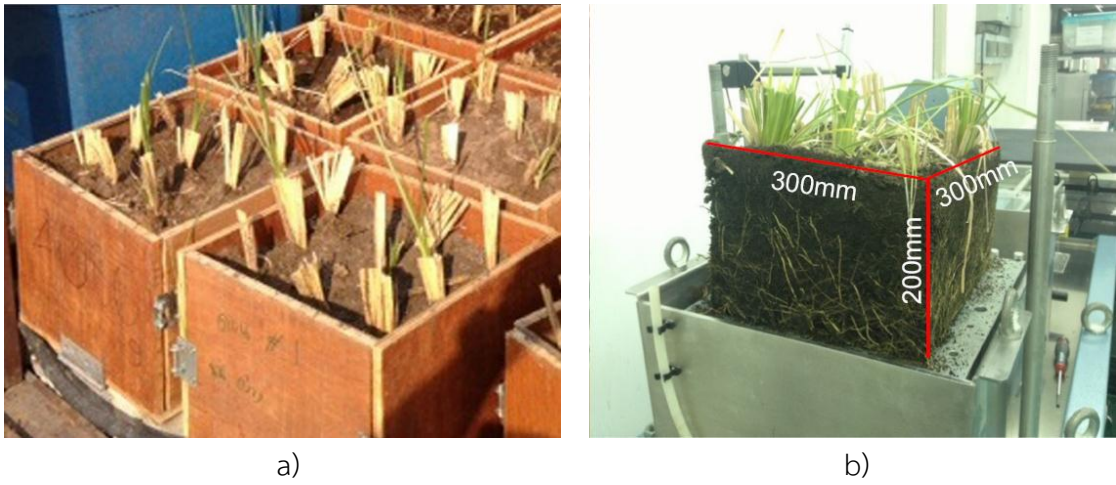


Figure 3-14: Group vetiver grass planting sample: a) planting in wood box and b) before testing

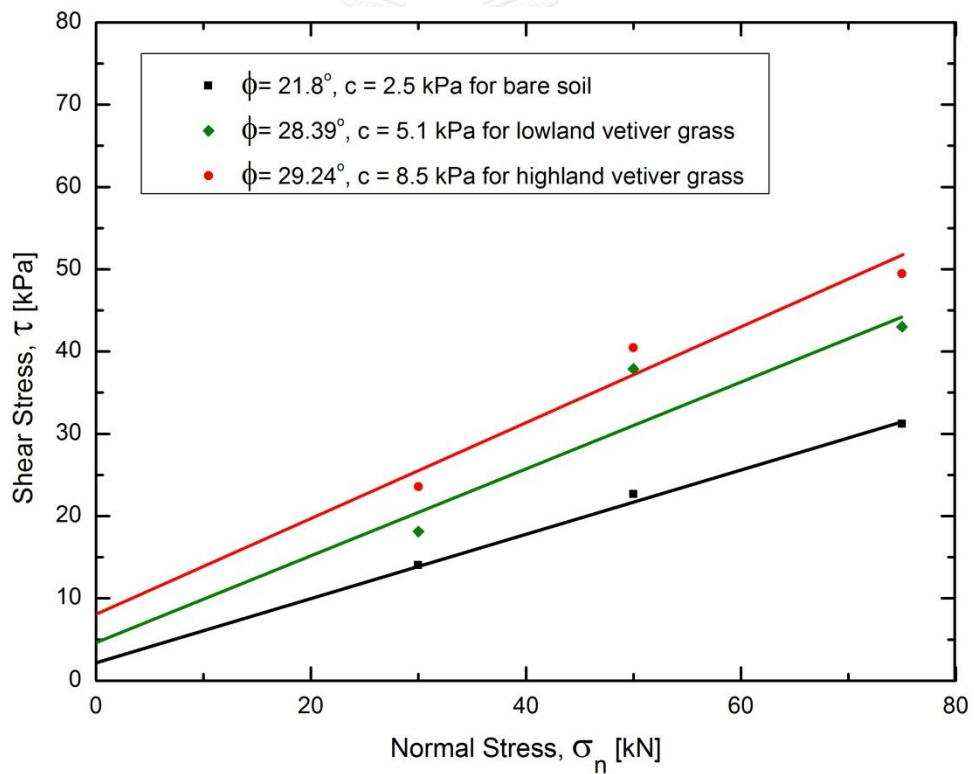


Figure 3-15: 6 months old group vetiver grass from large direct shear test

3.5 Image processing

Moreover, the root observations of the group vetiver roots can be defined by a root area ratio (Fig. 3.16). The term root area ratio refers to the fraction of the total cross-sectional area of a soil that is occupied by roots (Gray & Sotir, 1996). The root area

ratio plays an important role for a contribution of root fibres on shear strength when it is directly defined by the cross-sectional area in the shear plane (Fig. 3.16a). However, the root area ratio measured in the plane perpendicular to the root-growth direction is really difficult to determine and it is also varied with depth. The parallel plane measurement of the root area ratio, which is easier to observe and represents an average of root fibre contribution in the soil, was used in this study (Fig. 3.16b). (Alsheimer & Hughes, 2007) has reported the technique of using image processing to observe root distribution in a large direct shear specimen. The photographs of root and soil were taken with a digital camera and transferred to binary image via the histogram function of Photoshop software. The black and white pixels of the image could be distinguishably counted between soil and root. The ratio between the pixels of root and total pixels can be loosely defined as a root area ratio. Figure 3-17 is a photo of 6 months highland vetiver specimen which is taken by the digital camera. And Figure 3-18 is the binary image, which converted from digital photograph (Fig. 3.17), has presented the method to estimate the roots area ratio based on the colour in the image. For example, the white and black colours represent the soil and void space, respectively; on the other hand, the grey colour represents the root area. Hence, the roots area ratio can be defined by the total pixels of roots and total pixels. Table 3-2 show the results of the average root area ratio of the group vetiver at 6 months for both highland and lowland.

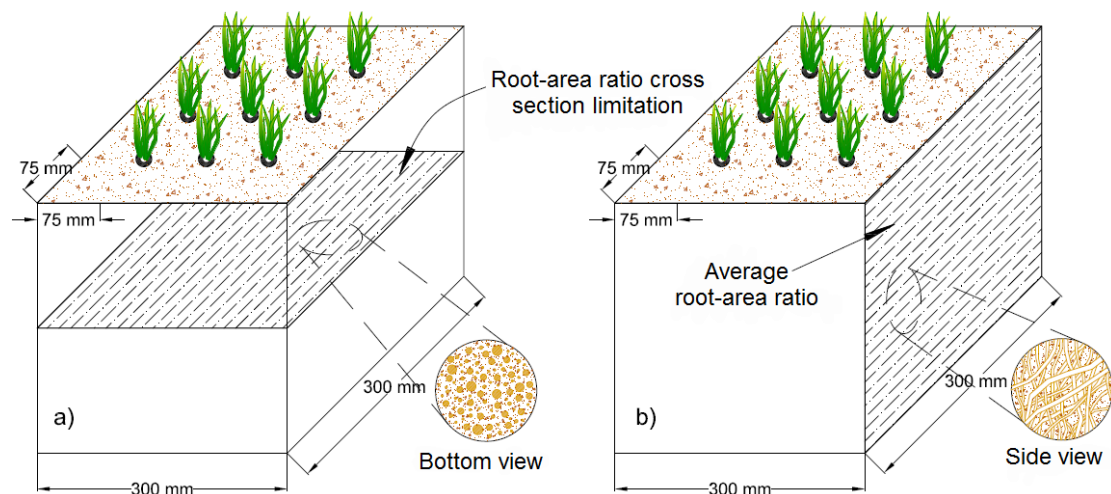


Figure 3-16: Definition of root-area ratio: a) in the shear plane and b) parallel plane

Table 3-2: Results of root area ratio

6 months Specimen	Water content (%)	Bulk density (kg/m^3)	Root area ratio (%)
Bare soil	20.85	1030	0
Lowland	25.49	1110	3.36
Highland	24.86	1103	4.56



Figure 3-17: Root photograph taken from the 6 months group vetiver

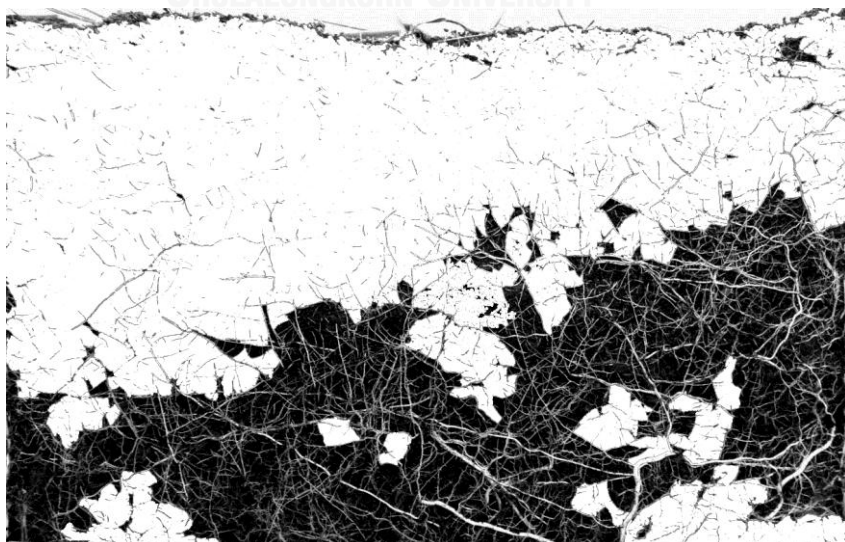


Figure 3-18: Binary image processing by using Photoshop

3.6 Results and discussion

According to the roots observation results, the growth rate of vetiver roots is relatively high comparing to others (Lyr & Hoffmann, 1967). The maximal depth development of vetiver root system could go up to 200 cm in first year and the average daily increment of root is approximately 10 mm. As shown on the plotting graph in Figure 3-9, the current study of vetiver (highland and lowland) has shown a slightly higher growth rate of vetiver when comparing to the data from (Kaewsaeng, 2000). The difference is probably caused by planting condition and measurement method. The data from (Kaewsaeng, 2000) was observed from the specimen planted in the soil and the root measurement required plant removal.

Based on shear strength results, the increasing of cohesion of shear strength of soil for the single vetiver specimen was higher than the group specimen (see Table 3-3). The difference is probably caused by the scale effect of tests. Due to the size of direct shear box is smaller than large direct shear box, the scale effect of the shear test have been involved in the shear process (shear zone) where the mechanism of localisation occurs. (Cerato & Lutenegeger, 2006) and (Moayed & Alizadeh, 2011) have reported the results of differences specimen size and the scale effect of direct shear test on sands and silty sand. The results were indicated that the friction angle have been decreased due to the increase of specimen size of direct shear box. However, the test results indicate that the vetiver roots significantly enhance the soil shear strength especially on the cohesion of soil. This result agrees well with the observation by (Ali & Osman, 2008).

Table 3-3: Results of direct shear tests

Test	Specimen	Shear strength parameters	Increasing in cohesion (kPa)
Standard direct shear test	Bare soil	$c = 6.8 \text{ kPa}; \phi = 22.8^\circ$	0.9
	4 months old lowland single vetiver grass	$c = 7.7 \text{ kPa}; \phi = 29.7^\circ$	
	4 months old highland single vetiver grass	$c = 13.7 \text{ kPa}; \phi = 28.8^\circ$	5.9
Large direct shear test	Bare soil	$c = 2.5 \text{ kPa}; \phi = 21.8^\circ$	2.6
	6 months old lowland group vetiver grass	$c = 5.1 \text{ kPa}; \phi = 28.4^\circ$	
	6 months old highland group vetiver grass	$c = 8.5 \text{ kPa}; \phi = 29.2^\circ$	6.0

4 CHAPTER PHYSICAL MODELLING

4.1 Introduction

Evaluating the soil slope stability is an important, interesting, and challenging aspect of civil engineering. Over the past decades, the experiences of soil slope behavior and their failure have improved the understanding of the change in soil properties. As it has been illustrated in chapter two that centrifuge modelling is a physical model testing and now widely used in geotechnical research or design. And since slope stability is a gravity-dependent problem, the major advantage of using centrifuge modelling is to enable researchers to test reduced-scale physical models at a correct stress level by increasing g-level (Taylor, 2003). In recent years, occurrence of slope failure induced by rainfall has been increasing not only in Thailand, but also all over the world especially in the tropical region. In the North and South of Thailand, the natural slope failures due to the heavy rainfall usually occur during rainy season. Hence, centrifuge modelling can be used to model of rainfall induced landslides by controlling material properties, and boundary conditions to provide an understanding of the triggering mechanisms of landslides due to rainfall. Previous researches have investigated on the mechanism of rainfall-induced slope instability based on the laboratory tests and field monitoring and as well as using centrifuge. For example, (Lumb, 1975) has been reported the role of rainfall induced slope failure by focusing on the infiltration water into the residual soil. (W. Mairaing, Jotisankasa, & Soralump, 2012) has made the field monitoring of the slope based on the surface flow and moisture infiltration due to the heavy rainfall. To understand strength reduction of the soil due to the water infiltration, laboratory tests to simulate the rainfall induced slope failure by reducing suction have also been carried out by (Chen, Lee, & Law, 2004). Plus, (Ling, Wu, Leshchinsky, & Leshchinsky, 2009) has studied the series of centrifuge modelling in slope

instability with rainfall simulator. And (Montrasio & Valentino, 2007) has been studied as well on the soil slope with shallow failure due to the rainfall by using the physical 1-g model. To solve this rainfall induced slope failure problem, several methods have been used such as; soil nail, retaining wall, geosynthetic reinforcement and shotcrete. All these methods are too expensive for the natural slope protection and they also require some maintenance. However, a soil-bioengineering approach is one of the approaches which are well known as the use of live materials such as the plants, vegetation and grass in protection of the slope against failure. The roots of vegetation could enhance the slope stability by increasing the shear strength of soil (Gray & Sotir, 1996). In addition, this method is used against the shallow failure and as well as for the soil surface erosion in the natural slopes. (Coppin & Richards, 1990; Greenway, 1978; T. H. Wu, 1995) have been researched on the role of vegetation in relation to the slope stability. To model soil slopes reinforced with vegetation, a few researchers recently have introduced the centrifuge (Sonnenberg et al., 2011; Sonnenberg et al., 2010; A. Takahashi et al., 2014). However, it is still difficult to model the soil slope reinforced by vegetation with the effect of rainfall in a centrifuge. This chapter therefore presents a series of centrifuge model tests on soil slopes reinforced with model roots using a rainfall simulator to demonstrate effectiveness of roots in the shallow depth against slope failure. The centrifuge model tests were performed at Tokyo Institute of Technology in Japan.

4.2 Soil bioengineering

As mentioned above, centrifuge model tests have conducted to define the mechanism of effectiveness of root fibres in shallow depth against slope failure. Thus, this section describes the effect of vegetation on slope model in centrifuge. In chapter 2, soil bioengineering has been described the use of live materials such as vegetation which has seriously introduced by (Gray & Sotir, 1996). Vegetation within natural and man-made slopes can alter mechanical performance considerably through the reinforcing effects of roots and altered hydrology (Mickovski & van Beek,

2009). In common engineering design, the effects of vegetation are overlooked, with a potentially beneficial, cost-effective, and environmentally friendly approach to stabilize slopes not being fully realized. A vegetated slope will differ in response from fallow slopes in mainly two aspects: (1) Hydrological – vegetation roots may increase subsoil permeability and they will intercept rainfall at the same time with transpiring water, eventually leading to lower water pressures (i.e., higher suctions) in slope. (2) Mechanical – the presence of the root fibres will lead to reinforcement in the penetrated regions (Gray & Sotir, 1996). The typical stability of vetiver grass on slope as bioengineering can be illustrated in Figure 4-1.

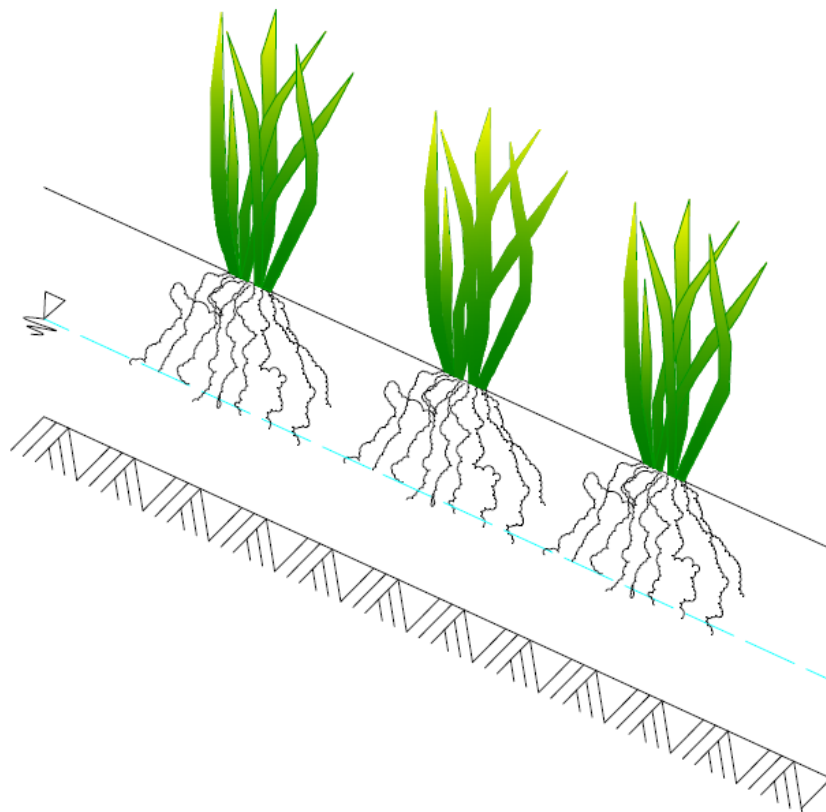


Figure 4-1: Stability of vetiver grass on Slope

Hydrology is strongly seasonal and many slope failures occur when trees have shed leaves and are not transpiring. It has even been argued that while transpiring, the net effect of plant transpiration on soil suction has minimal influence on slope stability compared with mechanical reinforcement (Greenwood, Norris, & Wint, 2004). Reinforcement by roots with typical tensile strengths of 5 – 50 MPa (Mickovski & van

Beek, 2009) can be significantly comparable to other materials used in engineering. As a result, various models have been developed to account for mechanical reinforcement by roots in the engineering analysis and design (Gray & Sotir, 1996; Tien H Wu et al., 1979). Difficulties with the analysis of slopes arise because plant roots grow under uncertain biological and environmental conditions. The mechanical properties of the roots vary with age, diameter and plant species as well as the distribution of roots. Due to the difficulty of planting vetiver grass into the slope model, this research has assumed the polyester fibres as equally to the root fibres. More detail about polyester fibres will be presented in the following section.

4.3 Instrumentation

4.3.1. Centrifuge apparatus

Centrifuge is kind of technique equipment for testing the physical model, which is used to solve the geotechnical problems such as slope stability. Centrifuge modeling has been conducted since last a few decades as it enables the study and analysis of design problems (Taylor, 2003). By the scaling law with the increasing g environment of a geotechnical centrifuge, the stress history of the prototype scale could be defined in the physical modeling which replicates the properties, dimension and in situ stresses change with depth. For any large-scale nonlinear problem in geotechnical engineering, centrifuge may be useful for scale modeling. The Tokyo Tech Mark III Centrifuge was used for the tests (Fig. 4.2). Specifications and details of the Mark III centrifuge are given by (Akihiro Takahashi, 2002).

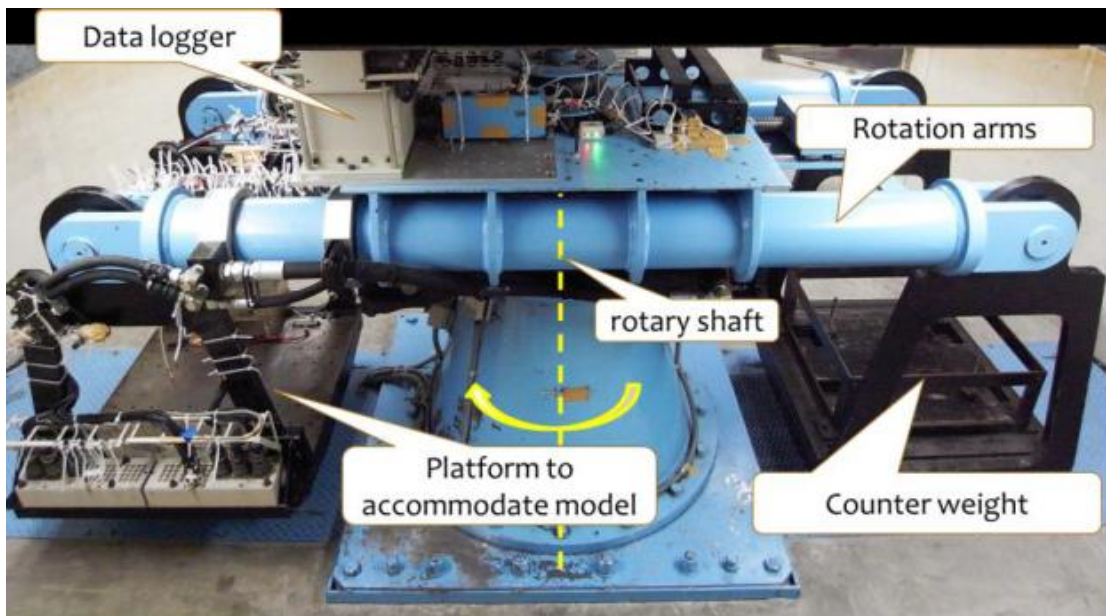


Figure 4-2: Centrifuge apparatus at Tokyo Institute of Technology (Tokyo tech)

4.3.2. Pore water pressure transducer and accelerometers

In the test, there are two type of transducers were used in the entire tests to measure pore water pressures change and the accelerations (displacement). There are nine pore pressure transducers and six accelerometers were installed properly in the model test. Figure 4-4 shows the arrangement of pore water pressure transducers and accelerometers inside the model. The size of transducers should be small enough to install inside the model test. The dimension of pore pressure transducers used in the experiment were 6 mm in diameter and 12 mm in length and fitted with a porous element to isolate the fluid pressure for measurement as shown in Figure 4-3a. The pore water pressure transducers have supplied with a porous stone that used to protect the diaphragm against the pressure applied by the soil. All these sensors were Druck miniature model PDCR81 based on GE Sensing and Inspection Technologies. The dimension of accelerometers used in the experiments was 4x4x10 mm as shown in Figure 4-3b.

All transducer sensors have to calibrate at 1 g acceleration to define the calibration factors which were used to convert the recorded data in voltage output of the

instrument into engineering units. The calibration factors for PPT and ACC were determined by manual calibration.



Figure 4-3: a) pore water pressure transducer and b) accelerometer

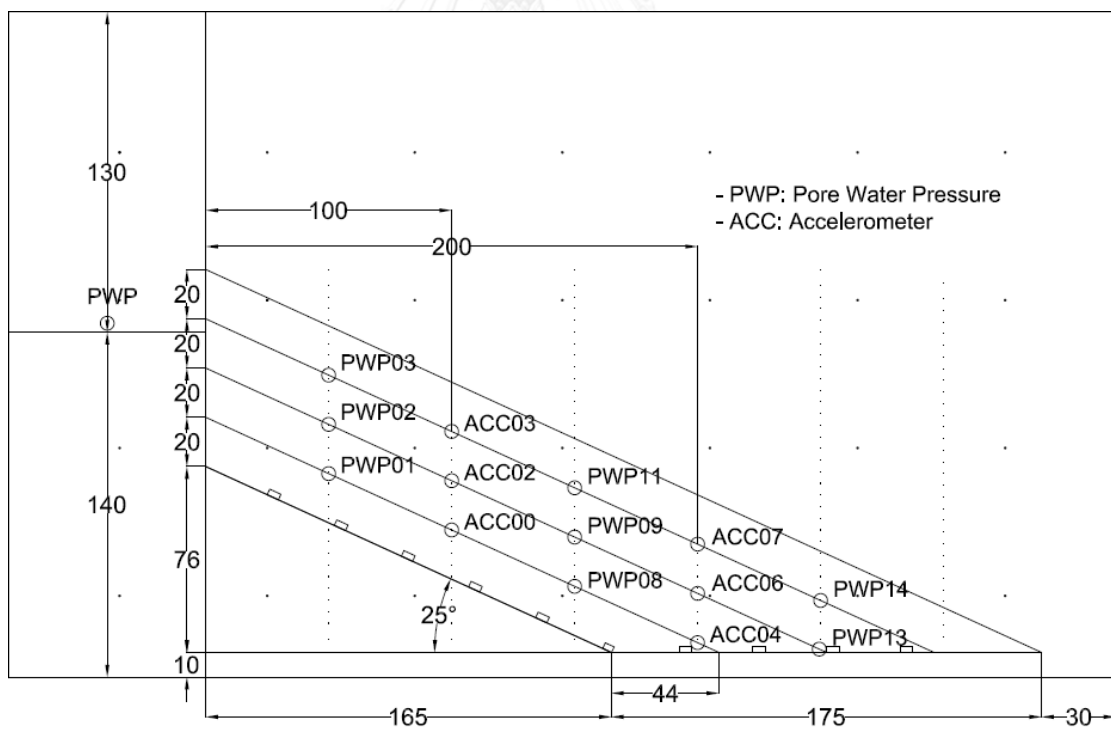


Figure 4-4: Pore water pressure transducers and accelerometers arrangement

4.3.3. Steel box and bedrock

Centrifuge model tests were conducted using the rectangular steel box as shown in Figure 4-5a. The steel box has a dimension of 450 mm \times 150 mm \times 270 mm by length, width and height, respectively. In front of the box is a transparent plastic glass which used to see through inside the box. Inside the steel box, a small water tank was installed and used as water storage tank. A small pipe also installed and put it close to the plastic glass to see the water level rise up during the test. At the bottom of bedrock inside steel box, there is a small drainage hole which used to drain the water out of the steel box. This container of steel box intends to simulate the behavior of a rainfall test and slope stability test. A triangular aluminium plate, with an inclination of 25°, was constructed to provide a rigid underlying layer for the soil slope. The top surface of this bedrock was roughened by paper sand and small aluminium plate which stuck them on the top as shown in Figure 4-5b. This sand paper and small aluminium plate have installed to prevent the soil slope from sliding down during soil preparation and as well as during the centrifuge spinning.

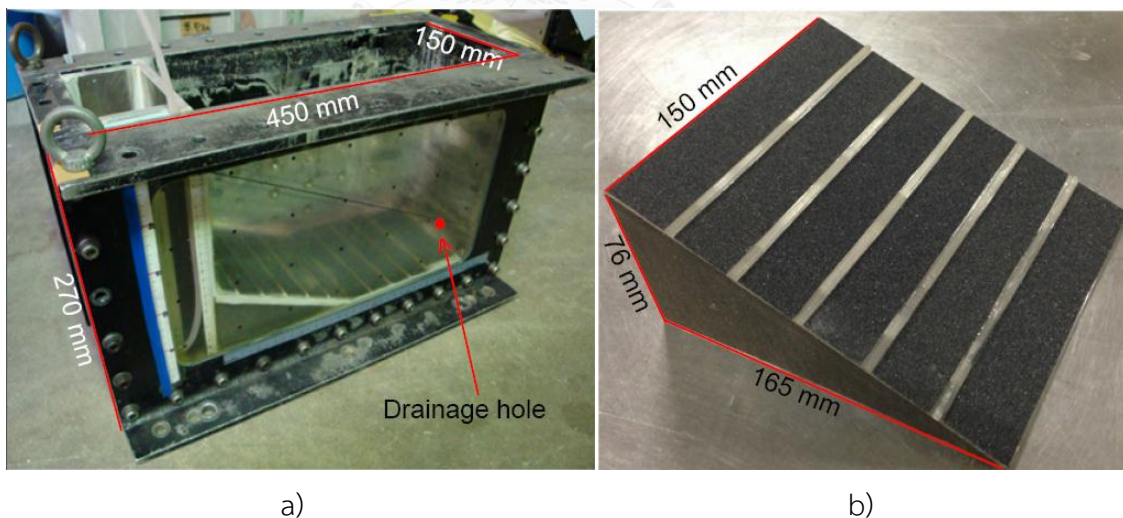


Figure 4-5: a) steel box and b) bedrock

4.4 Properties of soil and fibre used in the model

Edosaki Sand, a fine sand according to JGS0051 (Japan Geotechnical Society Standard), was used in the model slopes. Figure 4-6 shows the grain size distribution curve of the Edosaki sand. Only the sizes below 2mm were used in this study. Table 4-1 summary the engineering properties of the Edosaki sand. The polyester fibers (Teijin RA04FN, approximately 39 μm in diameter and 10mm in length) were used to model the fiber root. In the model tests, the 2% by mass of polyester fibers were mixed with the sandy soil for the vegetated slope surface cases. The amount of polyester fibres (2%) used to mix with Edosaki sand was based on the results of vetiver grass observation by direct shear test from chapter 3 (Fig. 3.12). Plus, it is noted that the 2% fibre mixing by mass is approximately 7% by volume, which is slightly higher than typical values of the root area ratio of 3 - 5% for small vegetation observed in literatures (Gary and Sotir, 1996). Figure 4-7 presents photos of the polyester fibers before and after mixed with the sandy soil. The engineering properties of soil mixed with 2% of polyester fibre are summarized in Table 4-1.

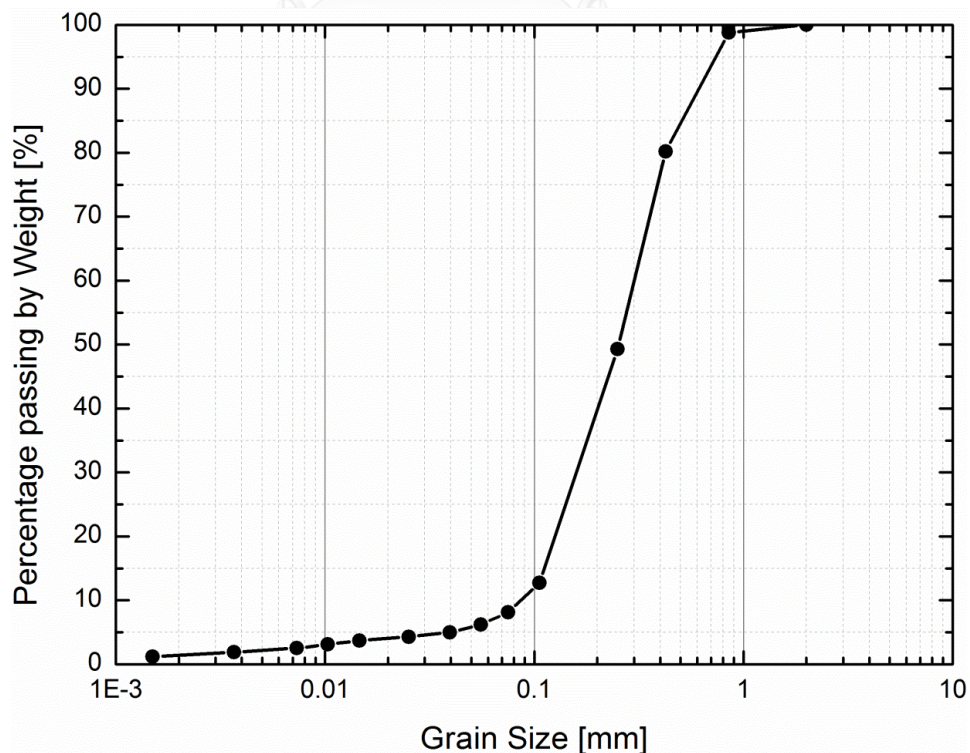


Figure 4-6: Grain size distribution curve of Edosaki Sand



Figure 4-7: Polyester fibers before and after mixed with Edosaki sand at 2% by mass:
a) Before mixing and b) After mixing

Table 4-1: Properties of compacted soils

Soil type	Edosaki Sand	Edosaki Sand + 2% by mass of polyester fibre
Specific gravity, G_s	2.65	-
Maximum dry unit weight, γ_d (kN/m^3)	12.94	12.94
Optimum water content, w_{opt} (%)	15.19	17.28
Degree of saturation, S_r (%)	39.85	-
Total unit weight, γ_t (kN/m^3)	14.91	15.18
Void ratio, e	1.01	-
Maximum void ratio, e_{max}	1.29	-
Minimum void ratio, e_{min}	0.87	-
Coefficient of permeability, k (cm/s)	3.25×10^{-5}	3.08×10^{-5}
Cohesion intercept, c (kPa)	4.8	18.9
Angle of shearing resistance, ϕ ($^\circ$)	28.58	31.45

4.5 Shear strength of soils

The shear strength of the soils was examined by the standard direct box shear test. The soil specimen was prepared in the cylindrical shape with 60 mm in diameter and 20 mm in height. In the tests, Edosaki sand with a water content of 15% was compacted to achieve a degree of compaction of 80%. For the case with the model fibre roots, water content of 17% was needed to mix with the fibres 2% to reach the final water content of 15%. The direct shear box tests were carried out to obtain the angle of shearing resistance (ϕ) and the cohesion intercept (c) of the soils both with and without fibres. Figure 4-8 shows the results of direct shear test for Edosaki sand with and without polyester fibres. By adding 2% of polyester fibre into the sand has increased the cohesion around 14 kPa and the friction angle around three degrees. The results are also summarized in Table 4-1. This result is similar to the evidence reported in chapter 3 (Fig. 4.9) and many researchers for the root-reinforced soils. The result exhibits that the fibre roots could increase the shear strength which mainly arises from the cohesion but not from the friction. The results have shown that the increasing of cohesion component of shear strength around 10kPa and is comparable to (Ali & Osman, 2008). Regarding to the hydraulic conductivity of the soils, the coefficient of the hydraulic conductivity of the soil with fibres was slightly smaller than that of the soil without fibres (see table 4-1).

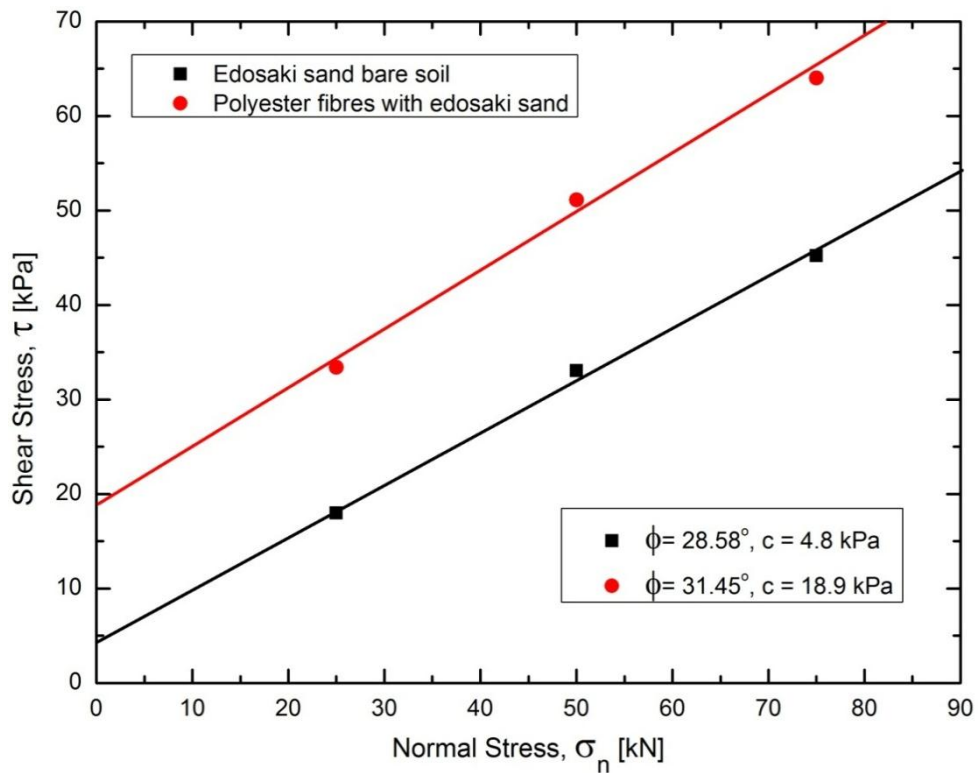


Figure 4-8: Edosaki sand specimens with and without 2% of polyester fibres

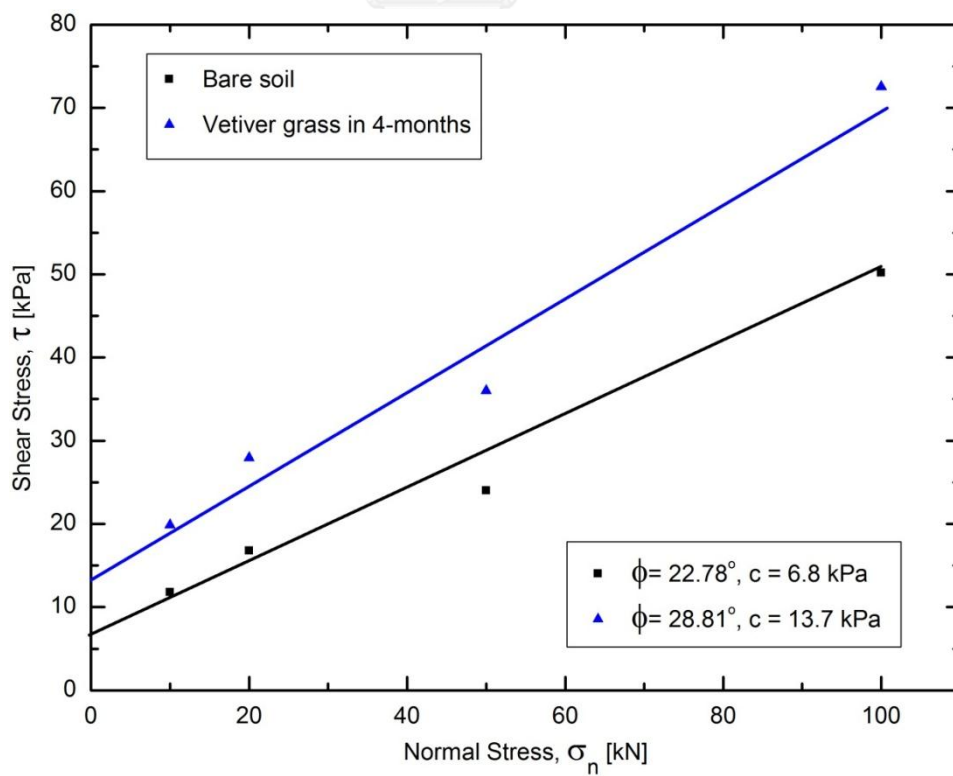


Figure 4-9: 4 months old single vetiver from direct shear test

4.6 Description of centrifuge model tests

Centrifuge model tests were conducted on the Tokyo Tech Mark III centrifuge at a 50g of centrifugal acceleration. The steps of centrifuge model tests have shown in the flow chart on Figure 4-10.

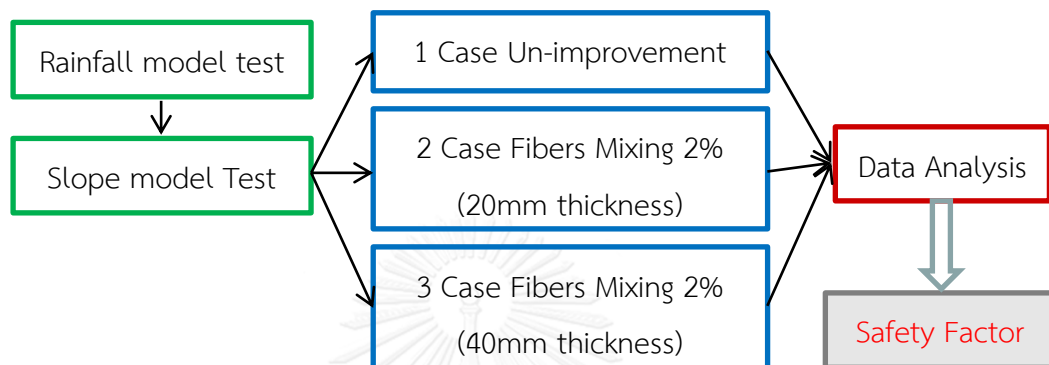
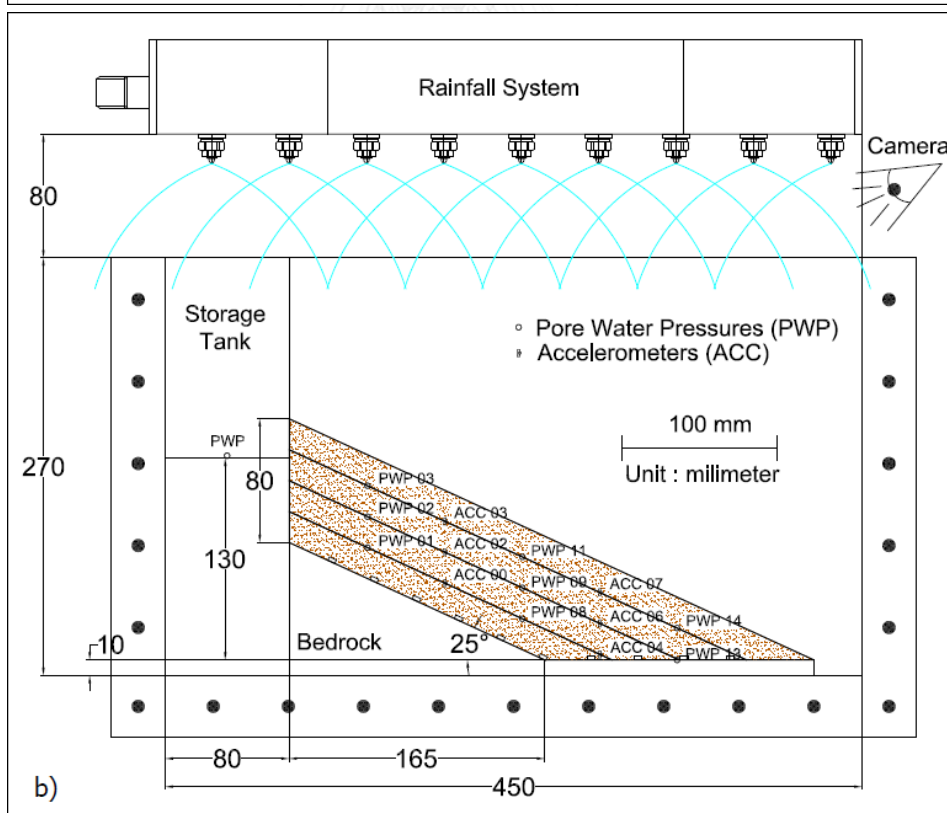
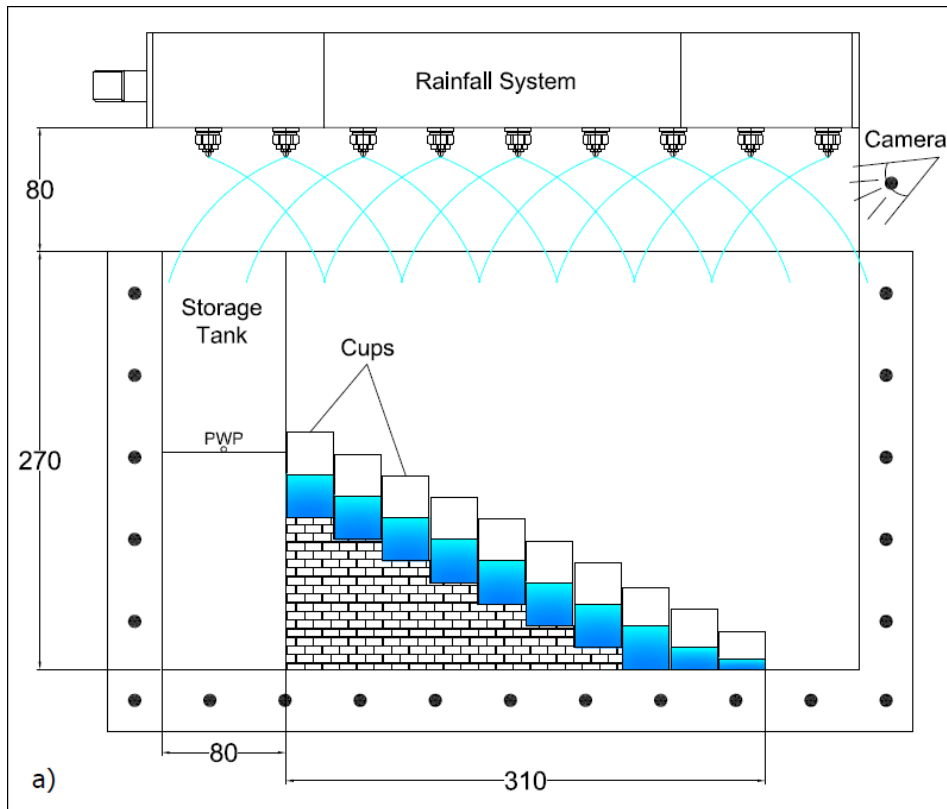


Figure 4-10: Flow chart of centrifuge model test

Figure 4-11 shows the model configurations of all the tests. As shown in the flow chart (Fig. 4.10), there are two steps in centrifuge model tests. First step, rainfall model test was performed at the first place before others started (Fig. 4.11a). This test was conducted to define the air pressure and water pressure which will be used in the second step. Second step, there are three different model geometries (case 1 to 3) (Fig. 4.11b, c, and d). All the models in this step have been performed for slope stability by using rainfall intensity from the first step. For case 1, the model simulated a homogeneous sandy soil profile (Edosaki sand) (Fig. 4.11b). For case 2, the model simulated a two layered of soil profile which is consisting of one Edosaki sand layer at the bottom and other one layer is 20 mm of Edosaki sand mixed with polyester fibres on the top surface (Fig. 4.11c). For case 3, the model simulated a two layered as well which is consisting of one Edosaki sand layer at the bottom and other one layer is 40 mm of Edosaki sand mixed with polyester fibres on the top surface (Fig. 4.11d).



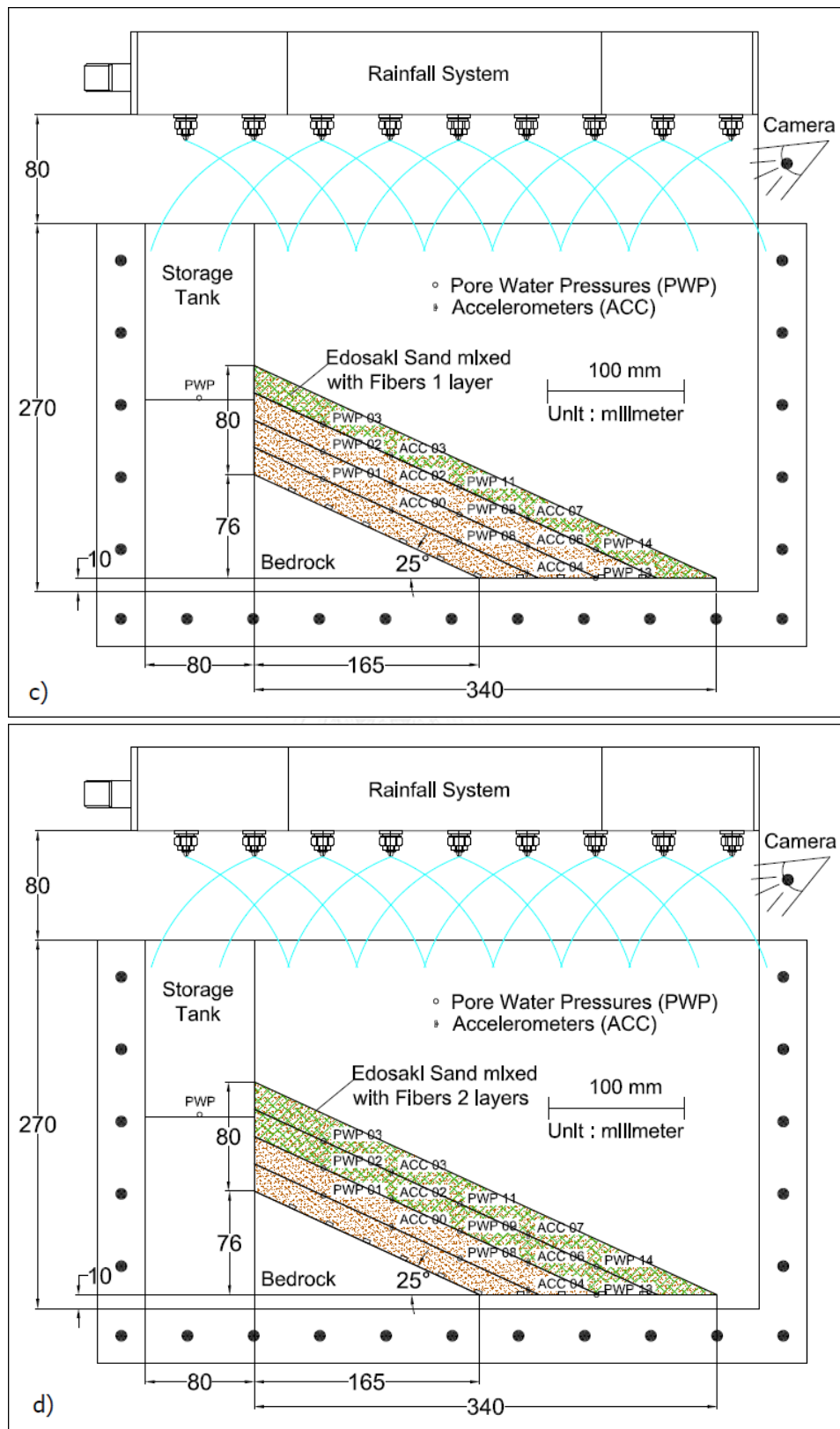


Figure 4-11: The detail schematic of centrifuge model tests: a) rainfall model test, b) case 1, c) case 2, and d) case 3

4.6.1. Rainfall model test

As the standard for heavy rainfall conditions in prototype scale, (Llasat, 2001) has mentioned the classification of rainfall intensity in the Table 4-2. The requirement to simulate the heavy rainfall is based on the air pressure and water pressure, which is important to obtain an impact pressure in the centrifuge. The pneumatic spray nozzle (BIMV45075) (see Fig. 4-12) was chosen for this rainfall simulation. Figure 4-13 shows the schematic of centrifuge for rainfall simulation system between the pressure supply air pressure (P_a) and water pressure (P_w). The rainfall simulator device of 9 nozzles was installed on the top of the steel box with 80 mm height. The small tank was installed as well in the left side of the steel box (Fig. 4-5a). This tank is called water storage tank. In addition, 50 cups were put inside the steel box on the 25° of the slope angle. These cups were used to store the water from the sprayer nozzle. The rainfall intensity was measured from the water storage tank and cups by the equation:

$$r = \left(\frac{R}{t} \right) \quad (4-1)$$

Where r is rainfall intensity, R is amount of rainfall drop, and t is rainfall time duration. During the spinning of the centrifuge, plastic sheets were put on the top covered on the steel box to prevent the effects of high speed wind on the rainfall drop. Based on the results of the various series of preliminary experiments, air pressure $P_a = 0.3$ MPa and water pressure $P_w = 0.45$ MPa were chosen for providing the rainfall onto the slope. Moreover, the combination of these two pressures could provide the rainfall intensity 33.75 mm/h in the storage tank and 19.1 mm/h on the slope area. Table 4-3 the summaries of the rainfall simulation results between model scale and prototype scale.



Figure 4-12: Rainfall simulator apparatus

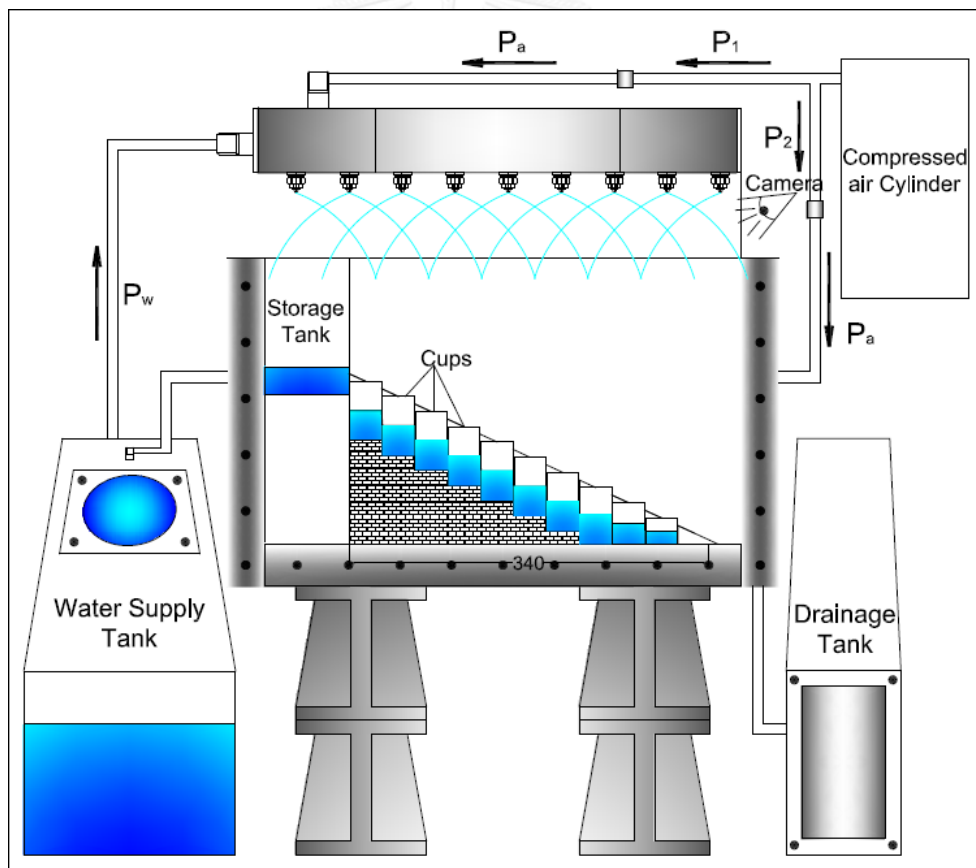


Figure 4-13: Schematic rainfall system in centrifuge test

Table 4-2: Classification of Rainfall intensity (Llasat, 2001)

Classification	Rainfall Intensity (mm/h)
Light	$I \leq 2$
Moderate	$2 < I \leq 15$
Heavy	$15 < I \leq 30$
Very heavy	$30 < I \leq 60$
Torrential	$I > 60$

Table 4-3: Summaries of the rainfall model test

Scale		Time (s)	A. Rainfall (mm)	R. Intensity
Location				
Model	Storage. T	32	15	0.47 (mm/s)
	Slope Area		8.48	0.27 (mm/s)
Prototype	Storage. T	22h22min	750	33.75 (mm/h)
	Slope Area		424.23	19.1 (mm/h)

4.6.2. Centrifuge slope stability model tests and testing procedure

The slope model was constructed inside the steel box, which has the inner dimensions of 450 mm × 150 mm × 270 mm (Fig. 4.5a)). A side view of the experimental system is schematically illustrated in Figure 4-14. The target of this study is the slope whose shallower portion is rooted. To examine the reinforcing effect of the roots against slope failure, the rooting depth, i.e., the thickness of the reinforced zone is selected as a parameter. The slope model consists of two parts, one is bedrock part and the other is soil part. The bedrock part (see Fig. 4.5b)) was made of aluminium plates and was placed on a 10 mm-thick acrylic plate. The soil slope part was made of Edosaki sand. It consists of four layers and its total thickness

is 80 mm high in the model scale. The soil was dynamically compacted with compaction degree of 80% for each layer. The pore water pressure transducers (PWPs) and the accelerometers (ACCs) were installed in the soil layers during the compaction to measure the pore water pressure and the soil slope displacement. The accelerometer was used as an inclinometer and the slope displacement was calculated by integrating the inclination along depth. After finishing the soil compaction, the noodles were installed between the model slope and the front transparent window so that deformation of the slope can be clearly observed. The soil displacements were measured with a combination of the accelerometer and the video record through the front transparent window of the steel box. In the test, three model cases were conducted as summarized in the flow chart (Fig. 4.10): (1) a case without reinforcement, (2) a case with a 20-mm of 2% fibre-reinforced surface layer, which is equivalent to 1 m deep of vegetation root (or approximately 4 months growth of vetiver) and (3) a case with a 40-mm of 2% fibre-reinforced surface layer, which is equivalent to 2 m deep of vegetation root (or approximately 6 months growth of vetiver). Figure 4-14 illustrates all three cases with the schematic of centrifuge modelling tests system. At the end of the model preparation, the soil slope and the steel box were placed onto the centrifuge platform.

For the test, the centrifuge had spun up to 50 times of Earth's gravity (50g); the slope model was 4 m height in the prototype scale. The air pressure and water pressure were set to the prescribed values and the rainfall test was provided by opening solenoid valves.

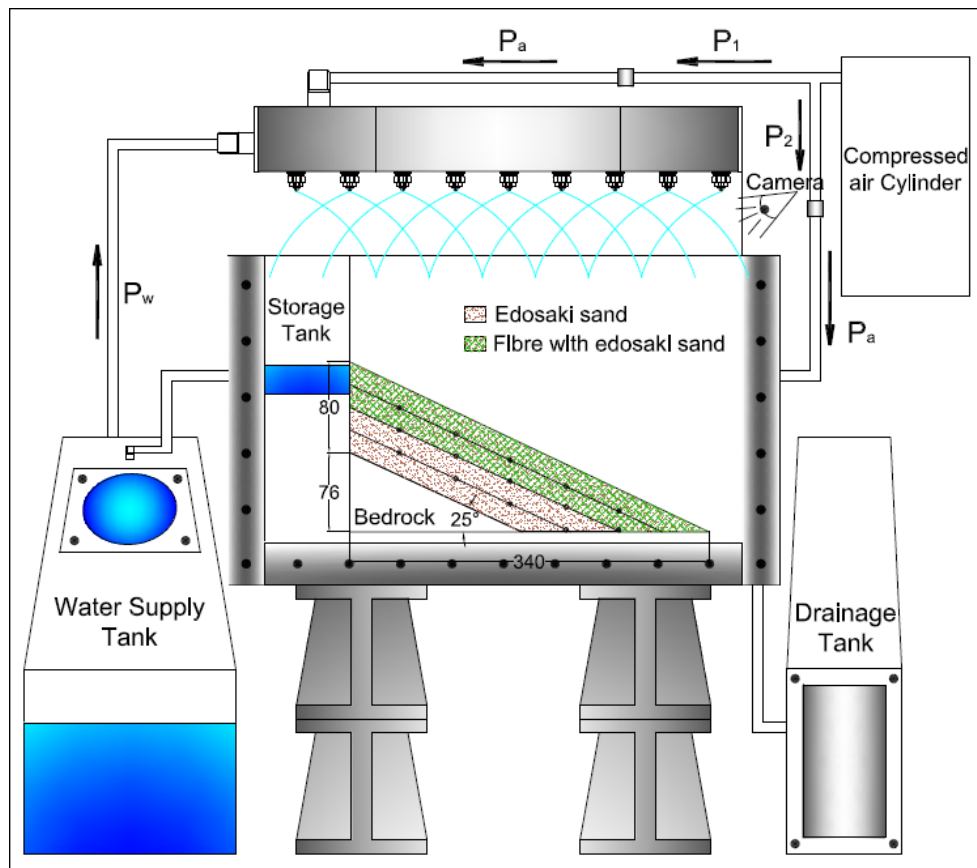


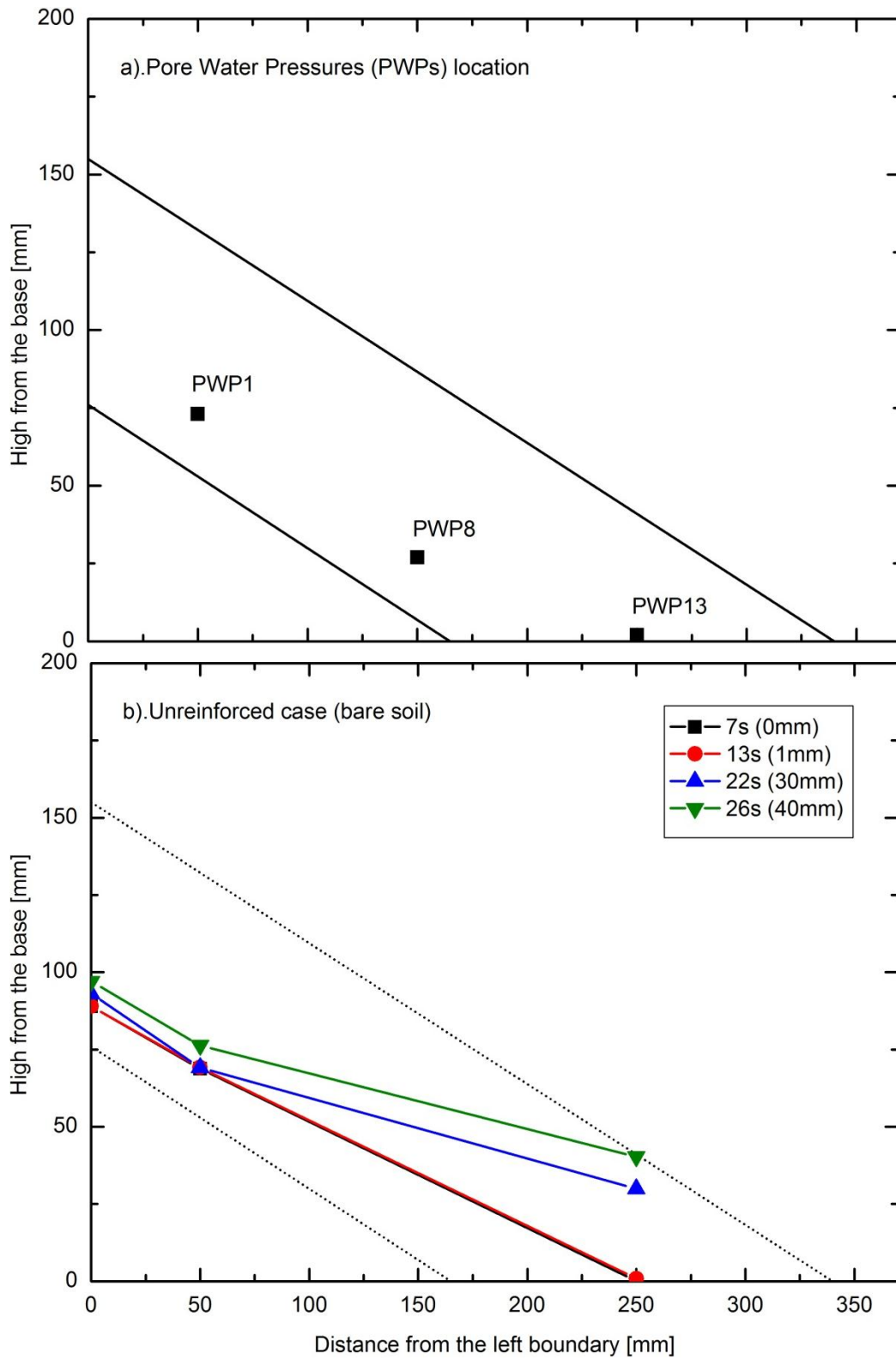
Figure 4-14: Schematic slope testing systems for centrifuge tests

4.7 Test Results and Discussion

4.7.1. Test results

4.7.1.1. Phreatic surface and slope displacement

Figure 4-15 shows the variations of phreatic surface within the soil slope. Position of the phreatic surface is calculated from the pore water pressure measured by the PWP's shown in Figure 4-15a). The phreatic surface for all cases was observed in which the phreatic lines are raised up at the toe of the slope between the boundary of soil and bedrock. Calculated slope displacements at the upslope and mid-slope using the accelerometers at relevant times are plotted in Figures 4-16 – 4-18 for all the cases.



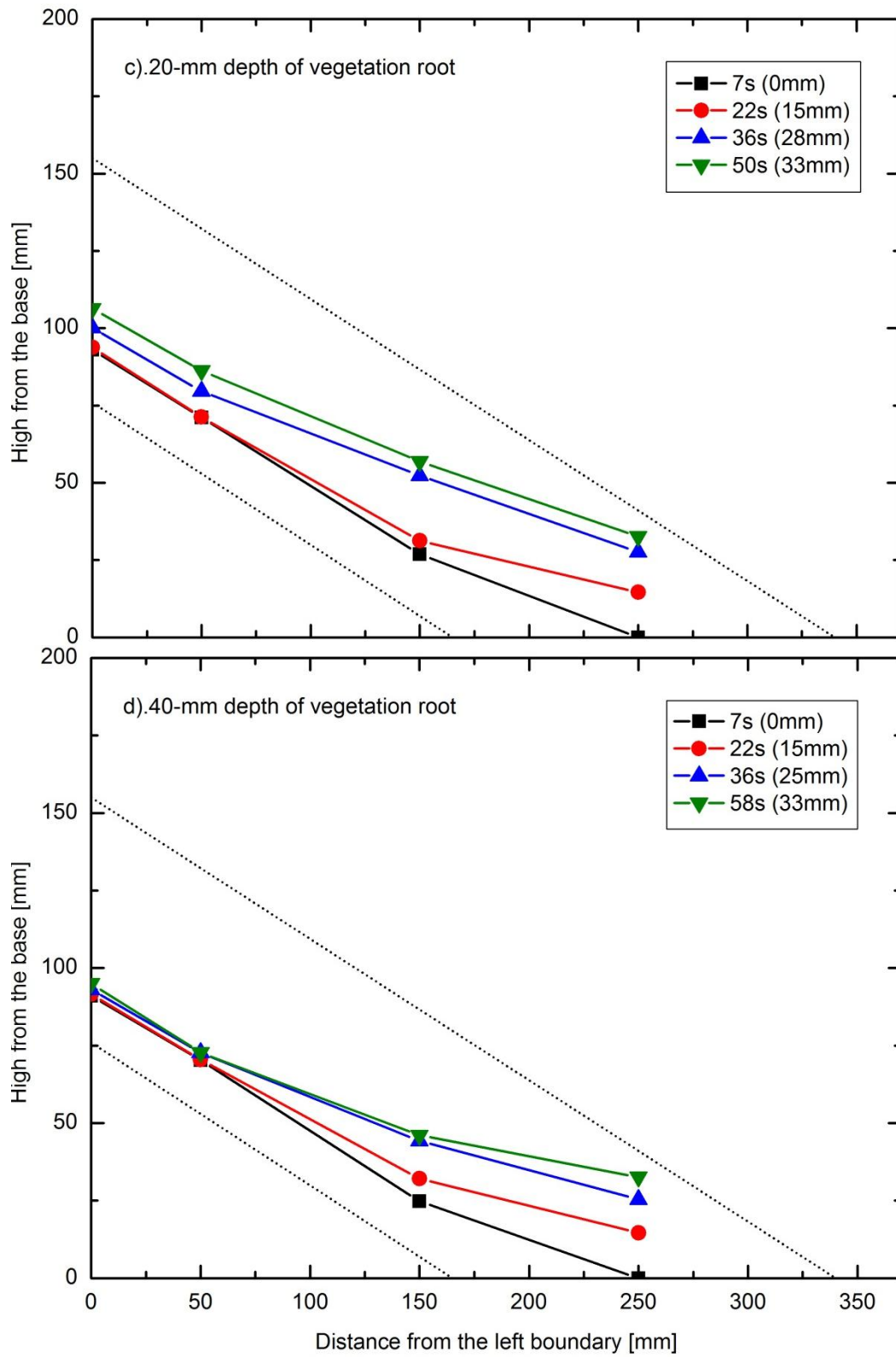


Figure 4-15: Variation of phreatic surface and location of pore water pressure gauges used: a) Pore water pressure location, b) Case 1, c) Case 2, and d) Case 3

In Case 1 (Fig. 4.15b), the rain was provided for 26s in the model scale ($\equiv 26s \times 50^2 = 65,000s \equiv 18\text{hr}$ in the prototype scale). Since the model slope was partially saturated before rainfall, the initial pore water pressure was negative due to suction. It is observed that the pore water pressure at PWP13 starts increasing around 1mm (5cm) at 13s in the model scale (9hrs in the prototype scale). The slope starts showing the movement based on the ACCs reading (Fig. 4.16a). At the time of 22s (15hr), the general failure of the slope has occurred at the toe slope with the pressure head around 30mm (1.5m) at PWP13. Once the pressure head reaches around 40mm at PWP13, the slope was collapsed with a relatively deep slip surface as shown in Figure 4-16b. According to the accelerometer reading (Fig. 4.16a) and the video observation has shown that the slope has started to collapse from the toe of the slope and progressively moves upward. In the cases with the model vegetation (Cases 2 and 3), at PWP13 the pore water pressure started showing change around 14s (10hr) for Case 2 (Fig. 4.15c) with 1.5mm (0.075m) of water head while Case 3 (Fig. 4.15d) is 1.3mm (0.065m) at this time and there is a very small change of the slope displacement in both cases (Fig. 4.17a and 4.18a). At the time 22s (15hr), the water head at PWP13 reached to 15mm (0.75m) for Case 2 and 14mm (0.7m) for Case 3. It was observed that once the phreatic surface reaches at 28mm (1.4m) for Case 2 and 25mm (1.25m) for Case 3 and the slope has deformed with small displacement (Fig. 4.17a and 4.18a) with time 36s (25hr). In this stage, the water head of Case 3 was slowly raised up due to the fibers mixing. Based on the permeability test shown that the infiltration of rainwater could be delayed by the fibers (see Table 4-1) and (H. Rahardjo et al., 2012) also mentioned on the effectiveness of the vetiver roots in minimising the infiltration into greater depth. At the end of the precipitation, the pressure head is reached to 33mm at 50s (35hr) and 33mm at 58s (40hr) for Case 2 and 3, respectively. The displacement in this stage has shown that the soil displacement is moderate for Case 2 (Fig. 4.17) and limited around the toe slope for Case 3 (Fig. 4.18), compared to Case 1. There is no collapse in Cases 2 and 3. This is caused by the effect of the model roots, which tie up the soil particles and prevent

formation of the crack on the slope surface. Rather uniform deformation of the slope in Cases 2 and 3 (see Figs. 4.17b and 4.18b) supports this effect of the fibers.

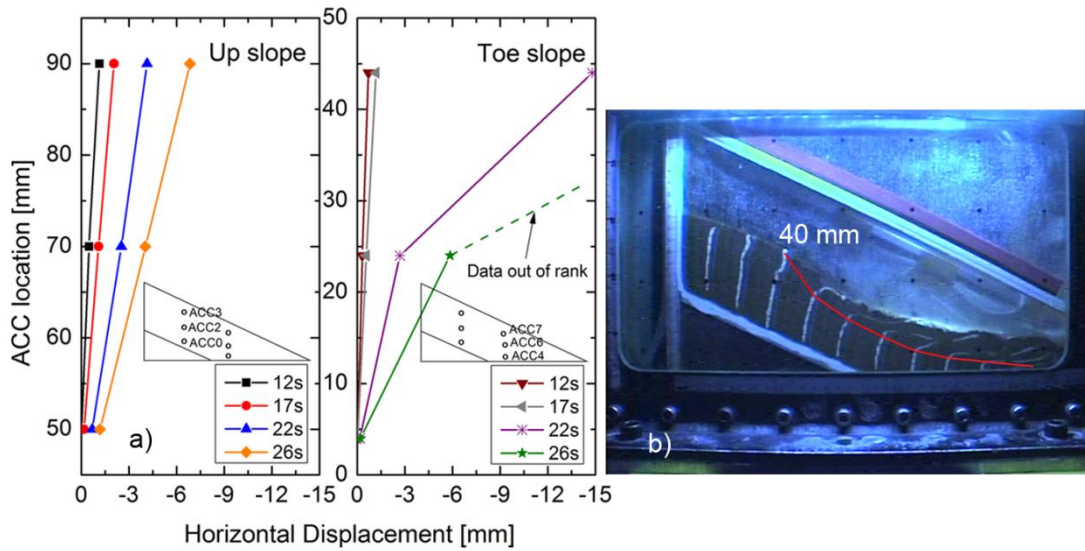


Figure 4-16: Slope displacement for case 1: (a) displacement calculated from ACCs; (b) slip surface of soil slope at 26 s

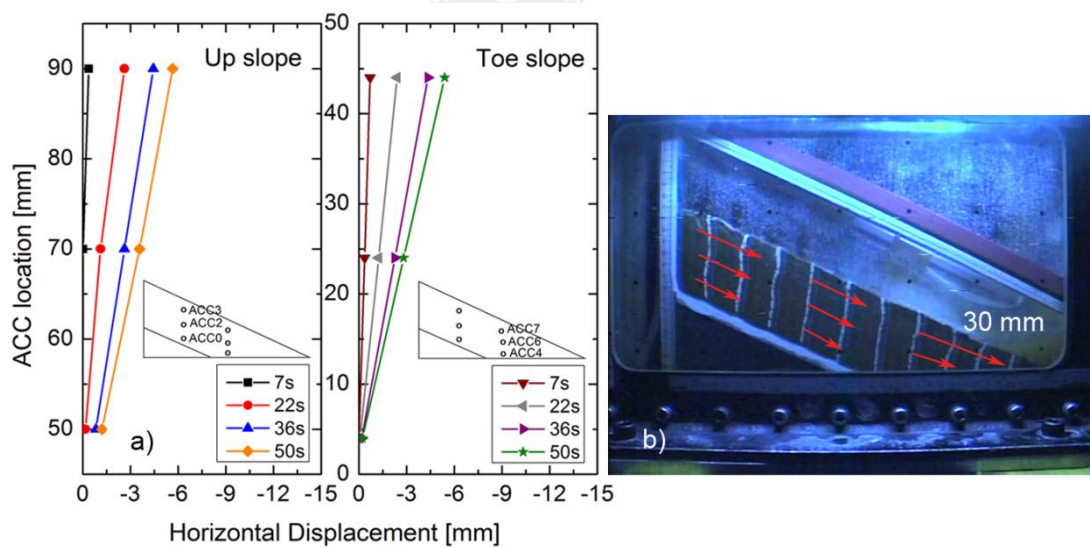


Figure 4-17: Slope displacement for case 2: (a) displacement calculated from ACCs; (b) exaggerated displacement vector at 50 s

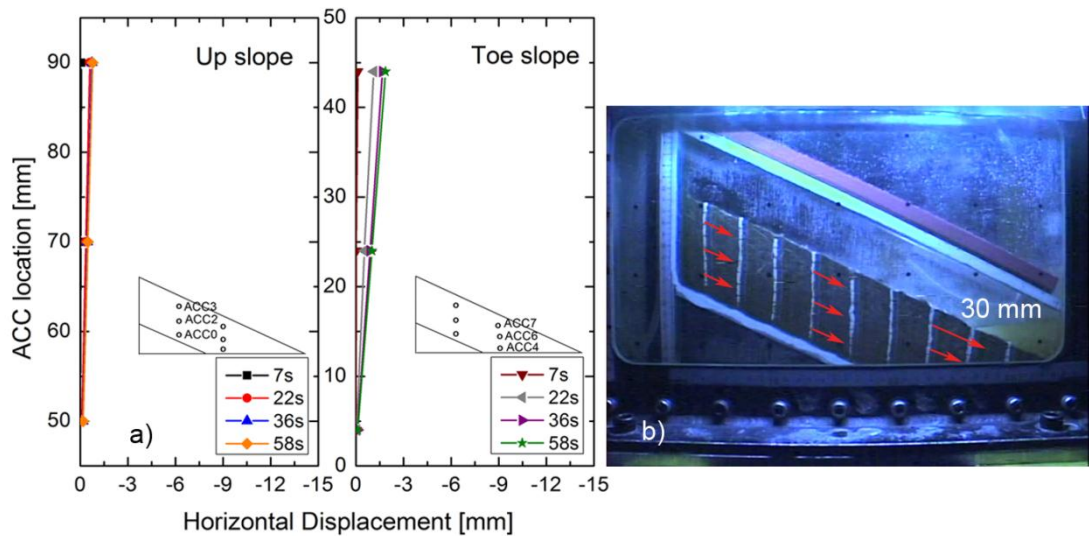


Figure 4-18: Slope displacement for case 3: (a) displacement calculated from ACCs; (b) exaggerated displacement vector at 58 s

4.7.1.2. Safety factor of slope model

Factor of safety for the slope model was determined by the infinite slope assumption which has assumed the water table is parallel to the soil slope. As mentioned in chapter 2 the safety factor that effect of vegetation on slope stability was calculated by using the equation from (Gray & Sotir, 1996). Figure 4-19 shows the results of the factors of safety calculated from the infinite slope assumption against the slope displacement. The initial factor of safety is 1.18 for all the cases. As can be seen in the figure, the infinite slope assumption could not be applied to root-reinforced case. This is due to the limitation of the infinite slope that the translational slip surface must pass to the weak stratum (i.e., between un-reinforced soil and bedrock). Therefore, the limit equilibrium method with a circular failure assumption might be a better approach to determine the factor of safety especially for the root-reinforce case. The analysis of safety factor for root reinforcement cases will be presented in chapter 5 by using the circular failure assumption from geoslope/w.

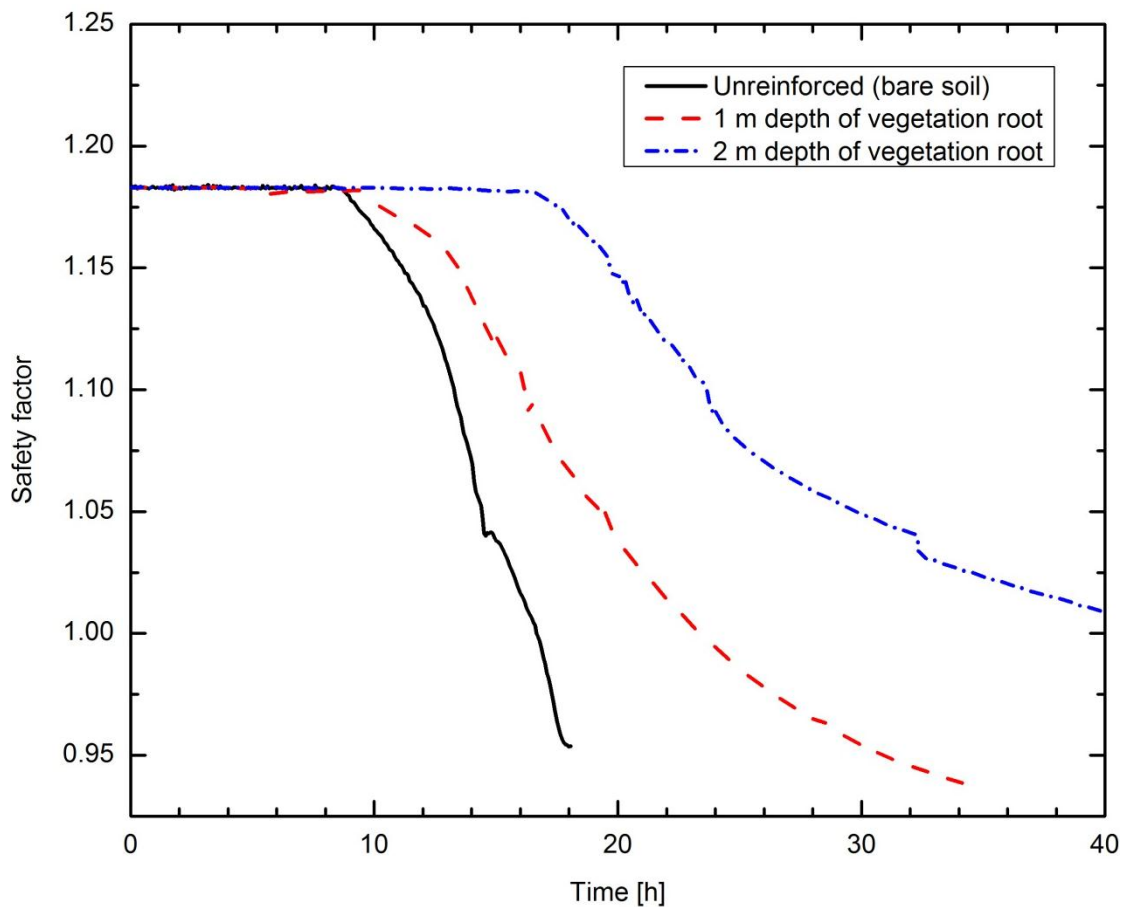


Figure 4-19: Relationships between safety factor with time history.

4.8 Results discussion

The results indicate that the bare soil slope was failed by raising the groundwater table, in which cracking started from the toe of the slope and progressively moved to the upslope. On the other hand, in the presence of the surface layer reinforced with fibres, the slopes deformed uniformly without collapse. This marked reinforcing effect is attributed to the sufficient reinforcement around the toe, otherwise the noticeable contribution of the reinforcement cannot be expected (e.g., (Sonnenberg et al., 2011; Sonnenberg et al., 2010)

Figure 4-20 plots changes of average water pressure head and displacement at the toe for all cases. Based on Figure 4-20a), the pressure head in Case 1 has reached to

1.2m at time 18hr while Case 2 is 1.3m at 35hr and Case 3 is 0.9m at 40hr. Hence, the pressure head of Case 1 is higher than the other two cases by comparing with time. Figure 4-20b), the displacement in Case 1 is shown a large displacement around 0.8m at time of 18hr and the other two cases just 0.3m at 35hr for Case 2 and 0.1m at 40hr for Case 3. According to the results, the tests have revealed that the fibers, i.e. the roots, could help to increase the soil strength of soil slope to prevent the failure and reduce the infiltration of rainfall into the ground to delay the groundwater table raising. These results are comparable to (H. Rahardjo et al., 2012). Table 4-4 summarises the test results.

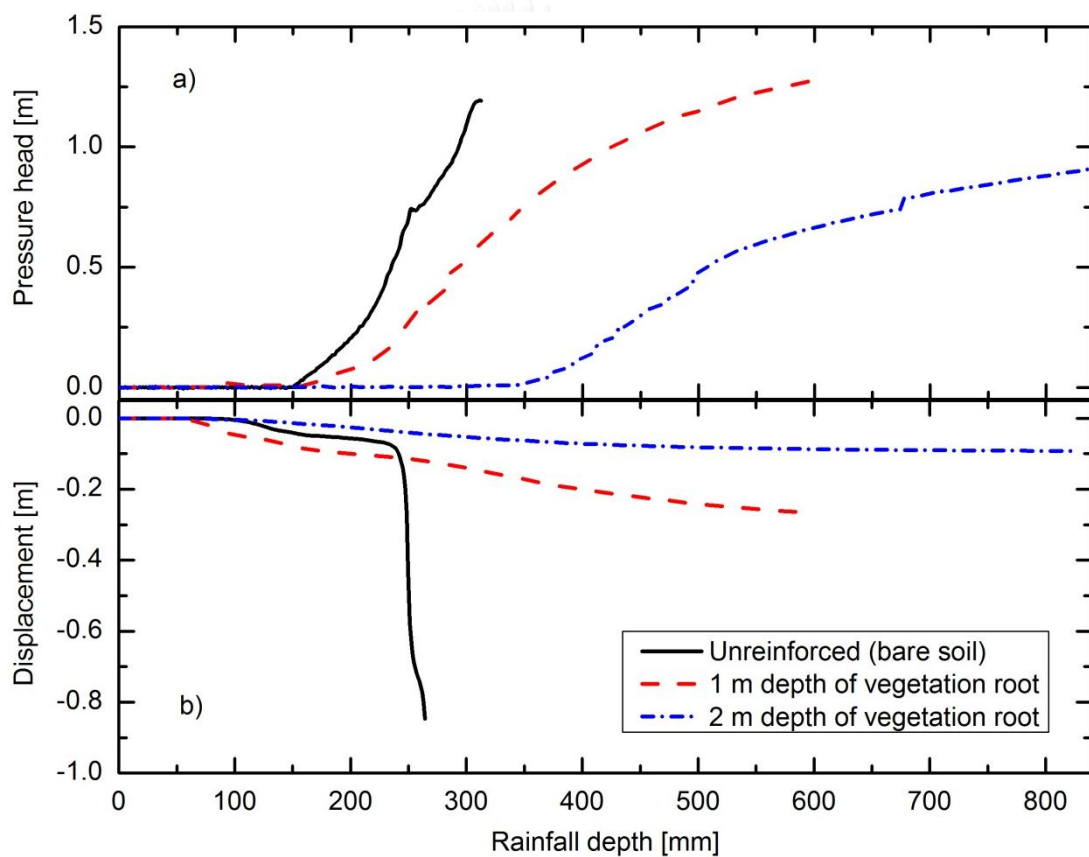


Figure 4-20: Evolutions of (a) average water pressure head; (b) displacement at toe slope

Table 4-4: Summaries of centrifuge tests

Case No.	Model case	Real case	Average of pressure head (m)	Total rainfall depth (mm)	Duration of rainfall (hr)	Slope deformation
1	Unreinforced	Bare soil	1.2	293.22	18	Collapsed
2	With 20-mm thick of fiber-reinforced surface layer	1-m depth of vegetation root (4 months growth of vetiver)	1.3	610.4	35	Moderate deformation (Uncollapsed)
3	40-mm thick of fiber-reinforced surface layer	2-m depth of vegetation root (6 months growth of vetiver)	0.9	835.2	40	Small deformation (Uncollapsed)

5 CHAPTER NUMERICAL MODELLING

5.1 Introduction

The slope stability analyses are performed to assess the safety and economic design of human made slopes or natural slopes (e.g. embankments, road cuts, open pit mining, excavation, and landfills). In the assessment of slopes, engineers primarily use the factor of safety values (SF) to determine how close or far slopes are from failure. When this ratio is greater than 1, the resistive shear strength is greater than the driving shear stress and the slope is considered stable. When this ratio is close to 1, the shear strength is nearly equal to the shear stress and the slope is close to failure. If FS is less than 1, the slope should have already failed. The limit equilibrium analysis method and the seepage finite element approach to the analysis of slope stability have been widely used for many years. Many numerical simulations with related software have been used in the slope stability analysis. To evaluate the influence of root vegetation during rainfall in the numerical analysis on the stability of unsaturated soil slopes, the limit equilibrium analysis method and the seepage finite element approach should be used. For example, (Tiwari, Bhandary, Yatabe, & Bhat, 2013) studied the finite element method with a new numerical scheme to observe the effects of root reinforcement on slope stability based on the effectiveness of root area ratio which helps to improve the level of safety. Limit equilibrium types of analysis for assessing the stability of earth slopes have been used for many decades in geotechnical engineering. The software code Slope/w (Geo-slope 2007 (Krahn, 2008)) allowed geotechnical engineers to carry out the limit equilibrium of slope stability analysis for existing natural slopes, un-reinforced man-made slopes, or slope reinforcement. The program uses many methods including Bishop's Modified method, Janbu's Simplified method, and Morgenstern-Price method, among others. Slope/w allows these methods to be applied to circular,

composite, and non-circular surfaces. In 1916, (Petterson, 1955) presented a stability analysis of slopes where the slip surface was divided into slices and was assumed as circular. The ordinary, or Swedish, method of slices was introduced by (Fellenius, 1936). (Janbu, 1954) and (A. W. Bishop, 1955) developed advances for the method. Transient seepage analysis is very powerful and useful in predicting rainfall-induced landslides. Based on the definition, the spatial and temporal change in the environmental conditions is defined by transient analysis as a time dependent analysis (Lu & Likos, 2004). Related to rainfall, the loss of the shear strength of the soil, seepage erosion, seepage force and the formation of tension cracks have caused many landslides to occur. (F. Cai & Ugai, 2004) studied the finite element analysis using transient flow through unsaturated soil to define the hydraulic characteristic, a method to consider boundary condition and rainfall intensity on water pressure in the soil slope.

5.2 Slope/W using limit equilibrium analysis

Slope/W is a kind of leading software product that is used to compute the level of safety of earth and rock slopes. With slope/W, the variety of the slip surface, pore-water pressure conditions, soil properties, analysis methods and loading conditions can be analyzed for both simple and complex problems. By using limit equilibrium, it can model slip surface geometry, complex stratigraphy, heterogeneous soil types, and variable pore-water pressure conditions with a large selection of soil models. slope/W provides essentially the same level of safety as the published solutions by (D. Fredlund, Krahn, & Pufahl, 1981), who used the stability programs from the University of Alberta and the University of Saskatchewan. This confirms that slope/W is formulated correctly.

The limit equilibrium method uses the Mohr-Coulomb criterion to compute the safety level of the slope. It has assumed that the soil shear strength along the potential circular slip surface is fully mobilized. The two-dimensional limit equilibrium analyses adopted here includes the Ordinary, Bishop, and Morgenstern-

Price methods and the calculations were performed using commercial Slope/W software (Krahn, 2008). Fredlund at the University of Saskatchewan developed a general limit equilibrium (GLE) formulation which is a method encompassing the key elements of all the other methods available in Slope/W (D. Fredlund & Krahn, 1977) (D. Fredlund et al., 1981). The GLE formulation is based on two safety factor equations. One equation provides the safety factor with respect to moment equilibrium F_m , while the other equation gives respect to horizontal force equilibrium, F_f (see chapter 2, section 2.10.1.1)

5.2.1. Ordinary of Fellenius method

The simplest form of the Ordinary factor of safety equation in the absence of any pore-pressures for a circular slip surface is given in the equation (5-1):

$$F.S = \frac{\sum (c\beta + N \tan(\phi'))}{\sum W \sin(\alpha)} = \frac{\sum S_{Resistance}}{\sum S_{Mobilized}} \quad (5-1)$$

Where, c is the cohesion, β is the slice base length, N is the base normal ($W \cos(\alpha)$), ϕ is the friction angle, W is the slice weight, and α is the slice base inclination.

5.2.2. Bishop's simplified method

In the 1950's simplified methods of (Janbu, 1954) included inter-slice normal forces but ignored the inter-slice shear forces. A simple form of the Bishop's simplified factor of safety equation without any pore water pressure is:

$$F.S = \frac{1}{\sum W \sin(\alpha)} \sum \left[\frac{c\beta + W \tan(\phi) - \frac{c\beta}{FS} \sin(\alpha) \tan(\phi)}{m_a} \right] \quad (5-2)$$

FS is on both sides of the equation as noted above. The equation is not unlike the Ordinary factor of safety equation except for the m_a term, which is defined as:

$$m_a = \cos(\alpha) + \frac{\sin(\alpha) \tan(\phi)}{FS} \quad (5-2.1)$$

5.2.3. Morgenstern-Price method

This method was developed by (Morgenstern & Price, 1965) and (Spencer, 1967), which considered not only the normal and tangential equilibrium but also the moment equilibrium for each slice in circular and non-circular slip surfaces. It resolved the issue of safety level analysis using the summation of forces tangential and normal to the base of a slice and the summation of moments about the base of each slice in the center. The equations were written for a slice of infinitesimal thickness. The force and moment equilibrium equations were combined and a modified Newton-Raphson numerical technique was used to compute the safety factor satisfying force and moment equilibrium. The solution required an arbitrary assumption regarding the direction of the resultant of the shear and normal forces at inter-slice.

5.3 Seep/W using transient analysis

Seep/W is defined as a finite element software product which is under Geostudio, used to compute the pore water pressure distribution and the movement of water flow through porous materials like soil and rock. It is defined on the basis of water flow through saturated soil by following Darcy's Law. The Seep/W model is formulated to solve 2-dimensional flow situations with single and/or multiple soil layers. The direction of groundwater flow can be analyzed in this seep/w. The difference between input flux and output flux is set to zero at all times for the under steady state condition. For finite element calculations, the Seep/W model is conducted by dividing the nodes and at each node the elevation of the water level is calculated. In the Seep/W models, the following two assumptions are made: 1) the aquifer is heterogeneous and isotropic, and (ii) the aquifer is partly confined and partly unconfined. Good quality output graphics allow a visual display of

equipotential lines and flow paths, and contours can be plotted for different properties like pore pressures, seepage velocities, and gradients. Computations include flow quantities and uplift pressures at user-selected locations in the model.

To understand how rainfall infiltration changes the unsaturation zone as well as the pore-water pressures in a slope, transient seepage analysis is needed. To solve the transient seepage problem, measured flow properties of unsaturated soils are needed. These are primarily the soil water content and the soil permeability as the function of soil suction. When these are determined, the differential equations governing flows through unsaturated soils can be solved iteratively by the FEM, as in programs like Seep/W, with the appropriate boundary conditions to simulate rainfall flux on the ground surface.

5.4 Unsaturated soil mechanics principle

Two stress state variables are required to describe the behaviour of unsaturated soil (D. G. Fredlund & Morgenstern, 1977): net normal stress ($\sigma - u_a$), and matric suction ($u_a - u_w$), where σ is total normal stress, u_a is the pore air pressure and u_w is the pore water pressure. The relationships between the shear strength or volume change with stress state variables are expressed as constitutive equations. All constitutive equations used to describe the mechanical behaviour of unsaturated soils can be presented as an extension of the equations used for saturated soils. Table 5-1 summarises several principle unsaturated soil mechanics equations.

To understand the significance of rainfall induced pore-water pressure changes on slope stability; two aspects of unsaturated soil behavior must be appreciated. The first is the components of the strength in unsaturated soils, and the second is the flow of water through unsaturated soils. The shear strength of unsaturated soils can be described by the extended Mohr-Coulomb criteria as shown in table 5-1 equation (5-4):

The significance of the strength equation is that the matric suction component is a function of the negative pore water pressure in the soils. The soil suction is reduced

with rainfall infiltration, which increases the pore-water pressure and hence reduces the soil shear strength. Also saturation of the soils above the vadose zone leads to a heavier soil mass, thereby increasing the loads on a potential slip surface.

Table 5-1: Principle and equations for unsaturated soil mechanics modified from (Harianto Rahardjo & Satyanaga, 2014)

Principle	Unsaturated soil	Equation
Stress state variables	$(\sigma - u_a)$ and $(u_a - u_w)$	(5-3)
Shear strength	$\tau = c' + (\sigma - u_a) \tan \phi' + (u_a - u_w) \tan \phi_b$	(5-4)
	$c = c' + (u_a - u_w) \tan \phi_b$	(5-5)
Flow law for water	$v_w = -k_w (u_a - u_w) (\partial h_w / \partial y)$	(5-6)
(Darcy's law)	$h_w = y + (u_w / \rho_w g)$	(5-7)

Where τ is shear strength, c' is effective cohesion, ϕ' is effective friction angle, ϕ_b is friction angle with respect to matric suction in unsaturated soils, $(\sigma - u_a)$ is net normal stress, $(u_a - u_w)$ is matric suction, k_w is unsaturated hydraulic conductivity, v_w is the low rate of water, $\partial h_w / \partial y$ is hydraulic head gradient in y-direction, g is gravitational acceleration, y is elevation at a certain point, ρ_w is the density of water, and h_w is hydraulic head.

5.4.1. Soil water characteristic curve

SWCCs can either be measured in the laboratory or predicted using a grain-size distribution curve taking into account such factors as dry density, porosity, and void ratio (Aubertin, Mbonimpa, Bussi re, & Chapuis, 2003; M. D. Fredlund, Fredlund, & Wilson, 1997; Gupta & Larson, 1979; Tyler & Wheatcraft, 1989). Figure 5-1 shows the volumetric of water content which is calculated by (van Genuchten, 1980) using grain size assumption from geo-slope 2007 for Edosaki sand with and without fibres.

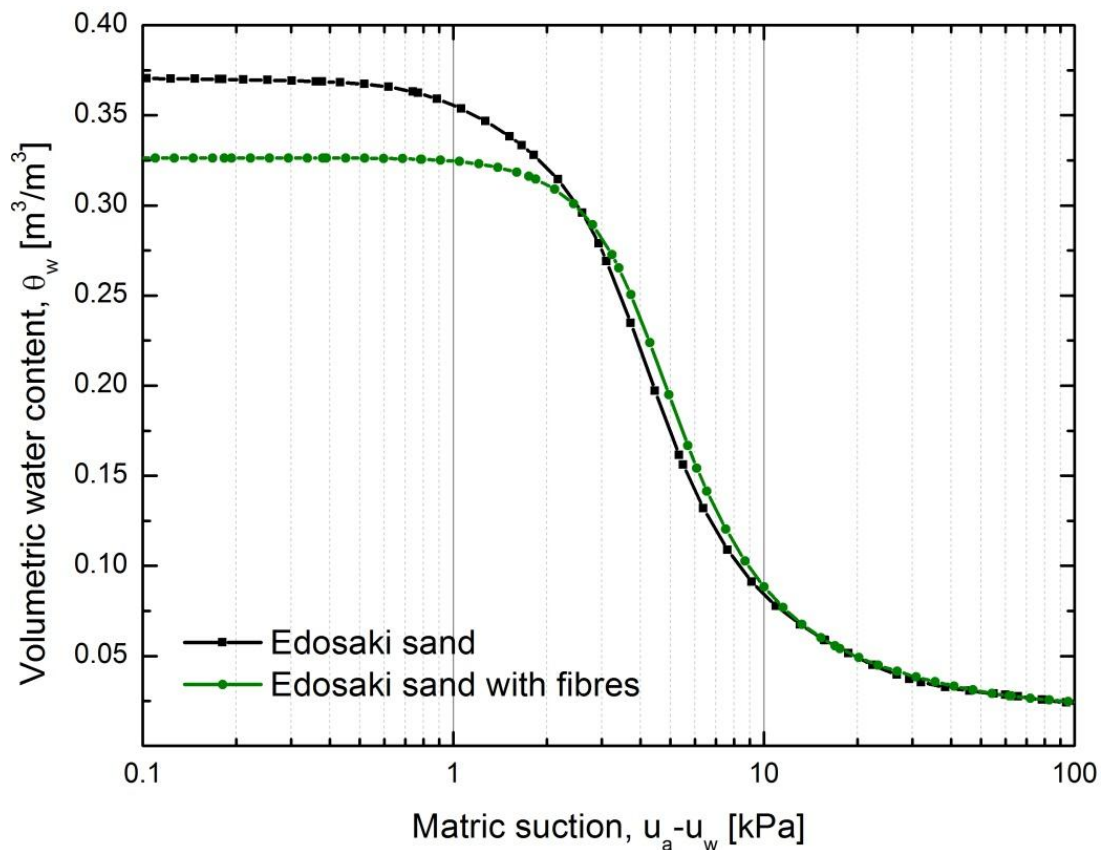


Figure 5-1: Fitting of soil water characteristic data using grain size assumption

5.4.2. Permeability function

Laboratory permeability tests were conducted to obtain saturated permeability k_s of the selected residual soils. The saturated permeability of Edosaki sand was then used in the parametric studies. Permeability functions of the investigated soils were determined indirectly from SWCC using grain size assumption from geo-slope 2007. The permeability functions of Edosaki sand soils with $k_s = 3.25 \times 10^{-5}$ m/s and the Edosaki sand with fibres is $k_s = 3.08 \times 10^{-5}$ m/s. Figure 5-2 shows two hydraulic conductivity coefficients of permeability of Edosaki sand with and without fibres. Nevertheless, predictive methods for unsaturated hydraulic conductivity have not advanced to a similar extent, nor have they been verified using laboratory measurements to a similar extent. Therefore, it is important to verify the accuracy of the unsaturated hydraulic conductivity predictive methods by comparing them with laboratory measurements.

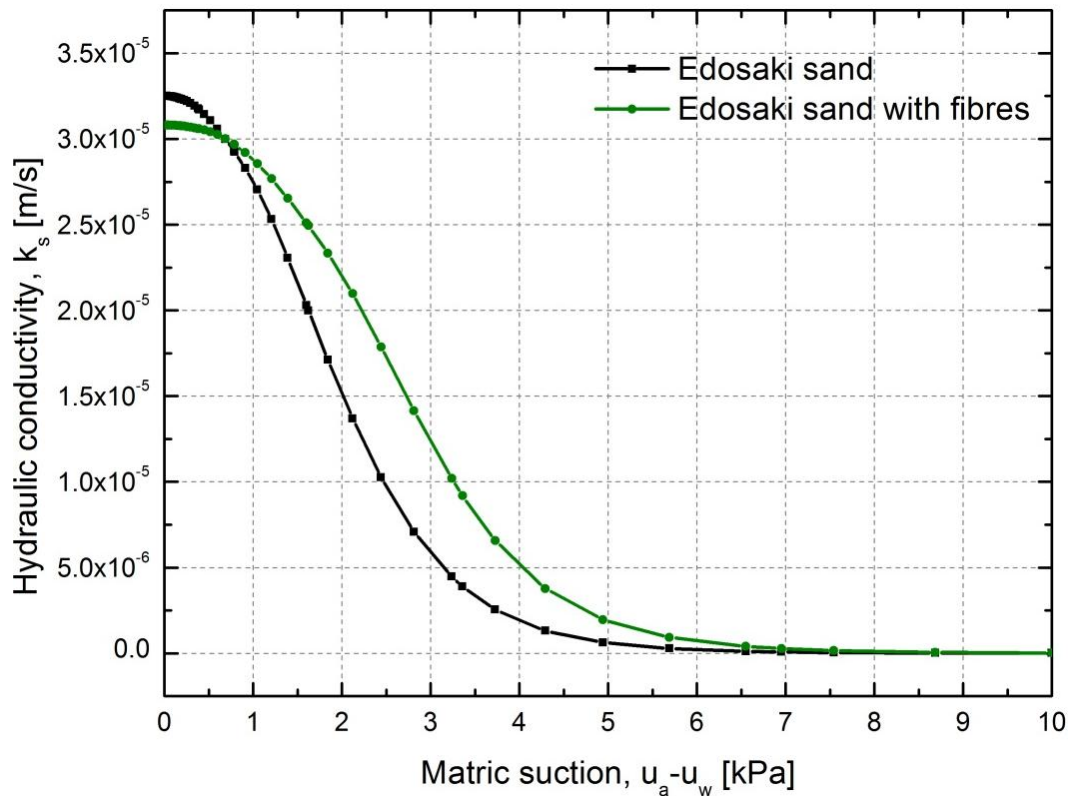


Figure 5-2: Hydraulic conductivity with soil suction using grain size assumption

5.5 Numerical analysis

Numerical analysis has been used to enhance the understanding of the effect of suction loss due to rainfall infiltration on slope stability. In the analysis, three cases were modelled (i.e., without reinforcement, 1 m depth root-reinforcement and 2 m depth root-reinforcement). Each model was performed by using transient analysis to define the pore water pressure change in the soil slope. The slope stability analysis was performed by inputting the results from seepage/w to define the factor of safety with time.

5.5.1. Model of root reinforcement

Recently, slope stability using the effect of vegetation roots as soil reinforcement was investigated by the finite element method. The slope geometry is broken down into

the small element by the discretisation process of the finite element method and this facilitates the incorporation of the effects of vegetation in the slope stability analysis. The individual soil element of soil properties, which is influenced by vegetation roots, has taken into account the slope stability analysis in the effect of vegetation. For example, the addition of apparent cohesion of root reinforcement can increase the value of the cohesion soil element on the top layer.

5.5.2. Seepage and slope stability modelling

Two-dimensional seepage analyses were performed in this study using the finite-element software Seep/W from geo-slope. Simplified slope profiles with a homogeneous soil layer (one layer) were used in the parametric study. Typical SWCC (Fig. 5.1) and hydraulic conductivity (Fig. 5.2) were used in the numerical analyses. Boundary conditions were applied to the slope model for the transient seepage analyses. Non-ponding boundary condition was applied in order to prevent excessive accumulation of rainfall on the slope surface. The flux boundary q equal to the desired rainfall intensity 20 mm/h was applied to the surface of the slope for each case. The potential seepage face was also applied at the toe of the slope model. Figure 5-3a) shows the geometry of boundary condition for seepage analysis. The pore-water pressures were calculated in Seep/W for every time step at each node of the finite-element mesh. The pore-water pressure output of the seepage analyses was incorporated into the slope stability analyses. Slope stability analyses were performed using slope/W from geo-slope. The finite-element mesh of the slope model in seep/W was imported to slope/W. Figure 5-3b) shows the geometry of slope stability in slope/w. Typical soil properties were used in the slope stability analyses using Bishop's simplified and Morgenstern- Price methods. Table 5-2 summarized the soil material input in slope/w. The pore-water pressure distribution was selected for each time increment, and the corresponding level of safety was calculated.

Table 5-2: Input soil material for slope stability

Material	Edosaki sand	Edosaki + fibers
Model	Un-reinforced	Root-reinforced
Cohesion, c (kPa)	4.84	18.9
Friction angle, ϕ ($^{\circ}$)	28.58	31.45
Total unit weight, γ_t (kN/m ³)	14.84	15.18
Optimum water content, w_{opt} (%)	15	17

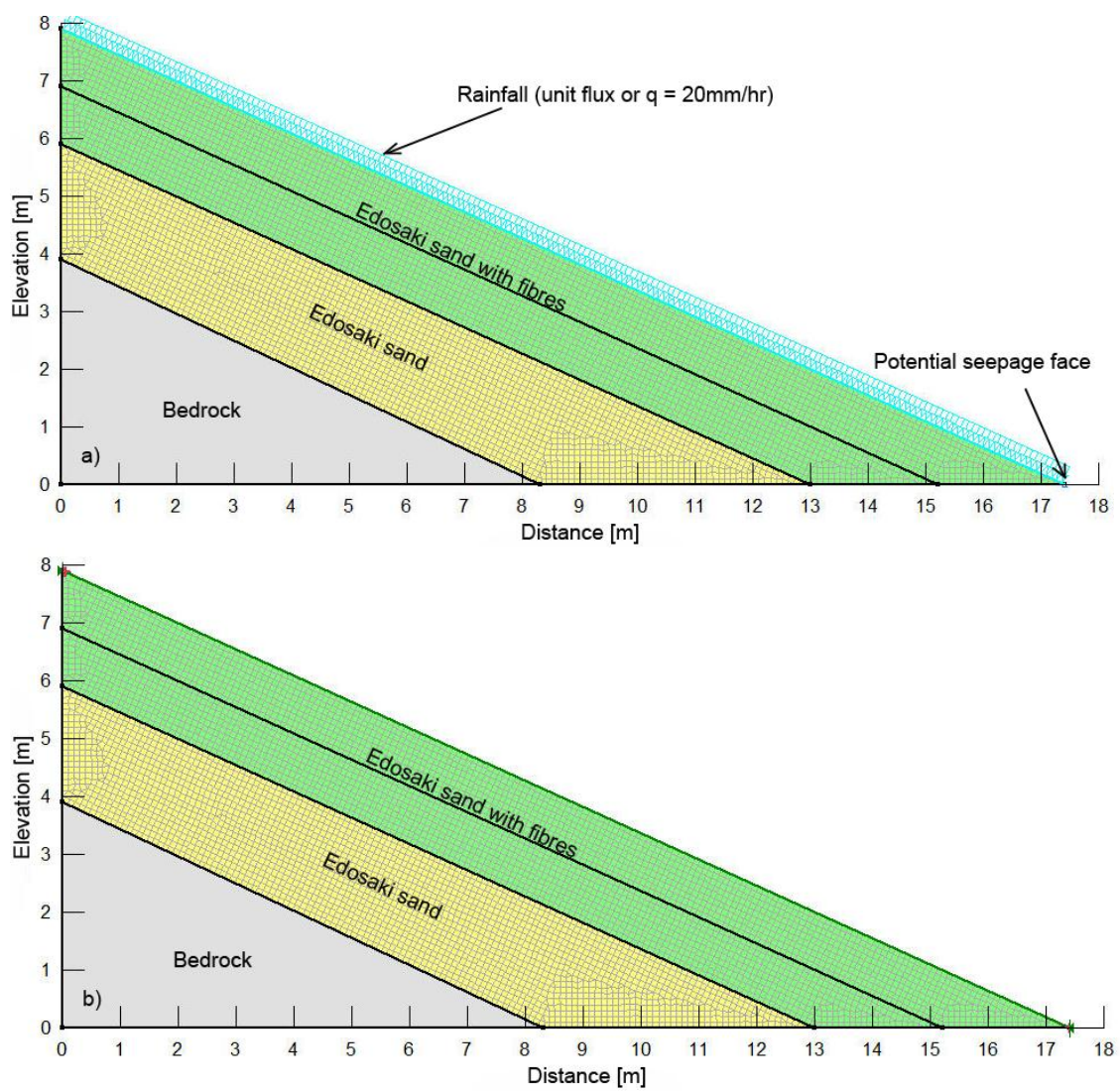


Figure 5-3: Geometry of boundary condition for slope models: a) for seepage analysis and b) for slope stability analysis

5.6 Results and discussion

5.6.1. Pore water pressure distribution

Figure 5-4 shows the pore water pressure contours distribution in the soil slope which is simulated from seepage/w with three different cases. The results showed that during rainfall pore water pressure in the soil slope moved gradually towards positive values. Figure 5-4a) shows the result for the un-reinforced case, where the pore water pressure increased 10 kPa from the toe of the slope while at the top slope showing a negative value with 18 hr duration of rainfall. For a 1 m depth of vegetation root case, Figure 5-4b) shows that a large amount of rainwater infiltrated into the slope and changed the pore water pressure from a negative to positive value with 20 kPa within 35 hr. For the last 2 m depth of vegetation root case (Fig. 5-4c)), pore water pressure increased up to 25 kPa within 40 hr. Based on these results, it is observed that pore water pressure increased from a negative value to a positive value due to the duration of rainfall.

5.6.2. Slip surface for factor of safety

Figure 5-5 shows the variation of slip surface and water table which was simulated from the slope/w. Due to the presence of the apparent root cohesion, the slip surface in the root-reinforced case was mostly developed along the bedrock of the slope (Fig. 5.5c)), while the slip surface was above the bedrock in the unreinforced case (Fig. 5.5a)) and 1 m depth of vegetation in the root case (Fig. 5.5b)). This might be due to the shear strength of the root fibre on the top layer being stronger than the soil layer below (Fig. 5.5c)). In addition, the analysis results indicate that the safety factor slightly increased from the case of the unreinforced to the case of the reinforced as summarized in Table 5-3. The safety factors calculated from the circular failure assumption are also comparable to those calculated from the infinite slope assumption for the case without reinforcement. According to the results, the shear strength of the unsaturated zone decreased and consequently the FS of the slope reduced during the rainfall. The minimum FS of 1.7 was observed at the end of rainfall ($t = 18$ hr). Figure 5-6 shows the variation of factor of safety for each case from Morgenstern & Price (1965) analysis computed by slope/W.

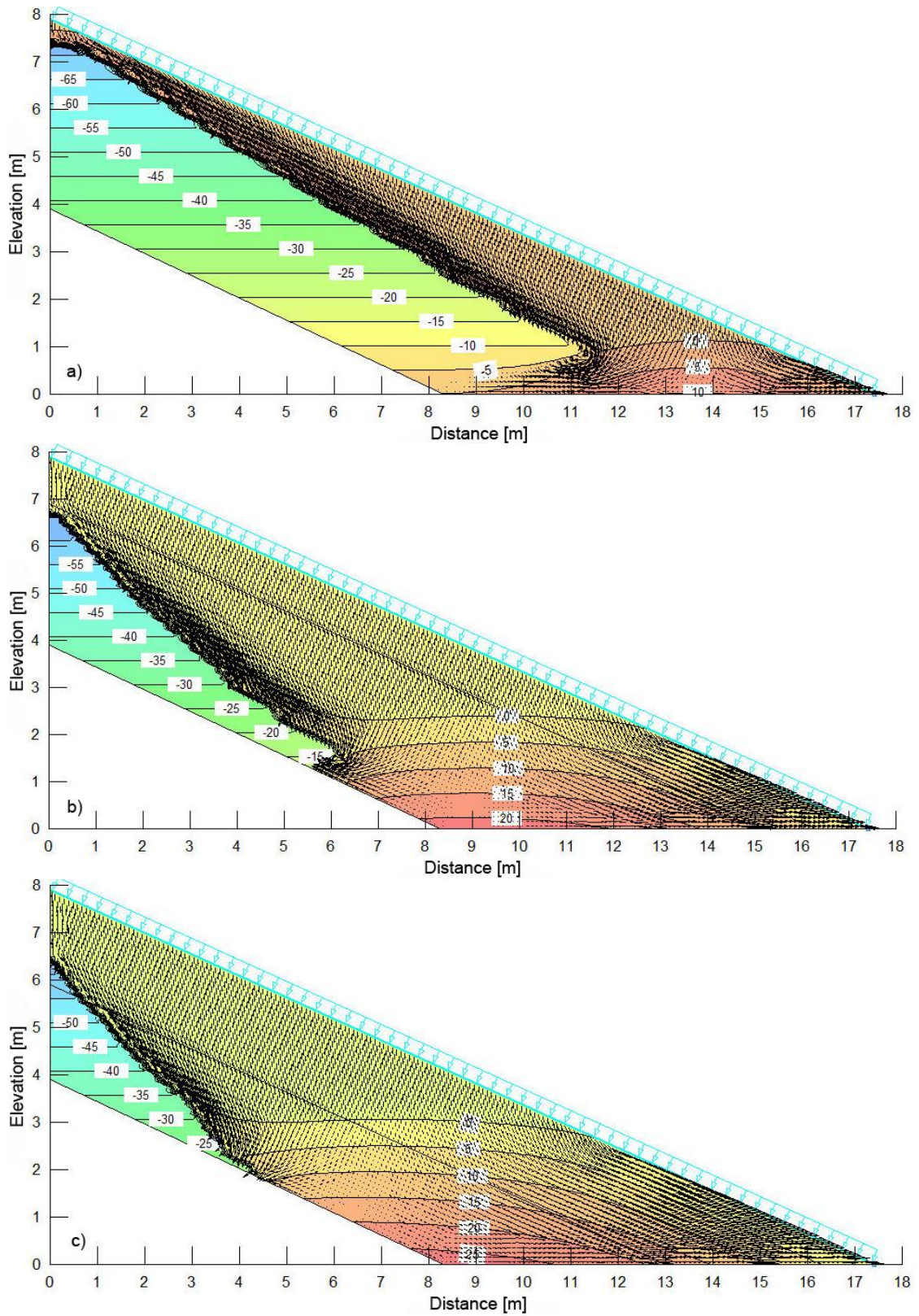


Figure 5-4: Results pore water pressure change at the end of rainfall: a) unreinforced case, b) 1 m depth of vegetation root case and c) 2 m depth of vegetation root case

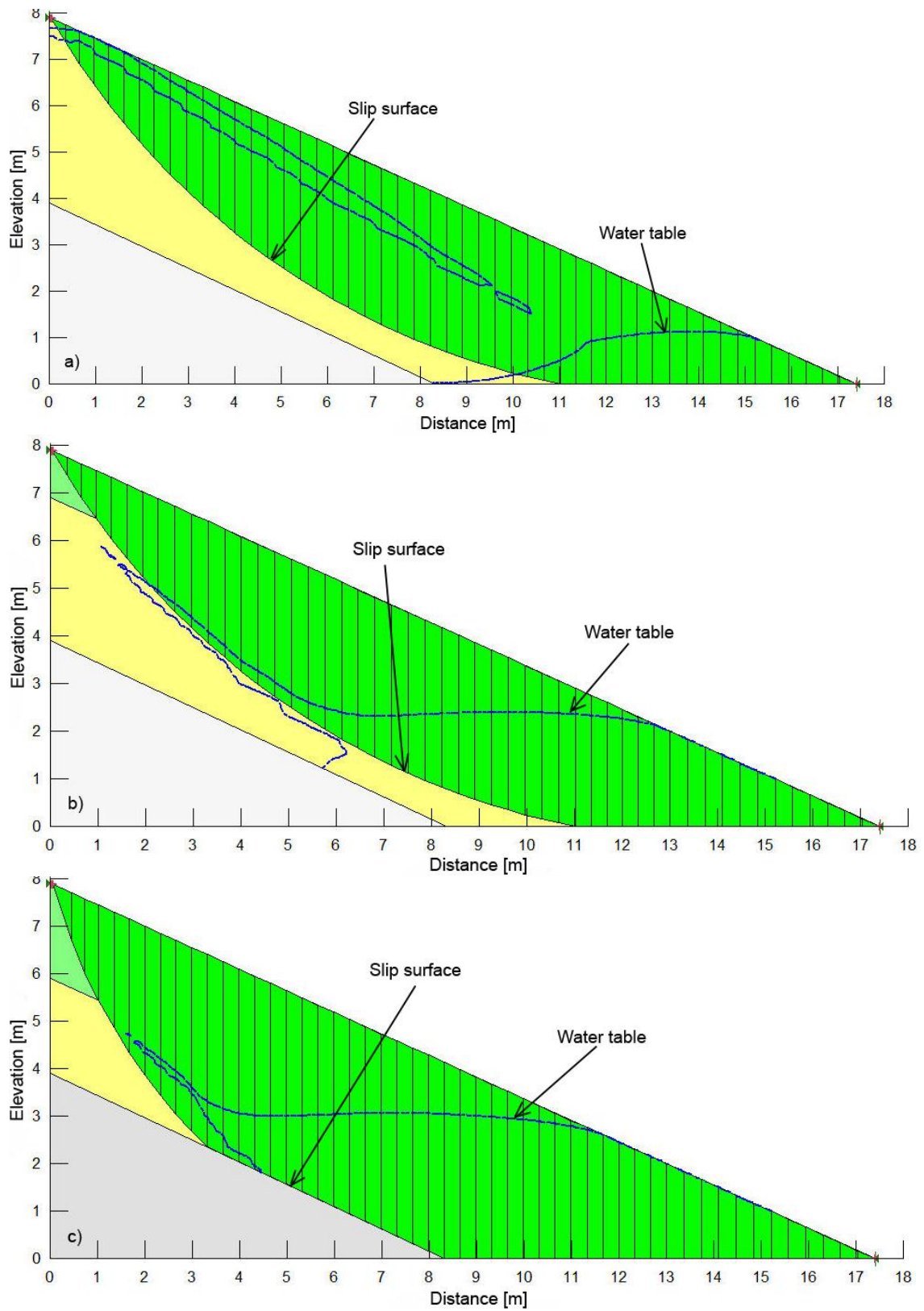


Figure 5-5: Results slip surface at the end of rainfall: a) un-reinforced case, b) 1 m depth of vegetation root case, and c) 2 m depth of vegetation root case.

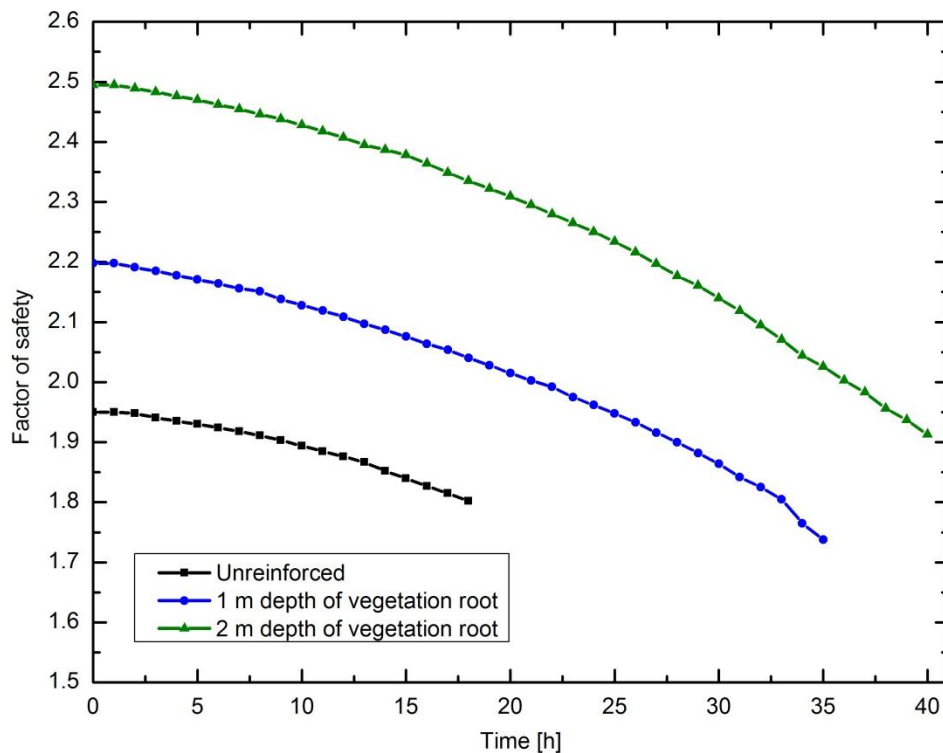


Figure 5-6: Variation of safety factor during rainfall

5.6.3. Pore water pressure comparison between centrifuge and geo-slope

Figure 5-7, 5-8, and 5-9 show the comparison of pore water pressure between the centrifuge and seepage/w for the unreinforced case, 1m depth of vegetation root, and 2m depth of vegetation root, respectively. Pore water pressure transducers 13 and 14 (PWP 13 and PWP 14) were selected to show in the graph due to their location at the toe slope where the most effective area is. According to the results from the centrifuge test in all cases (Fig. 5.7a), 5.8a) and 5.9a) it is shown that the pore water pressure started to change from zero while the result from seepage/w (Fig. 5.7b), 5.8b), and 5.9b)) show from the negative value for PWP 14. The differences are due to the limitation of pore water pressure transducer which was installed in the centrifuge test.

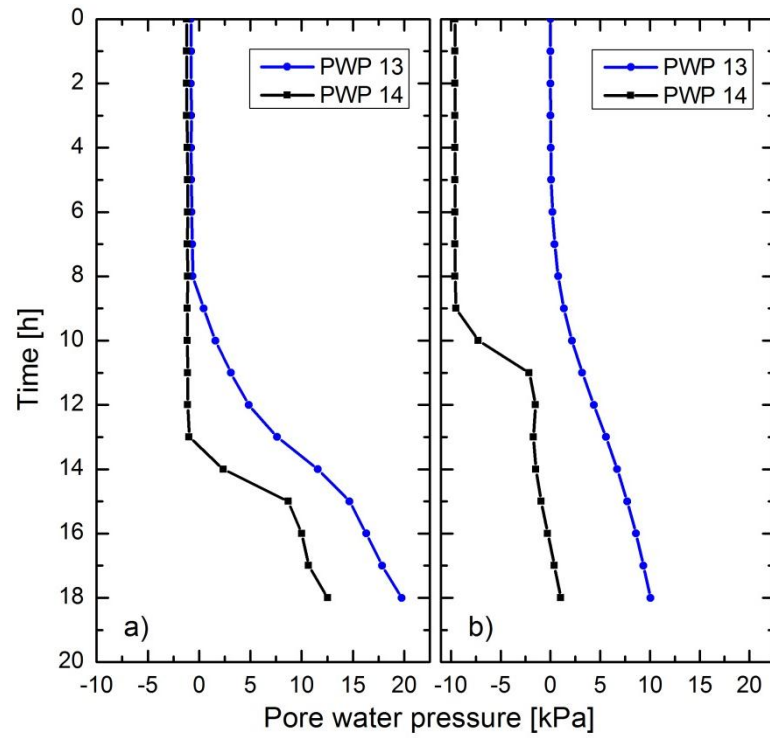


Figure 5-7: Comparison of pore water pressure change for unreinforced case: a) centrifuge result and b) seep/W result

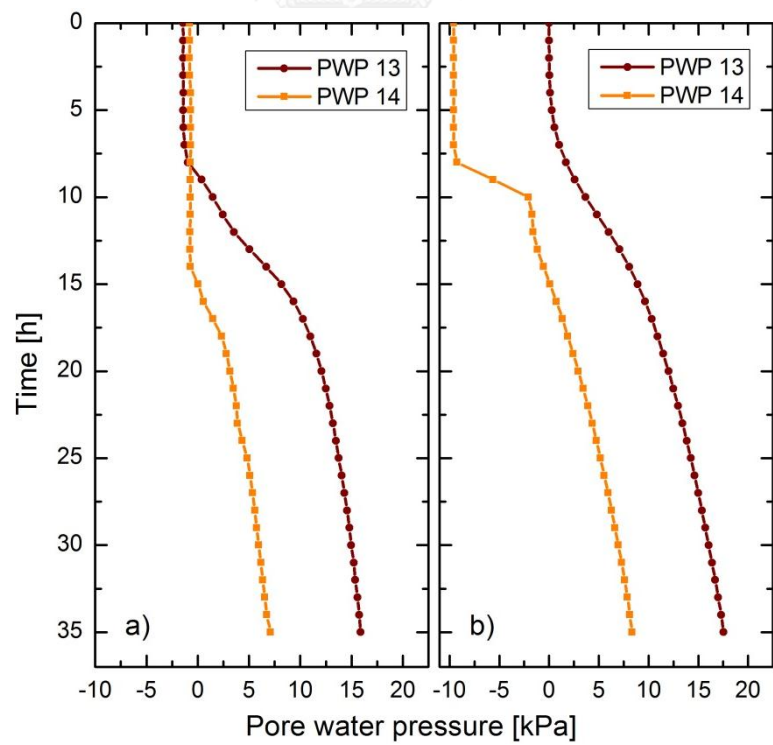


Figure 5-8: Comparison of pore water pressure change for 1m depth of vegetation root: a) centrifuge result and b) seep/W result

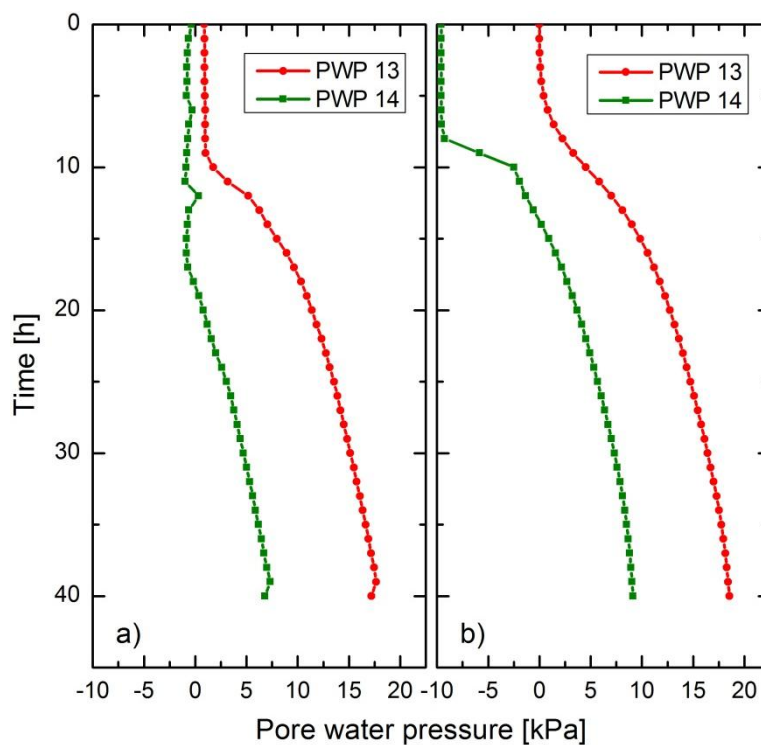


Figure 5-9: Comparison of pore water pressure change for 2m depth of vegetation root: a) centrifuge result and b) seep/W result

Table 5-3: Summarized of safety factors

Case		Circular failure assumption		Infinite slope assumption
Un-reinforced		Bishop method	1.7	0.95
		Morgenstern-Price method	1.8	
Root-reinforced	1 m depth	Bishop method	1.73	
		Morgenstern-Price method	1.74	
	2 m depth	Bishop method	1.92	
		Morgenstern-Price method	1.91	

6 CHAPTER CONCLUSION AND RECOMMENDATION

6.1 Conclusion

According to soil bioengineering concept and the observation results from vetiver grass, vegetation roots can increase the shear strength of the soil by mechanical reinforcement. The research confirms a significant contribution of the vegetation root on slope stability. The series of centrifuge model tests on slope whose surface is reinforced by model roots are conducted to understand the mechanism of the vegetation reinforcement against the rainfall-induced shallow failure. The conclusions of this study are as follows:

- 1) The roots significantly affect to the increase in the shear strength of soil. The shear strength of the root-reinforced soil depends on the roots length and the root area ratio.
- 2) The slope failure due to heavy rainfall is triggered by rising of the water table and starts around the toe of the slope. The rise of the water table causes the decreasing in the effective stress and results in the decrease in shear strength of the soil.
- 3) The presence of the root fibres on the slope surface helps to prevent the cracking on the soil slope.
- 4) The reinforcement efficiency increases with the rooting depth and the thicker reinforced zone makes the slope deformation less. In addition, the roots can delay the infiltration of rainfall into the ground to delay the groundwater table rising in the case of rainfall-induced failure.
- 5) Due to the numerical model using transient analysis in seep/W and limit equilibrium analysis in slope/W, the factor of safety of the slope have shown the increasing. Hence, the cohesion of fibres root helped to improve the shear strength of soil due to the length of the root.

6.2 Recommendation

- The study of vetiver grass should be performed in the field using the real scale model (full scale) to observe the real effect of the growing roots in the soil slope.
- To model slope stability on unsaturated soil with transient analysis in seep/w, SWCC (Soil Water Characteristic Curve) is the important parameter which used volumetric of water content and hydraulic conductivity as the function. Hence, the exact test result of SWCC should be well performed in laboratory with both un-reinforced and root-reinforced to avoid any error in the model.



REFERENCES

- Ali, F. H., & Osman, N. (2008). Shear Strength of a Soil Containing Vegetation Roots. *SOILS AND FOUNDATION Japanese Geotechnical Society*, 48(4), 587-596.
- Alsheimer, L., & Hughes, B. O. (2007). *Black and White in Photoshop CS3 and Photoshop Lightroom: Create stunning monochromatic images in Photoshop CS3, Photoshop Lightroom, and beyond*.
- Askarinejad, A. (2013). *Failure mechanisms in unsaturated silty sand slopes triggered by rainfall*. (Doctor of Sciences), Iran University of Science and Technology.
- ASTM-Standard-D98. (1998). Standard Test Method for Direct Shear Test of Soil Under Consolidated Drained Conditions (pp. 1-6). West Conshohocken, PA: American Society for Testing and Materials.
- Au, S. W. C. (1998). Rain-induced slope instability in Hong Kong. *Engineering Geology*, 51(1), 1-36. doi: [http://dx.doi.org/10.1016/S0013-7952\(98\)00038-6](http://dx.doi.org/10.1016/S0013-7952(98)00038-6)
- Aubertin, M., Mbonimpa, M., Bussière, B., & Chapuis, R. (2003). A model to predict the water retention curve from basic geotechnical properties. *Canadian Geotechnical Journal*, 40(6), 1104-1122.
- Bishop, A., & Morgenstern, N. (1960). Stability coefficients for earth slopes. *Géotechnique*, 10(4), 129-153.
- Bishop, A. W. (1955). The use of the slip circle in the stability analysis of slopes. *Géotechnique*(5), 7-17.
- Bishop, A. W. (1960). *The principles of effective stress*: Norges Geotekniske Institutt.
- Bishop, D. M., & Stevens, M. E. (1964). Landslides on logged areas in southeast Alaska. *US Forest Service research paper NOR*;-1.
- Blatz, J. A., Ferreira, N. J., & Graham, J. (2004). Effects of near-surface environmental conditions on instability of an unsaturated soil slope. *Canadian Geotechnical Journal*, 41(6), 1111-1126. doi: 10.1139/t04-058
- Brooks, R. H., & Corey, A. T. (1964). Hydraulic Properties of Porous Media *Hydrology Paper* (Vol. 3). Fort Collins, Colorado: Civil Engineering department, Colorado State University.

- Cerato, A. B., & Lutenegeger, A. J. (2006). Specimen Size and Scale Effects of Direct Shear Box Tests of Sands. *Geotechnical Testing Journal*, 29(6), 1-10.
- Chen, H., Lee, C., & Law, K. (2004). Causative mechanisms of rainfall-induced fill slope failures. *JOURNAL OF GEOTECHNICAL AND GEOENVIRONMENTAL ENGINEERING*, 130(6), 593-602.
- Childs, E. C., & Collis-George, N. (1950). The permeability of porous materials. *Proceedings of the Royal Society of London. Series A. Mathematical and Physical Sciences*, 201(1066), 392-405.
- Chinapan, W., Sukhasem, A., & Moncharoen, L. (1997). *Study on the ecotype comparison of vetiver grass in Thailand*. Paper presented at the Department of Land Development, Bangkok, Thailand.
- Coppin, N. J., & Richards, I. G. (1990). *Use of vegetation in civil engineering*: Butterworths.
- Duncan, J. M. (1996). State of the art: limit equilibrium and finite-element analysis of slopes. *Journal of Geotechnical Engineering*, 122(7), 577-596.
- Endo, T., & Tsuruta, T. (1969). The effect of the tree's roots upon the shear strength of soil. *1968 Annual Report of the Hokkaido Branch, Forest Exp. Sta.*, 157-182.
- F. Cai, & Ugai, K. (2004). Numerical Analysis of Rainfall Effects on Slope Stability. *INTERNATIONAL JOURNAL OF GEOMECHANICS*, 4(2), 69-78. doi: 10.1061//asce/1532-3641/2004/4:2/69
- Fellenius, W. (1936). *Calculation of the stability of earth dams*. Paper presented at the Transactions of the 2nd congress on large dams, Washington, DC.
- Fredlund, D., & Krahn, J. (1977). Comparison of slope stability methods of analysis. *Canadian Geotechnical Journal*, 14(3), 429-439.
- Fredlund, D., Krahn, J., & Pufahl, D. (1981). *The relationship between limit equilibrium slope stability methods*. Paper presented at the Proceedings of the International Conference on Soil Mechanics and Foundation Engineering.
- Fredlund, D., Rahardjo, H., Leong, E., & Ng, C. W. (2001). *Suggestions and recommendations for the interpretation of soil-water characteristic curves*. Paper presented at the Proceedings of the 14th Southeast Asian Geotechnical Conference, Hong Kong.

- Fredlund, D. G., & Morgenstern, N. R. (1977). Stress state variables for unsaturated soils. *JOURNAL OF GEOTECHNICAL AND GEOENVIRONMENTAL ENGINEERING*, 103(ASCE 12919).
- Fredlund, D. G., & Rahardjo, H. (1993). *Soil Mechanics for Unsaturated Soils*: Wiley.
- Fredlund, D. G., Rahardjo, H., & Fredlund, M. D. (2012). *Unsaturated soil mechanics in engineering practice*: John Wiley & Sons.
- Fredlund, D. G., Sheng, D., & Zhao, J. (2011). Estimation of soil suction from the soil-water characteristic curve. *Canadian Geotechnical Journal*, 48(2), 186-198.
- Fredlund, D. G., & Xing, A. (1994). Equations for the soil-water characteristic curve. *Canadian Geotechnical Journal*, 31(4), 521-532.
- Fredlund, M. D., Fredlund, D. G., & Wilson, G. (1997). *Prediction of the soil-water characteristic curve from grain-size distribution and volume-mass properties*. Paper presented at the Proc., 3rd Brazilian Symp. on Unsaturated Soils.
- Garnier, J., Gaudin, C., Springman, S., Culligan, P., Goodings, D., Konig, D., . . . Thorel, L. (2007). Catalogue of scaling laws and similitude questions in geotechnical centrifuge modelling. *International Journal of Physical Modelling in Geotechnics*, 7(3), 1-23.
- Ghestem, M., Sidle, R. C., & Stokes, A. (2011). The Influence of Plant Root Systems on Subsurface Flow: Implications for Slope Stability. *BioScience*, 61(11), 869-879. doi: 10.1525/bio.2011.61.11.6
- Gofar, N., Lee, L. M., & Asof, M. (2006). Transient seepage and slope stability analysis for rainfall induce lanslide: A case study. *Malaysian Journal of Civil Engineering*, 18(1), 1-13.
- Goodings, D. (1985). RELATIONSHIPS FOR MODELLING WATER EFFECTS IN GEOTECHNICAL CENTIFUGE MODELS. *Publication of: Balkema (AA)*.
- Gray, D. H., & Leiser, A. T. (1982). *Biotechnical slope protection and erosion control*: Van Nostrand Reinhold Company.
- Gray, D. H., & Sotir, R. B. (1996). *Biotechnical and soil bioengineering slope stabilization: a practical guide for erosion control*. New York: John Wiley & Sons.

- Greenfield, J. C. (1996). *Vegetative vs. mechanical soil conservation system as they affect moisture conservation and sustained production*. Paper presented at the Proceedings of the First International Conference on Vetiver. Office of the Royal Development Projects Board, Bangkok.
- Greenway, D. R. (1978). Vegetation and Slope Stability. In M. G. Anderson & K. S. Richards (Eds.), *Vegetation and Slope Stability* (pp. 187-230). Chichester: John Wiley and Sons.
- Greenwood, J., Norris, J., & Wint, J. (2004). Assessing the contribution of vegetation to slope stability. *Proceedings of the ICE-Geotechnical Engineering*, 157(4), 199-207.
- Gupta, S., & Larson, W. (1979). Estimating soil water retention characteristics from particle size distribution, organic matter percent, and bulk density. *Water resources research*, 15(6), 1633-1635.
- Helliwell, D. (1986). The extent of tree roots. *Arboricultural Journal*, 10(4), 341-347.
- Hengchaovanich, D., & Nilaweera, N. S. (1996). *An Assessment of Strength Properties of Vetiver Grass Roots in Relation to Slope*. Paper presented at the the First International Conference on Vetiver, Chain Kai.
- Hengchaovanich, D., & Nilaweera, N. S. (1996). *An assessment of strength properties of vetiver grass roots in relation to slope stabilization*. Paper presented at the International Conference on Vetiver, Chain Kai, Thailand.
- Islam, M. S., Nasrin, S., Islam, M. S., & Moury, F. R. (2013). Use of Vegetation and Geo Jute in Erosion Control of Slopes in a Sub Tropical Climate. *Engineering and Technology International Journal of Civil*, 7(1), 31-39.
- Janbu, N. (1954). *Application of composite slip surfaces for stability analysis*. Paper presented at the Proc. European Conf. on Stability of Earth Slopes, Stockholm, 1954.
- Janbu, N. (1968). Slope stability computations soil mechanics and foundation engineering report. *Technical University of Norway, Trondheim*.
- Jotisankasa, A. (2013). *Application of Local Plant Species for Live Stake as a Bio-Slope Stabilization Method in Thailand*. Paper presented at the Infrastructure Development, Tokyo Tech.

- Kaewsaeng, W. (2000). *Engineering Properties of Weathered Clay Soil Reinforced with Prachuap Khiri Khan Vetiveria Memorialis A.Camus Root for Slope Protection*. King Mongkut's University of Technology.
- Kimura, T., Takemura, J., Suemasa, N., & Hiro-Oka, A. (1991). *Failure of fills due to rain fall*. Paper presented at the Centrifuge.
- Kozłowski, T. T. (1971). *Growth and Development of Trees: Vol. II: Cambial Growth, Root Growth, and Reproductive Growth*: Academic Press.
- Krahn, J. (2008). *Stability Modeling with SLOPE/W 2007 Version: An Engineering Methodology*. Canada: GEO-SLOPE International Ltd.
- Krahn, J. (2009). *Seepage Modeling with SEEP/W 2007: An Engineering Methodology* (Fourth ed.). Canada: GEO-SLOPE International Ltd.
- Land-Development-Department. (1998). *Vetiver Grass Overview*. Land Development Department, Ministry of Agriculture and Cooperatives (pp. 115).
- Ling, H. I., Wu, M. H., Leshchinsky, D., & Leshchinsky, B. (2009). Centrifuge Modeling of Slope Instability. *JOURNAL OF GEOTECHNICAL AND GEOENVIRONMENTAL ENGINEERING*, 135(6), 758-767. doi: 10.1061//asce/gt.1943-5606.0000024
- Llasat, M. a.-C. (2001). An objective classification of rainfall events on the basis of their convective features: application to rainfall intensity in the northeast of Spain. *International Journal of Climatology*, 21(11), 1385-1400. doi: 10.1002/joc.692
- Lowe, J., & Karafiath, L. (1960). *Stability of earth dams upon drawdown*. Paper presented at the Proc. 1st. Pan American Conference on Soil Mechanics and Foundation Engineering, México.
- Lu, N., & Likos, W. J. (2004). *Unsaturated soil mechanics*: J. Wiley.
- Lumb, P. (1975). Slope failures in Hong Kong. *Quarterly Journal of Engineering Geology and Hydrogeology*, 8(1), 31-65.
- Lyr, H., & Hoffmann, G. (1967). Growth Rates and Growth Periodicity of Tree Roots (Vol. 2, pp. 181-236): International Review of FORESTRY RESEARCH.
- Mafian, S., Huat, B. B. K., & Ghiasi, V. (2009). Evaluation on Root Theories and Root Strength Properties in Slope Stability. *European Journal of Scientific Research*, 30(4), 594-607.

- Mairaing, W., Jotisankasa, A., & Soralump, S. (2011). *Some Applications of Unsaturated Soil Mechanics in Thailand: an Appropriate Technology Approach*. Paper presented at the Proceedings of the 5th Asia Pacific Conference on Unsaturated Soils., Pattaya, Thailand.
- Mairaing, W., Jotisankasa, A., & Soralump, S. (2012). Application of Unsaturated Soil Mechanics in Thailand: and Appropriate Technology Approach. *Geotechnical Engineering Journal of the SEAGS & AGSSEA*, 43(1), 1-11.
- Meisina, C., & Scarabelli, S. (2007). A comparative analysis of terrain stability models for predicting shallow landslides in colluvial soils. *Geomorphology*, 87(3), 207-223. doi: <http://dx.doi.org/10.1016/j.geomorph.2006.03.039>
- Menashe, E. (2001). *Bio-Structural Erosion Control: Incorporating Vegetation in Engineering Designs to Project Puget Sound Shorelines*. Paper presented at the Puget Sound Research.
- Michalowski, R. L., & Zhao, A. (1996). Failure of fiber-reinforced granular soils. *Journal of Geotechnical Engineering*, 122(3), 226-234.
- Mickovski, S. B., & van Beek, L. P. H. (2009). Root morphology and effects on soil reinforcement and slope stability of young vetiver (*Vetiveria zizanioides*) plants grown in semi-arid climate. *Plant and Soil*, 324(1-2), 43-56. doi: 10.1007/s11104-009-0130-y
- Moayed, R. Z., & Alizadeh, A. (2011). Effects of shear box size on the strength for different type of silty sands. In S. Jotisankasa, Soralump and Mairaing (Ed.), *Unsaturated Soil: Theory and Practice* (pp. 265-271).
- Montrasio, L., & Valentino, R. (2007). Experimental analysis and modelling of shallow landslides. *Landslides*, 4(3), 291-296.
- Morgenstern, N., & Price, V. E. (1965). The analysis of the stability of general slip surfaces. *Géotechnique*, 15(1), 79-93.
- Nasrin, M., Islam, M. S., & Moury, F. R. (2013). Use-of-Vegetation-and-Geo-Jute-in-Erosion-Control-of-Slopes-in-a-Sub-Tropical-Climate. *International Journal of Civil, Architectural, Structural and Construction Engineering*, 7(1), 31-39.

- Ng, C. W. W., & Shi, Q. (1998). A Numerical Investigation of the Stability of Unsaturated soil slope subjected to transient seepage. *Computer and Geotechnics*, 22(1), 1-28.
- O'Loughlin, C. L. (1974). The Effect of Timber Removal on the Stability of Forest Soils. *Journal of Hydrology, New Zealand*, 13(2), 121-134.
- Oblozinsky, P., & Kuwano, J. (2004). Centrifuge experiments on stability of tunnel face. *Slovak J Civil Eng*, 3, 23-29.
- Operstein, V., & Frydman, S. (2000). The influence of vegetation on soil strength. *Proceedings of the ICE-Ground Improvement*, 4(2), 81-89.
- Petterson, K. E. (1955). The early history of circular sliding surfaces. *Géotechnique*, 5(4), 275-296.
- Rahardjo, H., & Satyanaga, A. (2014). Application of unsaturated soil mechanics to open pit slope stability (Vol. 42, pp. 1-7). Singapore: Nanyang Technological University.
- Rahardjo, H., Satyanaga, A., & Leong, E. C. (2012). Unsaturated Soil Mechanics for Slope Stabilization. *Geotechnical Engineering Journal*, 43(1), 48-58.
- Richards, L. A. (1931). Capillary conduction of liquids through porous mediums. *Journal of Applied Physics*, 1(5), 318-333.
- Schofield, A. N. (1980). Cambridge geotechnical centrifuge operations. *Géotechnique*, 30(3), 227-268.
- Schofield, A. N. (1981). *Dynamic and earthquake geotechnical centrifuge modelling*. Paper presented at the First International Conference on Recent Advances in Geotechnical earthquake Engineering and Soil Dynamics (1981: April 26-May 3; St. Louis, Missouri).
- Schor, H. J., & Gray, D. H. (2007). *Landforming: An Environmental Approach to Hillside Development, Mine Reclamation and Watershed Restoration*: Wiley.
- Sonnenberg, R., Bransby, M. F., Bengough, A. G., Hallett, P. D., & Davies, M. C. R. (2011). Centrifuge modelling of soil slopes containing model plant roots. *Canadian Geotechnical Journal*, 49, 1-17. doi: 10.1139/T11-081
- Sonnenberg, R., Bransby, M. F., Hallett, P. D., Bengough, A. G., Mickovski, S. B., & Davies, M. C. R. (2010). Centrifuge modelling of soil slopes reinforced with

- vegetation. *Canadian Geotechnical Journal*, 47(12), 1415-1430. doi: 10.1139/t10-037
- Spencer, E. (1967). A method of analysis of the stability of embankments assuming parallel inter-slice forces. *Géotechnique*, 17(1), 11-26.
- Stone, E. L., & Kalisz, P. J. (1991). On the maximum extent of tree roots. *Forest Ecology and Management*, 46(1), 59-102.
- Sutton, R. (1969). Form and development of conifer root systems. *Technical Communication Commonwealth Agricultural Bureaux. Farnham Royal, Bucks., England.*(7).
- Swanston, D. N. (1970). Mechanics of debris avalanching in shallow till soils of southeast Alaska. *Research Papers. Pacific Northwestern Forest and Range Experiment Station*(PNW-103).
- Swanston, D. N. (1974). Slope stability problems associated with timber harvesting in mountainous regions of the western United States.
- Takahashi, A. (2002). *Soil-pile interaction in liquefaction-induced lateral spreading of soils*. (Doctor of engineering), Tokyo Institute of Technology.
- Takahashi, A., Nakamura, K., & Likitlersuang, S. (2014). *On the seepage-induced failure of vegetation-stabilised slopes*. Paper presented at the International Conference on Physical Modelling in Geotechnics, Perth.
- Takemura, J., Kondoh, M., Esaki, T., Kouda, M., & Kusakabe, O. (1999). Centrifuge model tests on double propped wall excavation in soft clay. *Soils and Foundations*, 39(3), 75-87.
- Taylor, R. e. (2003). *Geotechnical centrifuge technology*: CRC Press.
- Terwilliger, V. J., & Waldron, L. J. (1990). Assessing the contribution of roots to the strength of undisturbed, slip prone soils. *Catena*, 17(2), 151-162.
- Terzaghi, K., Terzaghi, K., Engineer, C., Czechoslovakia, A., Terzaghi, K., Civil, I., . . . Unis, E. (1943). *Theoretical soil mechanics* (Vol. 18): Wiley New York.
- Tiwari, R. C., Bhandary, N. P., Yatabe, R., & Bhat, D. R. (2013). New numerical scheme in the finite-element method for evaluating the root-reinforcement effect on soil slope stability. *Geotechnique*, 63(2), 129-139. doi: 10.1680/geot.11.P.039

- Truong, P., Van, T. T., & Pinners, E. (2008). *Vetiver System Applications: Technical Reference Manual* (2 ed.): CreateSpace Independent Publishing Platform.
- Tyler, S. W., & Wheatcraft, S. W. (1989). Application of fractal mathematics to soil water retention estimation. *Soil Science Society of America Journal*, 53(4), 987-996.
- van Genuchten, M. T. (1980). A close-form equation for predicting the hydraulic conductivity of unsaturated soils. *Soil Science Society of America Journal*, 44, 892-898.
- Waldron, L. (1977). The shear resistance of root-permeated homogeneous and stratified soil. *Soil Science Society of America Journal*, 41(5), 843-849.
- Waldron, L., & Dakessian, S. (1981). Soil reinforcement by roots: calculation of increased soil shear resistance from root properties. *Soil science*, 132(6), 427-435.
- Wu, T. H. (1976). *Investigation of landslides on prince of Wales Island, Alaska*: Ohio State University.
- Wu, T. H. (1995). *Slope stabilization*. In: *Slope stabilization and Erosion Control: A Bioengineering Approach* (R. P. C. Morgan & R. J. Rickson Eds.). Longdon.
- Wu, T. H., Bettadapura, D. P., & Beal, P. E. (1988). A statistical model of root geometry. *Forest Science*, 34(4), 980-997.
- Wu, T. H., McKinnell III, W. P., & Swanston, D. N. (1979). Strength of tree roots and landslides on Prince of Wales Island, Alaska. *Canadian Geotechnical Journal*, 16(1), 19-33.
- Wu, T. H., McKinnell, W. P., & Swanston, D. N. (1979). Strength of tree roots and landslides on Prince of Wales Island. *Canadian Geotechnical Journal*, 16, 19-33.
- Wu, T. H., & Swanston, D. N. (1980). Risk of landslides in shallow soils and its relation to clearcutting in southeastern Alaska. *Forest Science*, 26(3), 495-510.
- Ziemer, R. R. (1981). *The role of vegetation in the stability of forested slopes*. Paper presented at the Proc. First Union of For. Res. Org., Div. I, XVII World Congress, Kyoto, Japan.

Ziemer, R. R., & Swanston, D. N. (1977). *Root strength changes after logging in southeast Alaska* (Vol. 306): Dept. of Agriculture, Forest Service, Pacific Northwest Forest and Range Experiment Station.





APPENDIX

จุฬาลงกรณ์มหาวิทยาลัย
CHULALONGKORN UNIVERSITY

Appendix: Rainfall simulator



微霧発生ノズルBIMシリーズ/小噴量形

小噴量扇形 BIMV---液加圧---

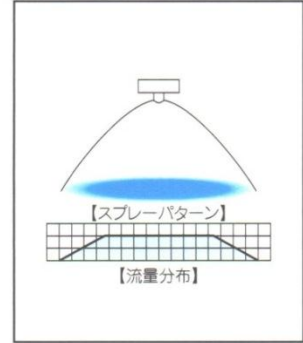


注:写真はSN形アダプターを使用

【特 性】

- 平均粒子径が100マイクロン以下(※1)の“微霧”を発生する2流体扇形ノズル。
- 噴霧液に0.1~0.3MPa程度の圧力をかけて噴霧する液加圧タイプで、幅広い流量調節範囲を持つ。
- 噴霧角度は110°、80°、45°の3種類。
- 扇形の全域にわたり均等な分布と、中央が強く両端にかけて次第に弱まる山形分布を1つのノズルで使い分けられます。

※1 レーザードップラー法による測定値。



【主用途】

- 散布: 塵型剤、消臭剤、油、表面処理剤、防錆剤、潤滑剤、ハチミツ、防虫剤、尿素水、その他。
- 冷却: 金型、ガス、鋼板、鋼片、鋳物、車体、塗装物、板硝子、プラスチック、その他。
- 潤湿: 紙、廃ガス、セラミック、コンクリート、その他。
- 洗浄: 精密基板、ガラス管、その他。

【構造と材質】

- ノズルチップ+コア+キャップ+アダプターの4部品(アダプターの種類についてはP.23, 24を御覧下さい。)
- 材質: S303 (SUS303) (オプション材質S316L)

【寸法とネジサイズ】

- BIMVシリーズの寸法と取付ネジサイズはP.25をご覧ください。

【付属品】

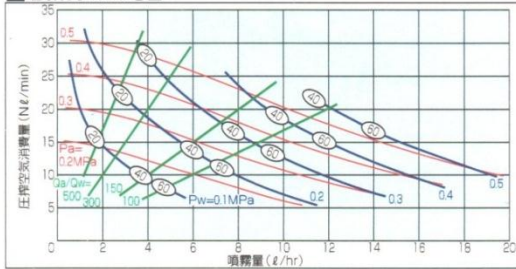
- ノズルを使用箇所に取り付けるための自在ホルダーを用意しています。P.26をご覧ください。

流量線図

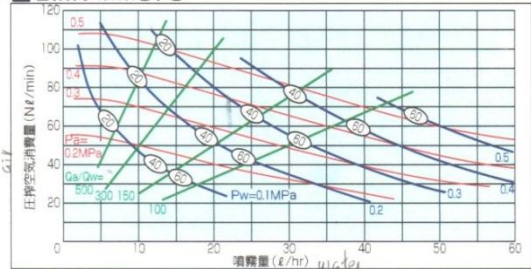
■線図の読み方

- ① 噴霧量 (ℓ/hr) は、1個のノズルのそれを示します。
- ② 赤色の線は圧搾空気圧力Pa (MPa)、
青色の線は液圧力Pw (MPa)、
緑色の線Qa/Qwは気水比を示します。
- ③ ○内の数値はレーザードップラー法によるサウター平均粒子径 (μm)。
- ④ ※には噴角の区分が入ります。

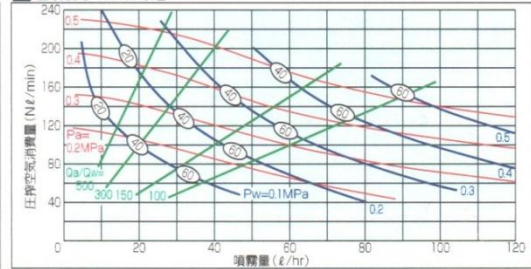
■BIMV ※※02



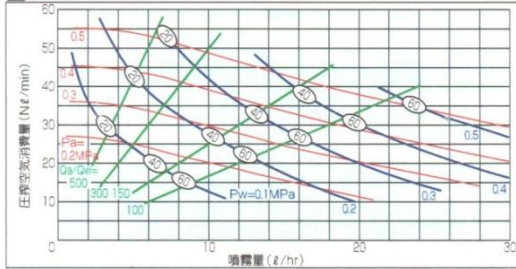
■BIMV ※※075



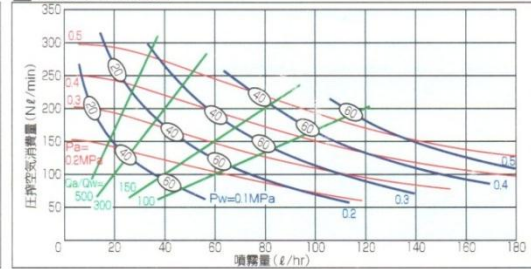
■BIMV ※※15



■BIMV ※※04



■BIMV ※※22

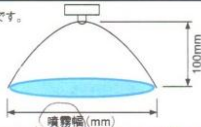


微霧発生ノズルBIMシリーズ/小噴量形

小噴量扇形 BIMV---液加圧---

噴角の区分 ※1	空気消費量の区分	Air 空気圧 (MPa)	噴霧量 (ℓ/hr) / 空気消費量 (Nℓ/min)					噴霧幅 (mm) ※2			平均粒子径 (μm)	異物通過径 (mm)			
			液圧 (MPa)					液圧 (MPa)				レーザー ドップラー法	チップ 噴口	アダプター	
			0.1	0.15	0.2	0.25	0.3	0.1	0.15	0.25				液	空気
110°	02	0.2	2.2 / 14	5.3 / 11	—	—	—	280	340	—	15 100	0.2	0.9	0.7	
		0.3	1.0 / 20	2.5 / 19	4.6 / 17	8.3 / 12	14.3 / 7	220	250	420					
		0.4	—	1.4 / 25	2.3 / 24	4.0 / 23	6.3 / 20	—	230	340					
	04	0.2	4.5 / 25	9.5 / 20	17.0 / 13	—	—	300	360	—	15 100	0.3	0.9	0.9	
		0.3	2.0 / 36	4.7 / 35	8.5 / 31	13.1 / 27	19.6 / 20	230	270	430					
		0.4	—	2.8 / 45	4.8 / 44	7.7 / 41	11.4 / 37	—	250	350					
	075	0.2	8.7 / 51	18.4 / 42	33.3 / 29	—	—	320	380	—	15 100	0.5	1.2	1.4	
		0.3	4.0 / 74	8.8 / 71	15.5 / 64	24.3 / 54	38.5 / 40	240	300	450					
		0.4	—	5.6 / 91	9.1 / 89	14.8 / 82	21.8 / 74	—	270	370					
	15	0.2	16.8 / 107	34.8 / 90	64.4 / 60	—	—	340	400	—	15 100	0.8	1.8	1.9	
		0.3	8.0 / 150	17.7 / 144	30.8 / 130	50.0 / 108	74.5 / 87	270	320	470					
		0.4	—	11.2 / 190	18.3 / 183	29.1 / 172	42.9 / 154	—	280	380					
22	0.2	22.3 / 140	45.6 / 116	92.1 / 76.9	—	—	350	420	—	15 100	0.9	2.1	2.2		
	0.3	11.5 / 200	23.9 / 189	41.3 / 169	68.5 / 138	107 / 103	280	330	490						
	0.4	—	15.3 / 245	24.5 / 238	39.1 / 220	57.7 / 198	—	300	400						
80°	02	0.2	2.2 / 14	5.3 / 11	—	—	—	200	260	—	15 100	0.3	0.9	0.7	
		0.3	1.0 / 20	2.5 / 19	4.6 / 17	8.3 / 12	14.3 / 7	170	210	300					
		0.4	—	1.4 / 25	2.3 / 24	4.0 / 23	6.3 / 20	—	200	250					
	04	0.2	4.5 / 25	9.5 / 20	17.0 / 13	—	—	200	260	—	15 100	0.4	0.9	0.9	
		0.3	2.0 / 36	4.7 / 35	8.5 / 31	13.1 / 27	19.6 / 20	170	210	310					
		0.4	—	2.8 / 45	4.8 / 44	7.7 / 41	11.4 / 37	—	200	260					
	075	0.2	8.7 / 51	18.4 / 42	33.3 / 29	—	—	200	270	—	15 100	0.6	1.2	1.4	
		0.3	4.0 / 74	8.8 / 71	15.5 / 64	24.3 / 54	38.5 / 40	170	210	310					
		0.4	—	5.6 / 91	9.1 / 89	14.8 / 82	21.8 / 74	—	200	260					
	15	0.2	16.8 / 107	34.8 / 90	64.4 / 60	—	—	210	280	—	15 100	0.9	1.8	1.9	
		0.3	8.0 / 150	17.7 / 144	30.8 / 130	50.0 / 108	74.5 / 87	180	220	320					
		0.4	—	11.2 / 190	18.3 / 183	29.1 / 172	42.9 / 154	—	200	270					
22	0.2	22.3 / 140	45.6 / 116	92.1 / 76.9	—	—	210	280	—	15 100	1.1	2.1	2.2		
	0.3	11.5 / 200	23.9 / 189	41.3 / 169	68.5 / 138	107 / 103	180	220	330						
	0.4	—	15.3 / 245	24.5 / 238	39.1 / 220	57.7 / 198	—	210	280						
45°	02	0.2	2.2 / 14	5.3 / 11	—	—	—	100	130	—	15 100	0.4	0.9	0.7	
		0.3	1.0 / 20	2.5 / 19	4.6 / 17	8.3 / 12	14.3 / 7	80	110	150					
		0.4	—	1.4 / 25	2.3 / 24	4.0 / 23	6.3 / 20	—	100	130					
	04	0.2	4.5 / 25	9.5 / 20	17.0 / 13	—	—	100	130	—	15 100	0.5	0.9	0.9	
		0.3	2.0 / 36	4.7 / 35	8.5 / 31	13.1 / 27	19.6 / 20	80	110	150					
		0.4	—	2.8 / 45	4.8 / 44	7.7 / 41	11.4 / 37	—	100	130					
	075	0.2	8.7 / 51	18.4 / 42	33.3 / 29	—	—	100	140	—	15 100	0.9	1.2	1.4	
		0.3	4.0 / 74	8.8 / 71	15.5 / 64	24.3 / 54	38.5 / 40	80	110	160					
		0.4	—	5.6 / 91	9.1 / 89	14.8 / 82	21.8 / 74	—	100	140					
	15	0.2	16.8 / 107	34.8 / 90	64.4 / 60	—	—	110	150	—	15 100	1.2	1.8	1.9	
		0.3	8.0 / 150	17.7 / 144	30.8 / 130	50.0 / 108	74.5 / 87	90	120	170					
		0.4	—	11.2 / 190	18.3 / 183	29.1 / 172	42.9 / 154	—	110	150					
22	0.2	22.3 / 140	45.6 / 116	92.1 / 76.9	—	—	110	160	—	15 100	1.6	2.1	2.2		
	0.3	11.5 / 200	23.9 / 189	41.3 / 169	68.5 / 138	107 / 103	90	120	180						
	0.4	—	15.3 / 245	24.5 / 238	39.1 / 220	57.7 / 198	—	110	150						

注：※1 噴角は空気圧0.3MPa、液圧0.1MPaのときのものです。
 ※2 噴霧幅は噴霧距離100mmのときのものです。



構成とお引き合い要領

BIMV (扇形ノズル) シリーズ 液加圧タイプのノズル品番は、噴角の区分と空気消費量の区分の組み合わせで選定し、配管への取付けに応じ、N形、T形、ND形、SP形、SN形などの8種類のアダプターと組み合わせてください。

形番はチャートをご覧ください、下記のように表示してください。

<例>

BIMV 11002S303+NS303

BIMV

110

噴角の区分
 ■110°
 ■80°
 ■45°

02

空気消費量の区分
 ■02
 ■04
 ■075
 ■15
 ■22

S303 +

N

アダプターの種類
 ■N形
 ■T形
 ■ND (UND) 形
 ■SP (USP) 形
 ■SN (USN) 形

S303

アダプターの材質SUS303

アダプターの詳細はP.23, 24をご覧ください。

VITA

Mr. Kreng Hav EAB was born in Kompong Cham Province, Eastern part of Cambodia, on February 28th, 1987. After finishing high school at the Stung Trang High School in 2004, he did pass the entrance exam to study Bachelor's degree of Rural Engineering in the division of Infrastructure and Water Resources at Institute of Technology of Cambodia (ITC) for 5 years. Shortly, after his graduation in June 2009, he had awarded a scholarship, which is supported by Indonesian Government under the AUN/Seed-Net Program (JICA), to study a Master's Degree in Geological Engineering department at Gadjah Mada University, Indonesia. After his successful graduation, his Master's degree in August 2011, he attained for a scholarship award in Sandwich Program under the support of AUN/Seed-Net Program (JICA) for his Doctoral's degree in Civil Engineering department at Chulaongkorn University, Thailand. He had two international journals within his doctoral degree. One is published in Géotechnique Letters and another is published in Soil and Foundation. Plus, he already submitted one proceeding: the 27th KKHTCNN Symposium, Shanghai, China. This thesis is a partial fulfillment of the requirements for the degree.